

CHAPTER 2:

Development and implementation of Non-linear models within GlnaFit framework

2.1 *GlnaFIT Modelling Framework:*

GlnaFIT (Geeraerd *et al.*, 2005) is a freely available predictive modelling program implemented in Microsoft Excel. The program was originally designed to provide access to predictive models for end-users within industry unfamiliar with advanced non-linear regression techniques (Geeraerd *et al.*, 2005). There are ten non-linear functions that allow models to be fit to data. Each model is designed to describe a particular type of underlying response. The model types provided within GlnaFIT are described following the approach of Geeraerd (2013).

The traditional log-linear model (Type I) (Bigelow and Esty, 1920) can be used to describe first-order kinetics. The model assumes that cells within a population exhibit equivalent sensitivity to heat. An additional variation of first-order kinetic models generate survival curves that incorporate a shoulder-effect prior to showing a log-linear decrease (Type II) (Geeraerd *et al.*, 2000). Expanded first-order kinetic models can be fit to data that incorporate an asymptotic function for describing a tailing effect following a log-linear decrease (Type III) (Geeraerd *et al.*, 2000). First-order kinetic models may also be fit to data that show a sigmoidal response by exhibiting a shoulder-effect, followed by a log-linear decrease in survival prior to an asymptote effect (tailing) (Type IV) (Geeraerd *et al.*, 2000). Concave (Shape V) and convex (Type VI) survival curves can be fitted to data using the Weibull model developed by Marfart *et al.* (2002). By contrast, concave or convex survival curves (Type VII) may be fit to data using a Weibull model with an asymptotic function to describe tailing effect (Marfart *et al.* 2002; Albert and Marfart, 2005). Models that generate biphasic survival curves (Type VIII) can be fit to data using the model described by Cerf (1977). Models can be fit to data that show a complex sigmoidal response using an expanded biphasic model proposed by Geeraerd *et al.* (2005) where a shoulder-effect describes the resistance of an initial subpopulation followed by a log-linear decrease in survival, and a further decrease in survival of an additional subpopulation (Type IX). Finally, a mixed Weibull distribution model (Coroller *et al.*, 2006) can be fit to data that exhibit double concave or convex response curves (Type X). The model assumes the presence of two subpopulations. The first subpopulation shows greater sensitivity to stress, whereas the second subpopulation shows increased resistance in response to biochemical and/or biophysical challenge.

2.2 Model Building:

The model framework outlined above was used to generate predicted survival curves for *Campylobacter* strains following exposure to each temperature profile and a combination of pH and temperature as a function of time. The underlying response of each *Campylobacter* strain to biophysical and biochemical stress was modelled independently using the GlnaFIT (1.6) (Geeraerd *et al.*, 2005). Where it was possible to use more than one model was to describe the underlying response of an individual strain, the goodness-of-fit statistic was used to select between competing models. The Root Mean Sum of Squared Error (RMSE) quantifies the goodness of fit for both linear and non-linear models and is calculated by determining the difference between observed and predicted values. A model is considered a good fit to data when RMSE is close to zero. In addition, the adjusted coefficient of determination (R^2_{adj}) was also provided as a measure of overall fit of the model to the data.

In addition, a Generalized Least Squares (GLS) modelling approach (Pineiro *et al.*, 2014) was used to examine differences in decimal reduction time (D-value) of *Campylobacter* strains according to time-temperature simulations (56°C, 60°C and 64°C). Time to first decimal reduction was also assessed for combined pH and time-temperature simulations where pH was defined factor (pH 4.5, pH 5.5, pH 6.5, pH 7.5 and pH 8.5) and temperature was represented as a three-level factor (56°C, 60°C and 64°C). The explanatory variables were incorporated multiplicatively as an interaction term. The D-values for each strain generated for each time-temperature simulation are provided in Tables 203, 218 and 233. The D-values calculated for combined pH and time-temperature simulations are provided in tables 248, 269 and 289. Analyses were undertaken using R (3.1.2) (R Core Development Team, 2014).

2.3 RESULTS:

2.3.1 Time-temperature Simulations

Parameter estimates for predictive models of experimental simulations undertaken at 56°C are shown in tables 207 – 220. Predicted response curves for corresponding models are shown in figures 232 – 245. The parameter estimates relating to predictive models for experimental simulations undertaken at 60°C are shown in tables 222 – 235 and predicted response curves for associated models are provided in figures 246 – 259. Parameter estimates of models generated for simulations undertaken at 64°C are shown in tables 237 – 250 and predicted response curves for associated models are shown in figures 260 – 273.

2.3.1.1 Assessment of Model Fit:

Goodness-of-fit statistics for individual models for each time-temperature profile are provided in Table 206, 221 and 236. The values for two measures of goodness-of-fit, RMSE and R^2_{adj} indicate that models were generally a good fit to data (Table 206). Nevertheless, the Weibull model fit to data for strain 12745 (ST-257, CC-257) was a poor fit in comparison to models generated for other strains (RMSE = 0.618, R^2_{adj} = 0.869) (Table 206). Visual examination of the corresponding predicted response curve illustrates that experimental heterogeneity in the recovery of cells at 6.00 - 8.00 minutes as a potential cause for lack of fit (Figure 240).

The goodness-of-fit of models for simulations undertaken at 60°C (Table 221) were comparable to those fit to data for simulations undertaken at 56°C (Table 206). The Weibull model fit to strain 12628 (ST-1773, CC-828) performed poorly in comparison to models generated for other strains (RMSE = 0.701, R^2_{adj} = 0.895) (Table 226). Similarly, visual examination of the predicted response curve illustrates that experimental heterogeneity in the recovery of cells between 6.00 - 7.00 minutes as the potential cause for lack of fit (Figure 250).

The goodness-of-fit of models generated for time-temperature simulations undertaken at 64°C (Table 236) is more varied than time-temperature simulations at 56°C and 60°C (Tables 206 and 221). An RMSE = 0.399 was observed for strain 11253 (ST-825, CC-828) indicating a good fit to the data, whereas the highest value was recorded for strain 12783 (ST-574, CC-574) suggested that the model was a poor fit to data. Visual examination of the predicted response curve indicates that experimental heterogeneity in recovery of cells between 2.00 – 6.00 minutes as a potential origin lack of fit.

2.3.1.2 Predicted Response Curves:

For simulations undertaken at 56°C models that incorporated a shoulder and/or tailing effect or those capable of fitting combined concave response curves were used to generate predictive models. However, strain 13121 (ST-45, CC-45) exhibited a concave response curve thus a biphasic model was used to generate the predictive model (Table 217, Figure 242). For time-temperature simulations undertaken at 60°C, biphasic and log-linear first-order kinetics models incorporating asymptotic functions, the Weibull model also incorporating an asymptotic function, and the mixed Weibull distribution model were used to generate predicted response curves (Tables 222 – 235).

Models generated for time-temperature simulations undertaken at 64°C were fit using expanded log-linear first-order kinetic models incorporating an asymptotic function (Type III) and biphasic models (Type VIII). Where the response of strains exhibited long tails, then log-linear models with an asymptotic function were used; for example, strain 11368 (ST-574, CC-574) (Table

238, Figure 247). Biphasic models were used to describe the underlying response of strains where survival trended towards zero. For instance, strain 11253 (ST-825, CC-828) (Table 237, Figure 246). By contrast, convex response curves or curves that integrated a shoulder-effect were not considered during the model building process.

Comparing the response of strains across different time-temperature Simulations suggests changes in the ability of a strain to resist stress. For example, the mixed Weibull distribution model was used to generate predicted response curves for strain 13126 (ST-45, CC-45) for simulations undertaken at 56°C and 60°C (Figure 243 and 257). In each instance, the resistance of the strain to heating is characterised by the convex curve fitted by mixed Weibull distribution model.

2.3.1.3 Assessment of Decimal Reduction:

The effects of heating on the survival of strains are illustrated by comparing the time to first decimal reduction (D-value). For example, for simulations undertaken at 56°C, the minimum D-value was recorded for strain 13121 (ST-45, CC-45) (D = 1.069 minutes) whereas the maximum value was observed for strain 12645 (ST-51, CC-443) (D = 3.708 minutes) (Table 206). Simulations describing the survival of strains at 60°C estimate that strain 13121 (ST-45, CC-45) to be the least resistant to stress (D = 0.475 minutes) whereas strains 11368 (ST-574, CC-574) (D = 1.476) and 13163 (ST-21, CC-21) (D = 1.393) and 11253 (ST-825, CC-828) (D = 1.382) exhibit greater resistance to biophysical stress (Table 218). By contrast, for simulations undertaken at 64°C the maximum estimated D-values was observed for strain 12628 (ST-1773, CC-828) D = 0.600 minutes. The minimum D-value was recorded for strain 12745 (ST-257, CC-257) D = 0.119 minutes. Findings suggest that strain 12628 (ST-1773, CC-828) may be more resistant to heating than other strains.

The range of D-values for each temperature simulation is shown in Figure 238. The estimated mean D-value for all strains following heating at 56°C is D = 2.388 minutes (Intercept). The estimated D-value for time-temperature simulations undertaken at 60°C was significantly lower than the estimate for simulations at 56°C (t-value = -4.960, P-value = 0.000). Similarly, there was a significant reduction in D-value for simulations undertaken at 64°C (t-value = 8.228, P-value = 0.000). The D-values for heating undertaken at 60°C and 64°C are calculated, in this instance, by subtracting the model estimated value generated for each temperature simulation from the intercept value at 56°C. For instance, at 60°C the D-value is D = 1.044 minutes. Correspondingly, for simulations following heating at 64°C, the D-value is D = 0.265 minutes.

Table 203. Results illustrating the comparison in time to first decimal reduction (D-value) following time-temperature simulations undertaken at 56°C, 60°C and 64°C ($R^2 = 0.913$).

	Estimate	Standard Error	t-value	P-value
(Intercept)	2.388	0.257	9.311	0.000
Temperature 60°C	-1.344	0.271	-4.960	0.000
Temperature 64°C	-2.123	0.258	-8.228	0.000

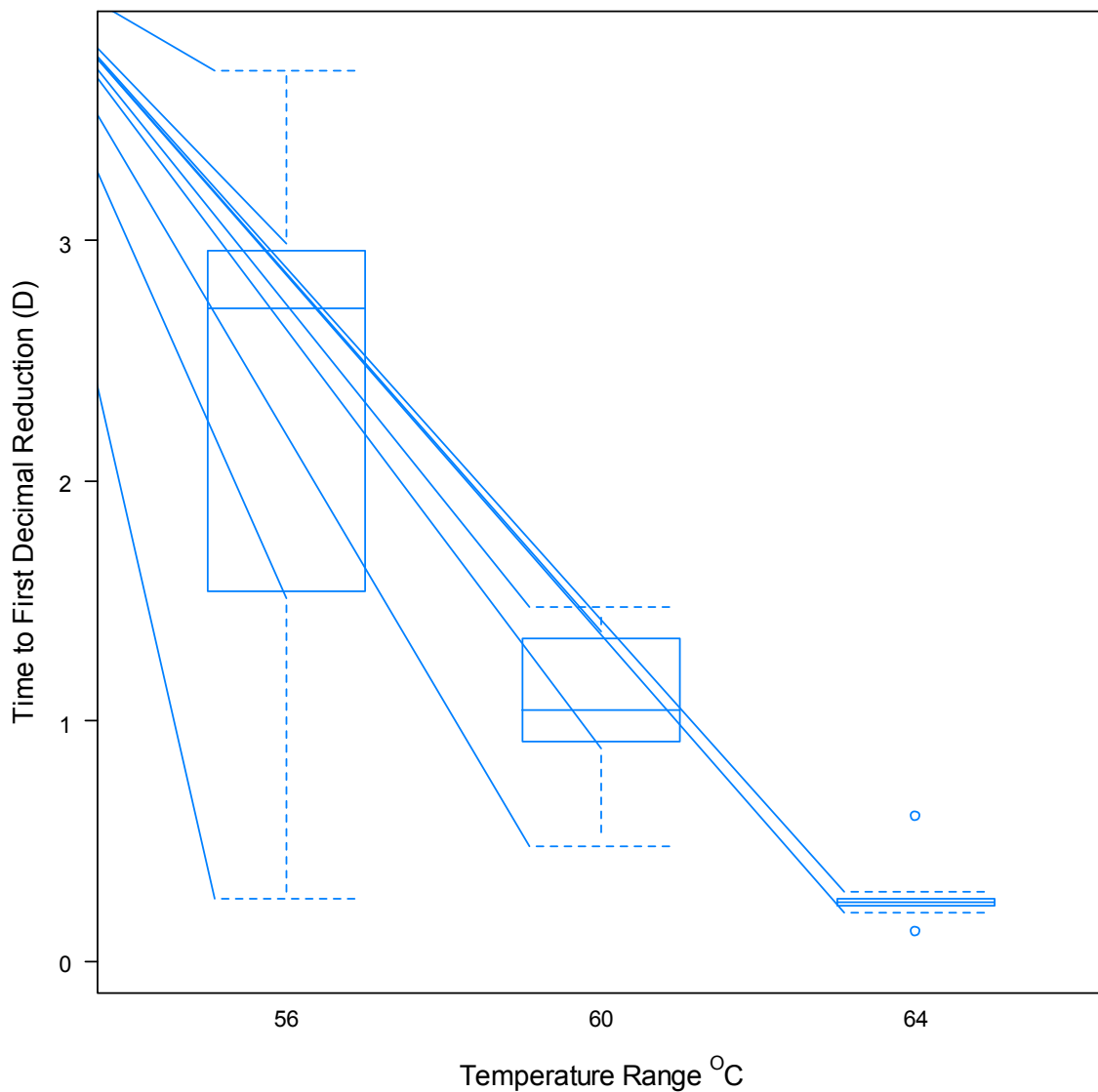


Figure 228. Summary box-plot illustrating the time to first decimal reduction following time-temperature simulations undertaken at 56°C, 60°C and 64°C.

2.3.2 pH and Time-temperature Simulations:

A summary of individual model fit is provided for each combined pH and time-temperature simulation (Tables 251, 272 and 292). Parameter estimates generated by predictive models for combined pH and time-temperature simulations undertaken at 56°C are shown in tables 252 – 271. Predicted response curves for corresponding models are shown in figures 274 – 293. The parameter estimates relating to predictive models for experimental simulations undertaken at 60°C are shown in tables 273 – 291 and predicted response curves for associated models are provide figures 294 – 312. Parameter estimates of models generated for simulations undertaken at 64°C are shown in tables 293 – 312 and predicted response curves for associated models are shown in figures 313 – 332.

2.3.2.1 Assessment of Model Fit:

An assessment of measures of goodness-of-fit indicates that the fit of models to data was depended on the combination of pH and temperature (Table 251, 272 and 292). Overall, goodness-of-fit indices indicate that models performed well when fit to data for simulations undertaken at pH 5.5 and pH 6.5. For example, strain 12662 (ST-257, CC-257) for simulations undertaken at pH 5.5 (RMSE = 0.265, $R^2_{adj.} = 0.963$) and pH 6.5 (RMSE = 0.228, $R^2_{adj.} = 0.969$) and strain 13136 (ST-45, CC-45) for simulations undertaken at pH 5.5 (RMSE = 0.203, $R^2_{adj.} = 0.987$) and pH 6.5 (RMSE = 0.251, $R^2_{adj.} = 0.973$) (Table 248). By contrast, goodness-of-fit was comparatively poor for strain 12628 (ST-1773, CC-828) for simulations undertaken at pH 5.5 (RMSE = 0.708, $R^2_{adj.} = 0.905$), strain 12662 (ST-257, CC-257) for simulations at pH 4.5 (RMSE = 0.627, $R^2_{adj.} = 0.901$) and strain 13136 (ST-45, CC-45) for simulations undertaken at pH 5.5 (RMSE = 0.723, $R^2_{adj.} = 0.870$). In each instance, experimental heterogeneity during the recovery of cells in the later observation periods may be the cause for a relative decrease model performance (Figure 262 and 266, respectively).

The goodness-of-fit of models fit to data following combined pH and time-temperature simulations undertaken at 60°C was similar irrespective of strain and the magnitude of biochemical challenge (Table 272). Overall, the degree of heterogeneity encountered during the recovery of cells was consistent between strains and reflected in marginally elevated values of RMSE (Table 269) when compared to goodness of fit for models generated for simulations undertaken 56°C (Table 248). Moreover, it was not possible to generate a model for strain 12628 (ST-1773, CC-828) at pH 4.5 due to high degree of heterogeneity during the recovery process.

The goodness-of-fit of models for combined pH and time-temperature simulations undertaken at 64°C were variable in response to increased heterogeneity during the recovery of cells (Table 292). The goodness-of-fit of models for strain 13136 (ST-45, CC-45) for simulations at pH 6.5

(RMSE = 0.365, $R^2_{adj} = 0.964$) and pH 7.5 (RMSE = 0.379, $R^2_{adj} = 0.963$) was adequate. In contrast, goodness-of-fit was comparatively poor for strain 12628 (ST-1773, CC-828) at pH 5.5 (RMSE = 0.613, $R^2_{adj} = 0.915$), and strain 13136 (ST-45, CC-45) at pH 4.5 (RMSE = 0.675, $R^2_{adj} = 0.900$) (Table 289). Visual examination of predicted response curves for each strain indicates that experimental heterogeneity is probable cause for a decrease in model fit (Figure 294 and 308 respectively).

2.3.2.2 Predicted Response Curves:

Strains demonstrated similar survival curves in response to combined pH and time-temperature simulations at 56°C. At pH 4.5 the biphasic model was used to generate predicted response curves for strains 12628 (ST-1773, CC-828) (Figure 274), 12662 (ST-257, CC-257) (Figure 279), 13126 (ST-21, CC-21) (Figure 284) and 13136 (ST-45, CC-45) (Figure 289). The use of first order kinetic models to generate response curves for simulations at pH 4.5 may indicate susceptibility of *Campylobacter* to acidic stress.

Survival curves for simulations undertaken at pH 5.5 – pH 8.5 demonstrated a high degree of similarity between strains. In all but one instance, variations of the Weibull model were used to generate predicted response curves. The mixed Weibull distribution model was used to describe the response of strain 12628 (ST-1773, CC-828) for pH 5.5 – pH 8.5 (Figures 275 – 278). The Weibull model incorporating an asymptotic function was used to generate the predicted response curve for strain 12662 (ST-257, CC-257) at pH 5.5 (Figure 280), the Weibull model was used at pH 6.5 (Figure 281). The Weibull model and asymptotic function was used again to generate a predicted response curve for simulations at pH 7.5 (Figure 282) and the mixed Weibull distribution model was used to generate a predicted response curve at pH 8.5 (Figure 283). The class of Weibull of models was also used for strain 13126 (ST-21, CC-21) where the Weibull with asymptotic function was fit to data for simulations at pH 5.5 (Figure 285). The mixed Weibull distribution model was used to generate predicted response curves for simulations undertaken at pH 6.5 (Figure 286) and pH 7.5 (Figure 287). By contrast, the underlying response at pH 8.5 differed from other strain insofar as a biphasic model and shoulder effect was used to generate a predicted response curve (Figure 288). Survival curves for strain 13136 (ST-45, CC-45) were similar to previous strains insofar as the Weibull class of models was again used to generate predicted response curves for simulations undertaken at pH 5.5 – 8.5. A Weibull model incorporating an asymptotic function was used to describe the underlying response at pH 5.5 (Figure 290), whereas the mixed Weibull distribution model was used to generate predicted response curves for simulations pH 6.5 (Figure 291), pH 7.5 (Figure 292) and pH 8.5 (Figure 293).

Survival curves for combined pH and time-temperature simulations undertaken at 60°C followed a pattern in use similar to those described above insofar as biphasic and log-linear first-order kinetic models were used to describe the response of some strains to extreme acid stress (pH 4.5 and pH 8.5) whereas variants of the Weibull class of models were predominately used to generate predicted response curves for simulations undertaken at pH 5.5, pH 6.5, pH 7.5.

The mixed Weibull distribution model was used to generate predicted response curves for strain 12628 (ST-1773, CC828) at pH 5.5 (Figure 294), pH 6.5 (Figure 293) and pH 7.5 (Figure 296). The biphasic model was used for simulations at pH 8.5 (Figure 297). Similarly, the biphasic model was used to generate predicted response curves for strain 12662 (ST-257, CC-257) for simulations undertaken at pH 4.5 (Figure 298) and pH 8.5 (Figure 302). The mixed Weibull distribution model was used to describe the underlying response at pH 5.5 (Figure 299) and pH 6.5 (Figure 300). The log-linear model incorporating an asymptotic function was used to generate a predicted response curve for simulations undertaken at pH 7.5 (Figure 307). The mixed Weibull distribution model was the only model used to generate predicted response curves for strain 13126 (ST-21, CC-21) across the entire spectrum of pH simulations undertaken at 60°C (Figures 303– 307). Variants of the Weibull class of models were used to generate predicted response curves for strain 13136 (ST-45, CC-45) for combined pH and temperature simulations undertaken at 60°C. The Weibull model was used to generate predicted response curve for pH 4.5 (Figure 308) and pH 8.5 (Figure 312) and the mixed Weibull distribution model generated predicted response curves for simulations at pH 5.5 (Figure 309), pH 6.5 (Figure 310) and pH 7.5 (Figure 311).

Predictive models used to describe survival curves of *Campylobacter* in response to combined pH and time-temperature simulations undertaken at 64°C varied according to strain and biochemical challenge. A Weibull model was used to describe the concave survival curve of strain 12628 (ST-1773, CC-828) at pH 4.5 (Figure 313). The biphasic model was then used to describe the response of strain 12628 (ST-1773, CC-828) for simulations undertaken at pH 5.5 (Figures 314), pH 7.5 (Figure 316) and pH 8.5 (Figure 317). The biphasic model incorporating a shoulder-effect was used to generate a predictive model for simulation at pH 6.5 (Figure 315). The biphasic first-order kinetics model was used to generate predicted response curves for strain 12662 (ST-257, CC-257) following simulations undertaken at pH 4.5 and pH 8.5 (Figures 318 and 322). By contrast, the mixed Weibull distribution model was used to describe the underlying response for simulations undertaken at pH 5.5, pH 6.5 and pH 7.5 (Figure 319 – 321). Similarly, the biphasic model was used to describe the response curves for strain 13126 (ST-21, CC-21) following simulations undertaken at pH 4.5 and pH 5.5 (Figures 323 – 324). The log-linear model incorporating an asymptotic function was used to generate predicted response curve for pH 6.5 (Figure 325). The mixed Weibull distribution model

was used to generate predicted response curves for simulations at pH 7.5 and pH 8.5 (Figures 326 – 327). The survival curves for strain 13136 (ST-45, CC-45) were modelled using the Weibull model incorporating an asymptotic function for pH 4.5, pH 5.5 and pH 6.5 (Figure 328 - 330), whereas the mixed Weibull distribution model was used to generate predicted response curves for simulations at pH 7.5 (Figure 331) and pH 8.5 (Figure 332).

2.3.2.3 Assessment of Decimal Reduction:

The combined effects of biochemical and biophysical challenge on the survival of strains can be demonstrated by comparing the time to first decimal reduction (D-value). In general, higher D-values were estimated for all strains for simulations undertaken at pH 5.5, pH 6.5 and pH 7.5 irrespective of temperature (Tables 251, 272 and 292). By contrast, D-values for simulations undertaken at pH 4.5 and pH 8.5 were comparatively lower. In general, higher D-values suggest an enhanced capability to resist combined biochemical and biophysical stress. Highest D-values were often observed for simulations undertaken at pH 5.5 and pH 6.5 (Tables 251, 272 and 292) which may suggest optimal acidic conditions for resistance to stress. For example, for combined pH and time-temperature simulations undertaken at 56°C, the recorded D-value for strain 12662 (ST-257, CC-257) at pH 5.5 was D = 5.624 minutes, and at pH 6.5 D = 5.492 minutes (Table 251). Similarly, combined simulations undertaken at 60°C, the recorded D-values at pH 5.5 (D = 1.769 minutes), pH 6.5 (D = 1.494 minutes) (Table 272). By contrast, estimated D-values for combined simulations undertaken at 64°C were comparatively lower than those recorded at lower temperatures. Nevertheless, a similar pattern was observed whereby higher D-values were recorded at pH 5.5 (D = 0.950 minutes) and pH 6.5 (D = 0.757 minutes) (Table 292).

Analyses of D-values for combined pH and time-temperature simulations were undertaken using Generalized Least Squares modelling approach (Table 204). Results provided confirmation of the patterns of enhanced resistance observed within individual strains. For instance, the estimated D-value for pH 4.5 at 56°C (Intercept) (D = 0.495) is significantly different from zero (t-value = 4.476, P-value = 0.001). Estimate of D-value for pH 5.5 is significantly greater than pH 4.5 (t-value = 5.909, P-value = 0.000). This is also the case for pH 6.5 (t-value = 6.373, P-value = 0.000), pH 7.5 (t-value = 7.007, P-value = 0.000) and pH 8.5 (t-value = 5.467, P-value = 0.000). The maximum D-value estimated at 56°C was generated for pH 5.5 indicating higher degree of resistance to biochemical stress (D-value = 4.531). D-values then declined as pH trended towards base values. For instance, at pH 6.5 D-value was estimated to be D = 4.089, at pH 7.5 the D-value decreased to D = 2.878 and at pH 8.5 the D-value was estimated at D = 1.694. While D-values after pH 5.5 declined towards base

values, there were nevertheless significantly higher than the estimate obtained for pH 4.5 (Table 204, Figure 229).

The estimated D-value for combined simulations undertaken pH 4.5 and 60°C was not statistically different from the corresponding estimate generated for pH 4.5 at 56°C (t-value -1.393, P-value = 0.171) (Table 204). By contrast, estimated D-values for remaining combined pH simulations undertaken at 60°C are significantly lower than corresponding estimates for simulations undertaken at 56°C for pH 5.5 (t-value -4.227, P-value = 0.0001) pH 6.5 (t-value -4.660, P-value = 0.000), pH 7.5 (t-value -4.364, P-value = 0.0001) and pH 8.5 (t-value -4.087, P-value = 0.0002) (Table 204). Similarly, estimated D-values generated for simulations at 60°C reach an optimum at pH 5.5 and then decrease subsequently (Table 204, Figure 229). At pH 4.5 the estimated D-value was $D = 0.272$, D-values subsequently increased as pH increased towards base values: at pH 5.5 ($D = 1.492$), pH 6.5 ($D = 1.323$), pH 7.5 ($D = 1.164$) and pH 8.5 ($D = 0.558$).

The estimated D-value for combined simulations undertaken pH 4.5 and 64°C was statistically different from pH 4.5 at 56°C (t-value -2.975, P-value = 0.005) (Table 204). Estimated D-values for remaining combined pH simulations undertaken at 64°C also significantly lower than corresponding estimates for simulations undertaken at 56°C for pH 5.5 (t-value -4.9642, P-value = 0.000) pH 6.5 (t-value -5.312, P-value = 0.000), pH 7.5 (t-value -5.701, P-value = 0.000) and pH 8.5 (t-value -4.092, P-value = 0.000) (Table 204). Similarly, estimated D-values generated for simulations at 64°C reach an optimum at pH 5.5 and then decrease slightly (Table 204, Figure 229). At pH 4.5 the estimated D-value was $D = 0.068$, D-values subsequently increased as pH increased towards base values: at pH 5.5 ($D = 1.061$), pH 6.5 ($D = 0.959$), pH 7.5 ($D = 0.747$) and pH 8.5 ($D = 0.643$).

Table 204. Results illustrating the comparison in time to first decimal reduction (D-value) following interaction between pH and time-temperature simulations undertaken at 56°C, 60°C and 64°C ($R^2 = 0.963$).

	Estimate	Standard Error	t-value	P-value
(Intercept)	0.495	0.111	4.476	0.000
pH 5.5	4.036	0.683	5.909	0.000
pH 6.5	3.594	0.564	6.373	0.000
pH 7.5	2.383	0.340	7.007	0.000
pH 8.5	1.198	0.219	5.467	0.000
60°C	-0.223	0.160	-1.393	0.171
64°C	-0.427	0.144	-2.975	0.005
pH 5.5 : 60°C	-3.004	0.711	-4.227	0.000
pH 6.5 : 60°C	-2.767	0.594	-4.660	0.000
pH 7.5 : 60°C	-1.678	0.385	-4.364	0.000
pH 8.5 : 60°C	-1.099	0.269	-4.087	0.000
pH 5.5 : 64°C	-3.471	0.699	-4.964	0.000
pH 6.5 : 64°C	-3.095	0.583	-5.311	0.000
pH 7.5 : 64°C	-2.096	0.367	-5.708	0.000
pH 8.5 : 64°C	-1.051	0.257	-4.092	0.000

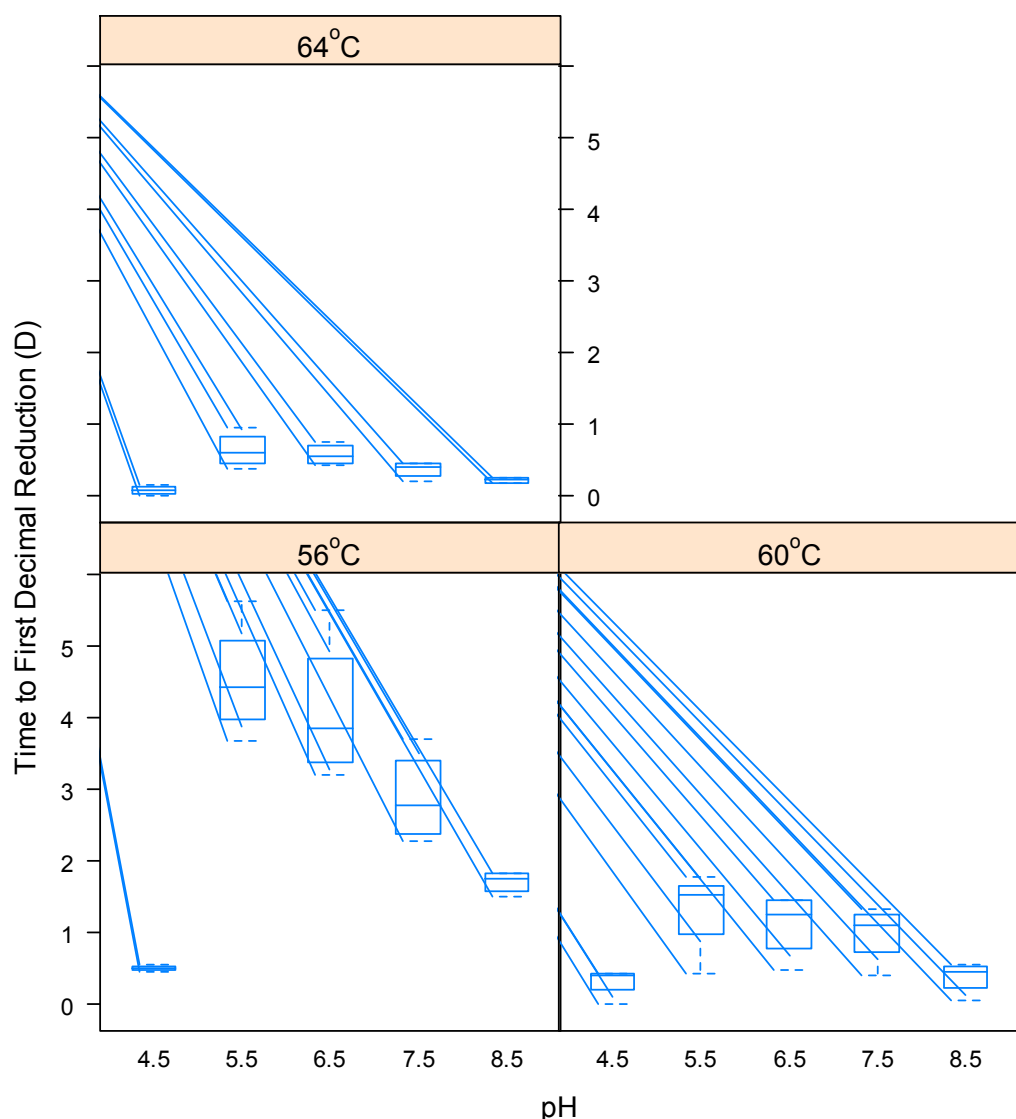


Figure 229. Summary box-plot illustrating the time to first decimal reduction following combined pH and time-temperature simulations undertaken at 56°C, 60°C and 64°C.

2.3.3 Exterior Food-matrices Time-temperature Simulations

A summary of individual model fit is provided for combined gradual and direct heating, time-temperature simulations (Tables 313, 320, 327, 336, 345, 352 and 359). Parameter estimates generated by predictive models for gradual heating of food-matrices at 56°C and 70°C are shown in Tables 313 and 320. The parameter estimates generated by predictive models for direct heating of food-matrices are also provided for simulations undertaken at 56°C (Table 327), at 60°C (Table 336) at 64°C (Table 345), at 68°C (Table 352) and 70°C (Table 359).

Predicted response curves are provided for combined gradual heating and time-temperature simulations undertaken at 56°C (Figure 333 – 338) and 70°C (Figures 339 – 344), and also for direct heating simulations undertaken at 56°C (Figure 345 – 352), 60°C (Figure 353 – 360), 64°C (Figure 361 – 366), 68°C (Figure 367 – 372) and 70°C (Figures 373 – 379).

2.3.3.1 Assessment of Model Fit

An assessment of goodness-of-fit indices suggests that the fit of models to the data was largely dependent and the temperature used during simulations. In addition, there was insufficient data to determine if model fit was affected by pre-chilling of food-matrices prior to heating.

During gradual heating at 56°C (Table 313) the lowest recorded value of goodness-of-fit was observed for strain 13136 (ST-45, CC-45) RMSE = 0.326 and $R^2_{adj.} = 0.856$, indicating an adequate fit to the model. By contrast, the highest recorded value of goodness-of-fit was observed for strain 13126 (ST-21, CC-21) RMSE = 0.515 and $R^2_{adj.} = 0.865$. There was a marked decrease in goodness-of-fit of models for gradual heating simulations undertaken at 70°C. For instance, the lowest recorded value for goodness-of-fit was observed for strain 12662 (ST-257, CC-257) RMSE = 0.495 and $R^2_{adj.} = 0.867$. The highest recorded value was observed for strain 13126 (ST-21, CC-21) RMSE = 0.857 and $R^2_{adj.} = 0.702$ (Table 320). Goodness-of-fit improved notably for all strains during direct heating and temperature simulations. For simulations undertaken at 56°C, RMSE = 0.279 and $R^2_{adj.} = 0.809$ was recorded for strain 12662 (ST-257, CC-257). However, model fit was comparatively poor for strain 13126 (ST-21, CC-21) RMSE = 0.765 and $R^2_{adj.} = 0.666$ (Table 327). Similarly, goodness-of-fit indices for direct heating simulations undertaken at 60°C demonstrates good model fit to strain 13136 (ST-45, CC-45) RMSE = 0.293 and $R^2_{adj.} = 0.878$. By contrast, the goodness-of-fit of the model to strain 13126 (ST-21, CC-21) was comparatively poor RMSE = 0.572 and $R^2_{adj.} = 0.742$ (Table 336). For direct heating simulations undertaken at 68°C, RMSE = 0.231 and $R^2_{adj.} = 0.956$ indicated a good fit of the model to strain 12662 (ST-257, CC-257) (Table 352). The goodness-of-fit of models generated for direct heating simulations undertaken at 70°C demonstrated a pattern similar to models developed for gradual heating simulations at 70°C, insofar as model fit was inferior when compared to simulations at lower temperatures. Goodness-of-fit for strain 12662 (ST-257, CC-257) was adequate, RMSE = 0.315 and $R^2_{adj.} = 0.921$. However, the model fit to strain 12628 (ST-1773, CC-828) was comparatively poor, RMSE = 0.762 and $R^2_{adj.} = 0.731$ (Table 359). Visual examination of the predicted response curves for models that demonstrated an inadequate fit suggests that heterogeneity in the recovery of cells may adversely affect model fit. For example, the predicted response curve generated for strain 13126 (ST-21, CC-21) following gradual heating at 70°C demonstrates heterogeneity in observations between 12:00 – 22:00 minutes (Figure 343).

2.3.3.2 Predicted Response Curves

For gradual heating simulations undertaken at 56°C, strains demonstrated similar survival concave curves with evidence of a tailing-effect at later observation points. The mixed Weibull distribution model was used to generate a predicted response curve for strain 12662 (ST-257, CC-257) (Figure 333), whereas food-matrices that were pre-chilled and then inoculated with an identical strain used a Weibull model incorporating an asymptotic function to generate the predicted response curve (Figure 334). The mixed Weibull model was also used to generate a predicted response curve for strain 13126 (ST-21, CC-21) (Figure 335). By contrast, the first-order kinetic log-linear model incorporating a combined shoulder and tailing effect was used to generate a predicted response curve for pre-chilled food matrices inoculated with the same strain (Figure 336). A mixed Weibull distribution model was used to generate predicted response curves for both un-chilled and pre-chilled food-matrices inoculated with strain 13136 (ST-45, CC-45) (Figures 337 – 338).

For gradual heating simulations undertaken at 70°C, the mixed Weibull distribution model was used to describe survival curves for un-chilled food-matrices inoculated with strains 12628 (ST-1773, CC-828) (Figure 339), 13126 (ST-21, CC-21) (Figure 343) and 13136 (ST-45, CC-45) (Figure 344). The Weibull model incorporating an asymptotic function to account for tailing effect was used to describe the response of pre-chilled food-matrices inoculated with strain 12628 (ST-1773, CC-828) (Figure 340) and strain 12662 (ST-257, CC-257) (Figure 342). By contrast, the predicted response curve for un-chilled food-matrices inoculated with strain 12662 (ST-257, CC-257) was generated using a Weibull model. However, the overall fit of this model is subject to heterogeneity at during later stages of observation and predictions may therefore be unreliable (Figure 340).

For direct heating simulations undertaken at 56°C, the Weibull model was used to assess the survival curves for un-chilled food-matrices inoculated with strain 13126 (ST-21, CC-21) (Figure 349), whereas the mixed Weibull distribution model was used to generate predictive response curves for un-chilled and pre-chilled food-matrices for strain 13136 (ST-45, CC-45) (Figures 351 – 352). By contrast, the first order log-linear model incorporating an asymptotic function was used to generate the predicted response curves for un-chilled and pre-chilled food-matrices inoculated with strains 12628 (ST-1773 CC-828) (Figures 345 – 346) and 12662 (ST-257, CC-257) (Figures 347 – 348). In addition, the log-linear model was also used to generate predicted response curve for pre-chilled food-matrices inoculated with strain 13126 (ST-21, CC-21) (Figure 348).

Predictive models generated for strains following simulations undertaken at 60°C demonstrated similar responses to those described at 56°C. The log-linear model incorporating an asymptotic function was also used to describe the survival curves for pre-chilled food-matrices inoculated with strain 12628 (ST-1773, CC-828) (Figure 354) and for un-chilled matrices inoculated

with strain 13126 (ST-21, CC-21) (Figure 357). Biphasic first-order kinetics models incorporating an asymptotic function were used to generate predictive response curves for un-chilled food-matrices inoculated with strain 12662 (ST-257, CC-257) (Figure 355) and for strains 13126 (ST-21, CC-21) (Figure 358) and 13136 (ST-45, CC-45) (Figure 360) following inoculation of pre-chilled food-matrices. The Weibull model, also incorporating an asymptotic function generated a concave survival response curve strains 12628 (ST-1773, CC-828) (Figure 353) and 13136 (ST-45, CC-45) (Figure 359).

The underlying response demonstrated by strains following direct heating at 64°C was again similar to those described at 56°C and 60°C, insofar as strains demonstrated an initial susceptibility to increased temperature followed by a period of enhanced resistance demonstrated by the tailing effect. The biphasic model was used to describe the survival curve for strain 12662 (ST-257, CC-257) (Figure 361). The log-linear model was used to describe the survival curves for un-chilled food-matrices inoculated with strains 12662 (ST-257, CC-257) (Figure 362) and 13126 (ST-21, CC-21) (Figure 363) and the Weibull model, incorporating an asymptotic function was used to generate predicted response curve for the survival of strain 13126 (ST-21, CC-21) (Figure 364).

For direct heating simulations undertaken at 68°C, the Weibull model incorporating an asymptotic function was used to generate predicted response curve for un-chilled food-matrices inoculated with strain 12662 (ST-257, CC-257) (Figure 367) whereas the log-linear model was used to generate predicted response curve for pre-chilled matrices inoculated with an identical strain (Figure 366). The log-linear model was also used to generate predicted response curves for un-chilled and pre-chilled food matrices inoculated with strains 13126 (ST-21, CC-21) (Figures 369 – 370) and 13136 (ST-45, CC-45) (Figures 371 – 372).

Similarly, for direct heating simulations undertaken at 70°C the biphasic model and log-linear models incorporating asymptotic functions were used to describes survival curves produced by un-chilled and pre-chilled food matrices inoculated with strain 12628 (ST-1773, CC-828) (Figure 373 and 374). The Weibull model incorporating an asymptotic function was used to generate a predicted response curve for un-chilled food-matrices inoculated with strain 12662 (ST-257, CC-257) (Figure 375) and a first-order kinetic log-linear model was used to generate predicted response curve for pre-chilled food matrices inoculate with an identical strain (Figure 376).The log-linear model was also used to generate predicted response curves for un-chilled and pre-chilled food matrices inoculated with strain 13126 (ST-21, CC-21) (Figures 377 – 378). By contrast, the biphasic model and asymptotic function generated predicted response curves for un-chilled and pre-chilled food matrices inoculated with strain 13136 (ST-45, CC-45) (Figures 379 – 380).

2.3.3.3 Assessment of Decimal Reduction:

Direct heating simulations undertaken at 56°C (Intercept) at 60°C (t-value = -2.401, P-value = 0.023), 64°C (t-value = -3.944, P-value = 0.000), 68°C (t-value = -4.039, P-value = 0.000) and 70°C (t-value = -3.990, P-value = 0.000). By contrast, no statistically significant differences in time to first decimal reduction were found between pre-chilled or un-chilled treatments of food-matrices (Table 3, Figure 3). The estimated D-value for food-matrices exposed to heating at 56°C (Intercept) following pre-chilling was D = 0.957 minutes. The time to first decimal reduction declined as temperature increased to 60°C (D = 0.369), 64°C (D = 0.107), 68°C (D = 0.095), 70°C (D = 0.109). Estimated D-values for simulations that used pre-chilled food-matrices were similar- at 56°C (D = 0.940), 60°C (D = 0.353), 64°C (D = 0.090), 68°C (D = 0.079) and 70°C (D = 0.093).

Inferential statistics were not used to assess differences between pre-chilled and un-chilled food matrices due to insufficient sample size as there were only three observations per treatment and temperature group (total n = 12). Nevertheless, a box-plot is provided to summarize the distribution of D-value, findings are however, inconclusive (Figure 231).

Table 205. Results illustrating the comparison in time to first decimal reduction (D-value) following direct heating of food matrix simulations undertaken at 56°C, 60°C, 64°C, 68°C and 70°C ($R^2 = 0.937$).

	Estimate	Standard Error	t-value	P-value
(Intercept)	0.957	0.212	4.503	0.000
60°C	-0.588	0.245	-2.401	0.023
64°C	-0.850	0.216	-3.944	0.00
68°C	-0.861	0.213	-4.039	0.000
70°C	-0.848	0.213	-3.990	0.000
Un-chilled	-0.017	0.014	-1.171	0.251

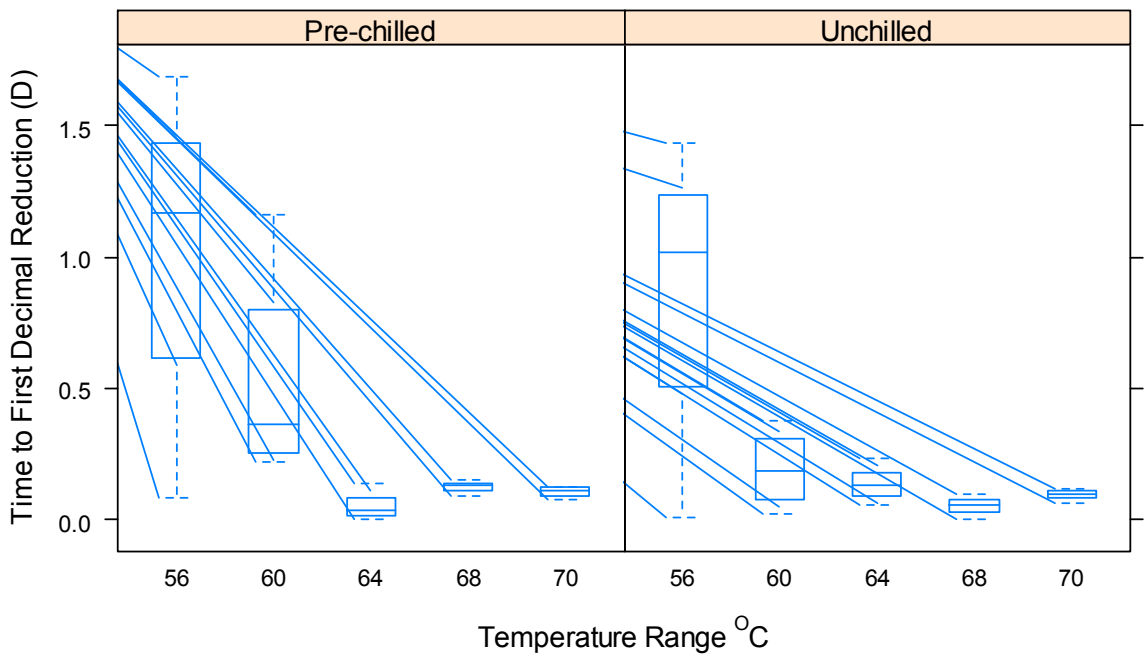


Figure 230. Summary box-plot illustrating the time to first decimal reduction following direct heating of food matrices at a range of temperatures.

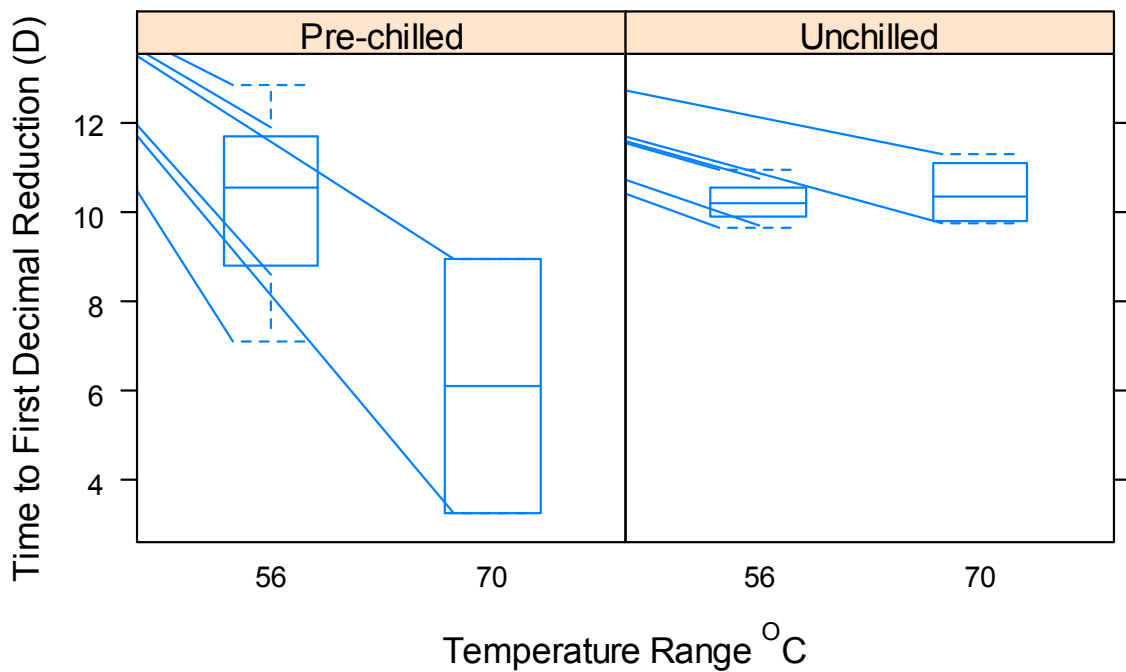


Figure 231. Summary box-plot illustrating the time to first decimal reduction following gradual heating of food matrices at 56°C and 70°C.

2.3.4 Interior Food-matrices Time-temperature Simulations

A summary of individual model fit is provided for combined gradual and direct heating, time-temperature simulations (Tables 368 and 375). Parameter estimates generated by predictive models for gradual heating of food-matrices at 64°C and 68°C (Tables 369 – 374) and direct heating of food-matrices interiors at 64°C and 68°C (Tables 376 – 382) are also provided.

Predicted response curves are provided for gradual heating for combined time-temperature simulations undertaken at 64°C and 68°C (Figures 381 – 386) and direct heating for combined time-temperature simulations undertaken at 64°C and 68°C (Figures 387 – 393).

2.3.4.1 Assessment of Model Fit

An assessment of goodness-of-fit indices suggests that the fit of models to the data was broadly consistent between gradual and direct heating simulations undertaken at each time-temperature profile. During gradual heating of interior tissues at 68°C, recorded values for goodness-of-fit was observed for strain 12662 (ST-257, CC-257) RMSE = 0.543 and $R^2_{adj.} = 0.885$, whereas during direct heating at 68°C, the highest recorded value of goodness-of-fit was observed for strain 12628 (ST-1773, CC-828) RMSE = 0.594 and $R^2_{adj.} = 0.846$, indicating a relatively poor fit of model to data. By contrast, the best performing models fit to data were observed for strain 12628 (ST-1773, CC-828) for gradual heating at 68°C (RMSE = 0.240, $R^2_{adj.} = 0.970$) and direct heating at 64°C (RMSE = 0.285, $R^2_{adj.} = 0.947$).

2.3.4.2 Predicted Response Curves

For gradual heating simulations undertaken at 64°C and 64°C, strains demonstrated similar convex survival curves. In all but one instance, the Weibull model incorporating an asymptotic function was used to generate predicted response curves for strains during gradual heating simulations (Figure 381 – 386). The log-linear model was used to describe the response of strain 13136 (ST-45, CC-45) (Figure 386). In some cases, with the exception of predicted response curve for strain 13136 (ST-45, CC-45) marginal evidence was found in support of a tailing-effect at later observation points.

In contrast, biphasic and log-linear first-order kinetics models incorporating asymptotic function were used to generate concave predictive response curves for strains in response to direct heating of tissue interiors at 64°C and 68°C. The response of strains to direct heating may be characterised by a decline in counts of cells of an initial subpopulation, before an elongated tailing effect indicative of increased resistance. These findings suggest that high counts of *Campylobacter* were able to survive for extended periods of time (between 10 and 20 minutes).

2.3.4.3 Assessment of Decimal Reduction:

The effects of gradual and direct heating on survival of strains within tissue interiors was evaluated by comparing the time to first decimal reduction (D-value). The estimated D-values for strains subjected to gradual heating varied between strains. Estimated values ranged from D = 4.420 minutes for strain 13136 (ST-45, CC-45) to D = 11.260 minutes for strain 12662 (ST-257, CC-257). Estimated time to first log reduction declined when heating was increased during simulation to 68°C. The estimated time to first log reduction varied between strains and ranged from D = 0.490 minutes for strain 12662 (ST-257, CC-257) to D = 5.280 minutes for strain 13136 (ST-45, CC-45). The evaluation of survival for strain 13136 (ST-45, CC-45) is particularly striking and indicates enhanced capability to survive within the interior of food at higher temperature. There was insufficient data with which to undertake a formal statistical comparison of time to first decimal reduction.

2.3.5 Time-temperature Simulations: 56°C

Table 206. Assessment of model fit for individual strains following heating at 56°C.

Strain	RMSE	$R^2_{adjusted}$	D-value
11253 (ST-825, CC-828)	0.348	0.972	2.599
11368 (ST-574, CC-574)	0.315	0.970	3.175
11762 (ST-829, CC-828)	0.263	0.981	2.942
12610 (ST-825, CC-828)	0.254	0.963	2.657
12628 (ST-1773, CC-828)	0.254	0.985	2.560
12645 (ST-51, CC-443)	0.288	0.976	3.708
12662 (ST-257, CC-257)	0.280	0.966	2.774
12720 (ST-51, CC-443)	0.242	0.982	3.235
12745 (ST-257, CC-257)	0.618	0.869	3.390
12783 (ST-574, CC-574)	0.315	0.969	2.960
13121 (ST-45, CC-45)	0.385	0.954	1.069
13126 (ST-21, CC-21)	0.292	0.978	2.463
13136 (ST-45, CC-45)	0.313	0.976	3.028
13163 (ST-21, CC-21)	0.228	0.983	2.907

Table 207. Mixed Weibull distribution model incorporating an asymptotic function for survival of strain 11253 (ST-825, CC-828) following heating at 56°C.

Parameters	Estimates	Standard Error
α	4.078	0.739
δ_1	2.599	0.374
ρ	1.758	0.320
N_0	8.225	0.198
δ_2	9.797	4.572

Table 208. Weibull model incorporating an asymptotic function for survival of strain 11368 (ST-574, CC-574) following heating at 56°C.

Parameters	Estimates	Standard Error
α	3.687	0.133
δ_1	3.175	0.402
ρ	1.867	0.336
N_0	7.997	0.170

Table 209. Mixed Weibull distribution model for survival of strain 11762 (ST-829, CC-828) following heating at 56°C.

Parameters	Estimates	Standard Error
α	3.832	0.283
δ_1	2.942	0.329
ρ	2.828	0.637
N_0	8.190	0.154
δ_2	11.323	2.336

Table 210. Mixed Weibull distribution model for survival of strain 12610 (ST-825, CC-828) following heating at 56°C.

Parameters	Estimates	Standard Error
α	3.971	0.673
δ_1	2.657	0.314
ρ	1.571	0.217
N_0	8.152	0.143
δ_2	13.258	9.922

Table 211. Log-linear model incorporation a shoulder effect and asymptotic function for survival of strain 12628 (ST-1773, CC-828) following heating at 56°C.

Parameters	Estimates	Standard Error
SI	1.521	0.213
K max	2.119	0.108
Nres	3.188	0.078
N_0	8.185	0.103

Table 212. Weibull model incorporating an asymptotic function for survival of strain 12645 (ST-51, CC-443) following heating at 56°C.

Parameters	Estimates	Standard Error
Nres	3.069	0.194
δ	3.708	0.393
ρ	1.787	0.232
N_0	7.985	0.147

Table 213. Weibull model for survival of strain 12662 (ST-257, CC-257) following heating at 56°C.

Parameters	Estimates	Standard Error
δ	2.774	0.414
ρ	1.121	0.120
<i>NO</i>	7.890	0.153

Table 214. Weibull model incorporating an asymptotic function for survival of strain 12720 (ST-51, CC-443) following heating at 56°C.

Parameters	Estimates	Standard Error
Nres	3.165	0.185
δ	3.235	0.335
ρ	1.543	0.166
<i>NO</i>	8.085	0.129

Table 215. Weibull model for survival of strain 12745 (ST-257, CC-257) following heating at 56°C.

Parameters	Estimates	Standard Error
δ	3.390	0.890
ρ	1.385	0.311
<i>NO</i>	7.890	0.323

Table 216. Weibull model incorporating an asymptotic function for survival of strain 12783 (ST-574, CC-574) following heating at 56°C.

Parameters	Estimates	Standard Error
Nres	3.382	0.166
δ	2.960	0.414
ρ	1.570	0.258
<i>NO</i>	7.799	0.172

Table 217. Biphasic model for survival of strain 13121 (ST-45, CC-45) following heating at 56°C.

Parameters	Estimates	Standard Error
F	0.998	0.002
Kmax1	2.162	0.226
Kmax2	0.520	0.119
<i>NO</i>	7.966	0.153

Table 218. Mixed Weibull distribution model for survival of strain 13126 (ST-21, CC-21) following heating at 56°C.

Parameters	Estimates	Standard Error
α	3.623	0.513
δ_1	2.463	0.335
ρ	1.682	0.335
N_0	8.047	0.170
δ_2	8.684	2.398

Table 219. Mixed Weibull distribution model for survival of strain 13136 (ST-45, CC-45) following heating at 56°C.

Parameters	Estimates	Standard Error
α	3.923	1.259
δ_1	3.028	0.440
ρ	1.685	0.331
N_0	8.138	0.179
δ_2	9.015	5.747

Table 220. Weibull model incorporating an asymptotic function for survival of strain 13163 (ST-21, CC-21) following heating at 56°C.

Parameters	Estimates	Standard Error
N_{res}	3.412	0.142
δ	2.907	0.300
ρ	1.443	0.148
N_0	8.006	0.124

2.3.6 Time-temperature Profile 56°C

Predicted Response Curves:

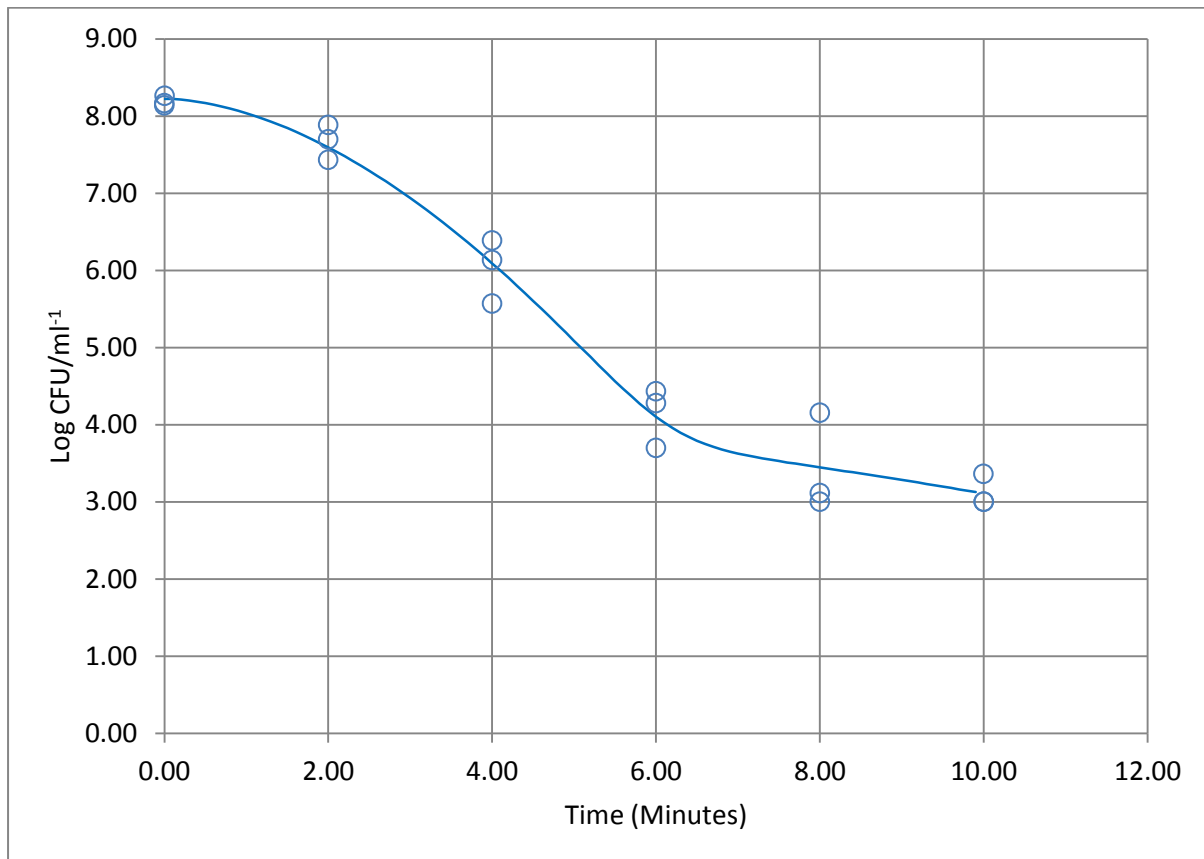


Figure 232. Plot illustrating predicted response curve using a mixed Weibull distribution model for strain 11253 (ST-825, CC-828) following heating at 56°C.

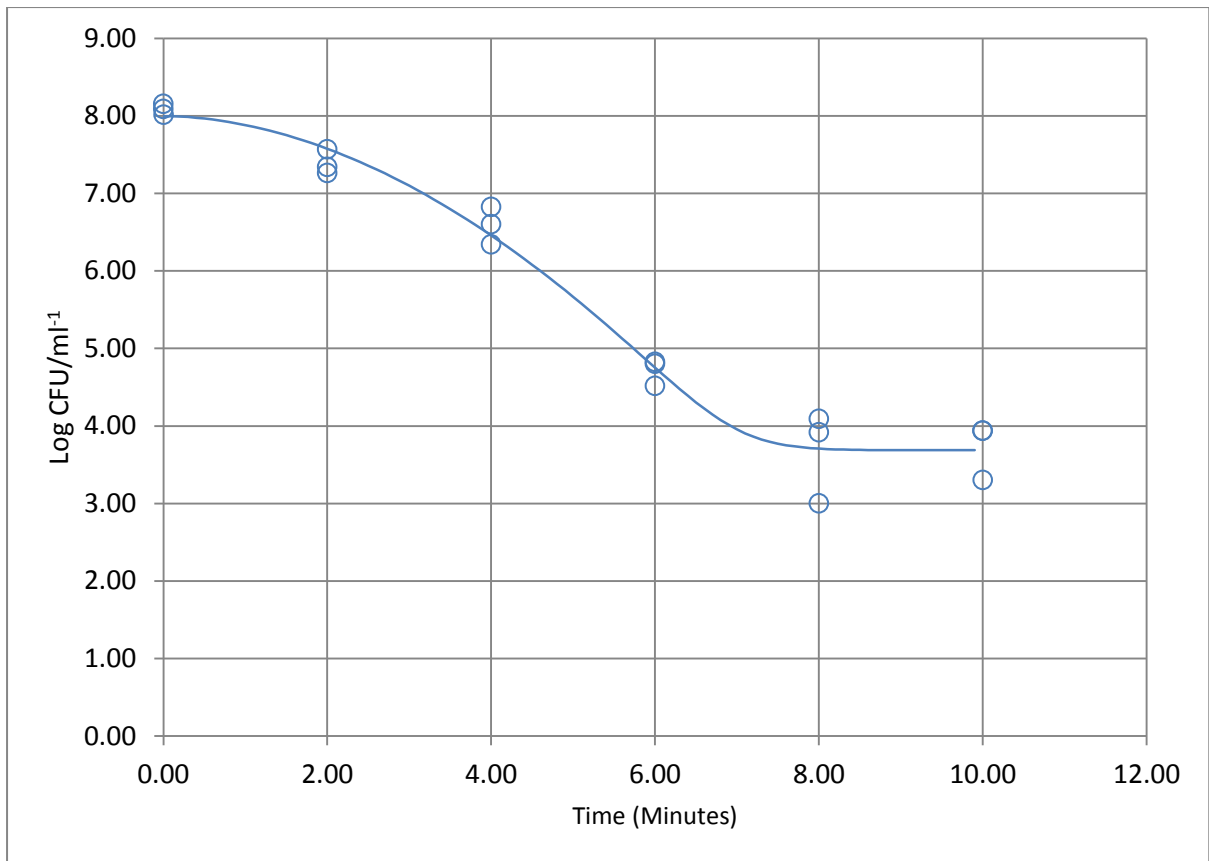


Figure 233. Plot illustrating predicted response curve using a Weibull model incorporating an asymptotic function for strain 11368 (ST-574, CC-574) following heating at 56°C.

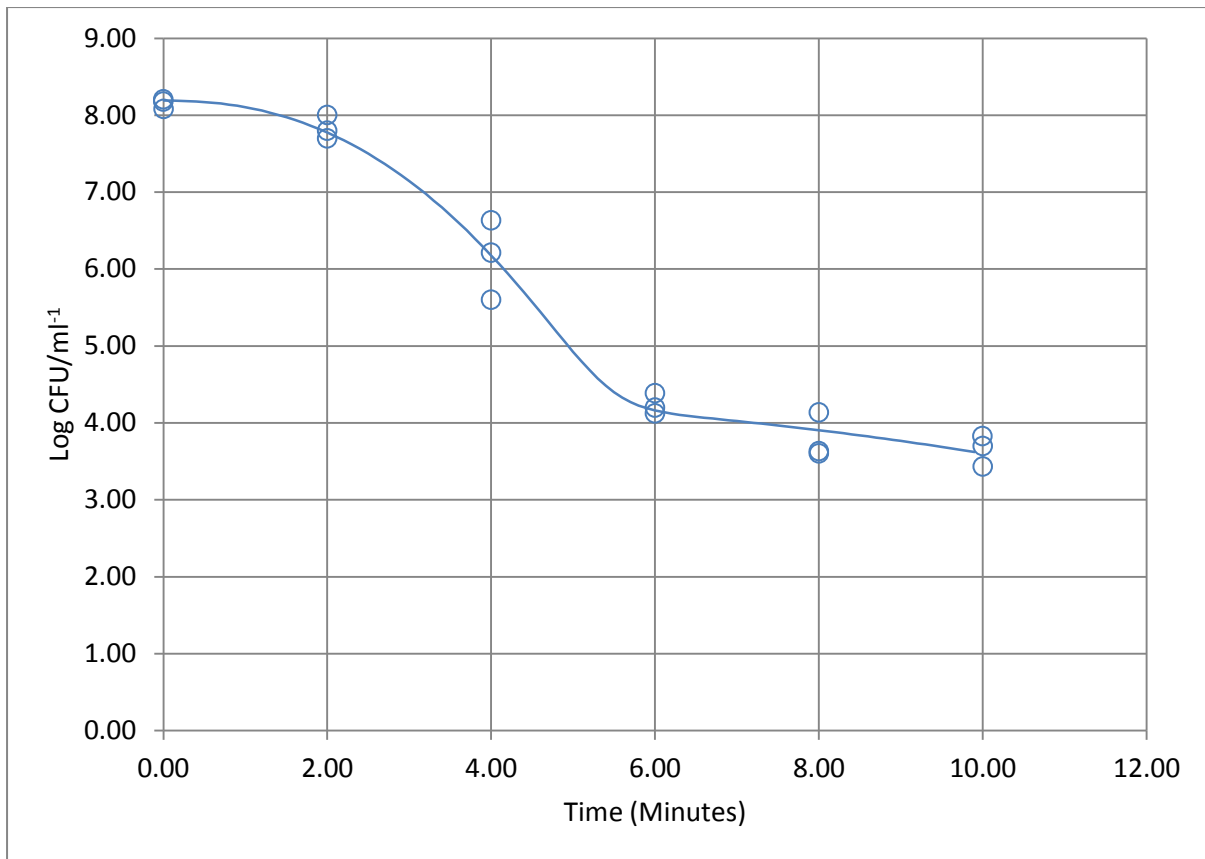


Figure 234. Plot illustrating predicted response curve using a mixed Weibull distribution model for strain 11762 (ST-829, CC-828) following heating at 56°C.

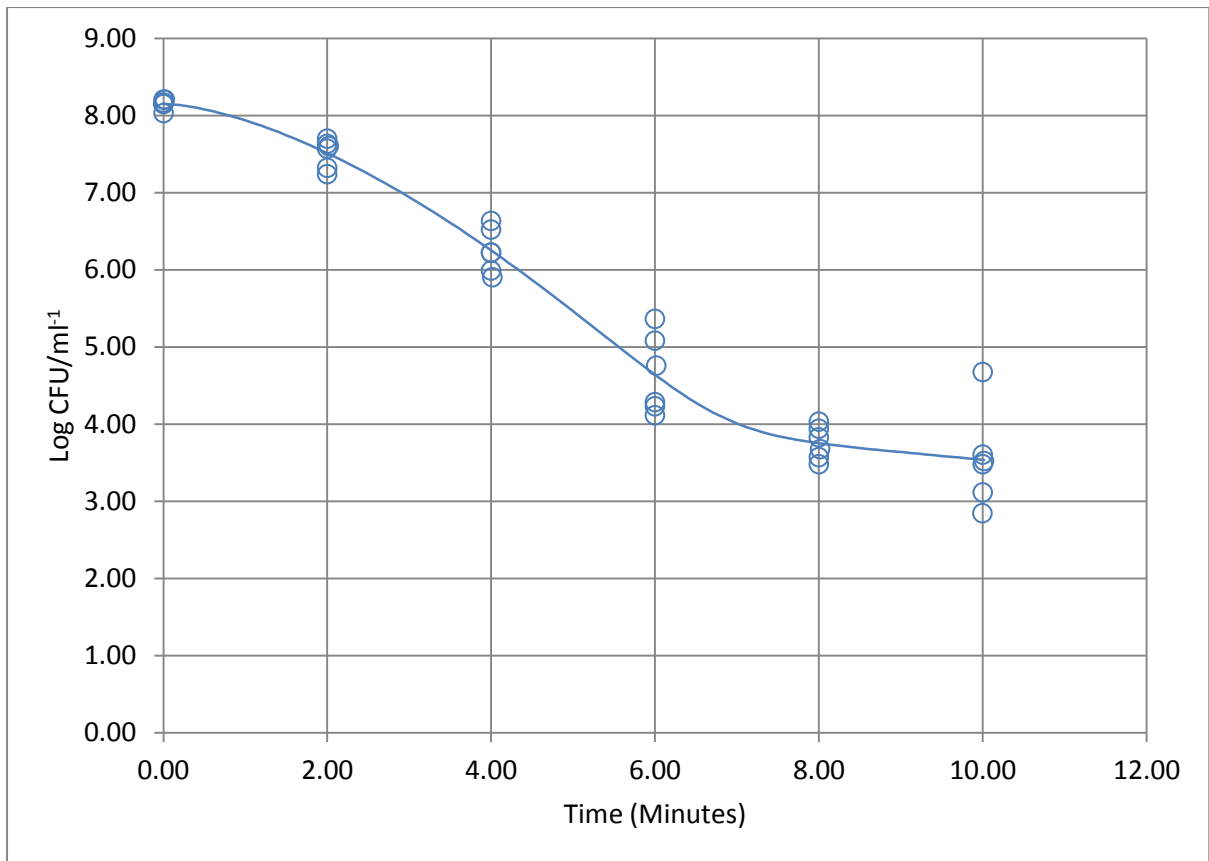


Figure 235. Plot illustrating predicted response curve using a Weibull distribution model for strain 12610 (ST-825, CC-828) following heating at 56°C.

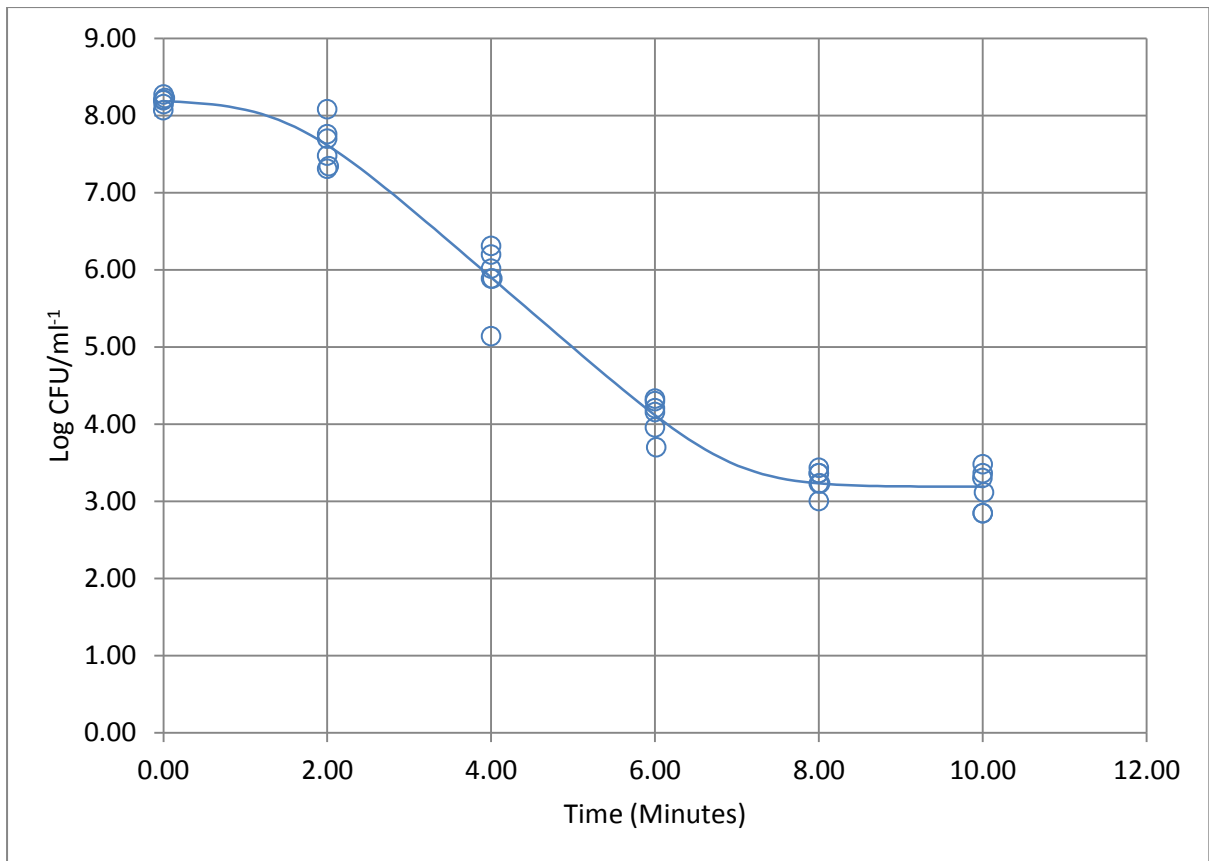


Figure 236. Plot illustrating predicted response curve using a log-linear model incorporating a shoulder effect and asymptotic function for strain 12628 (ST-1773, CC-828) following heating at 56°C.

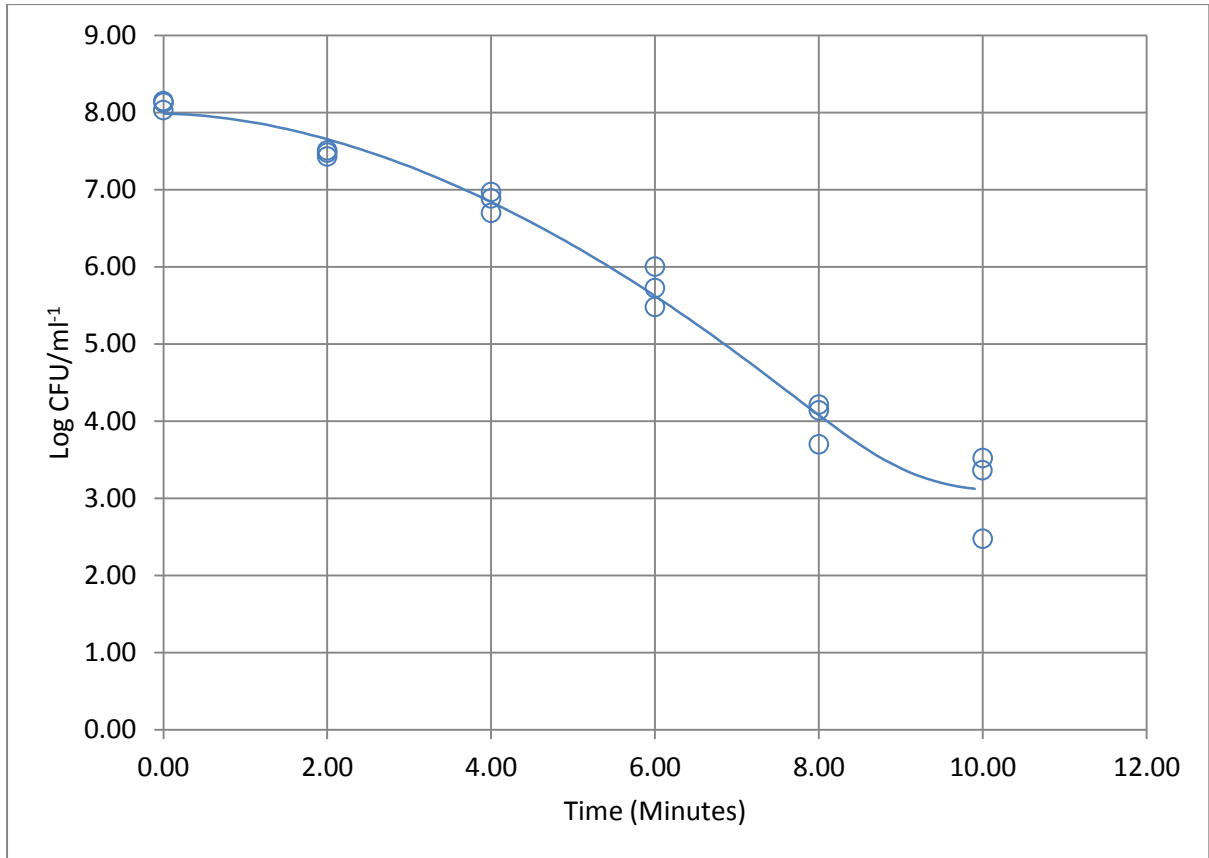


Figure 237. Plot illustrating predicted response curve using a Weibull model incorporating an asymptotic function for survival of strain 12645 (ST-51, CC-443) following at 56°C.

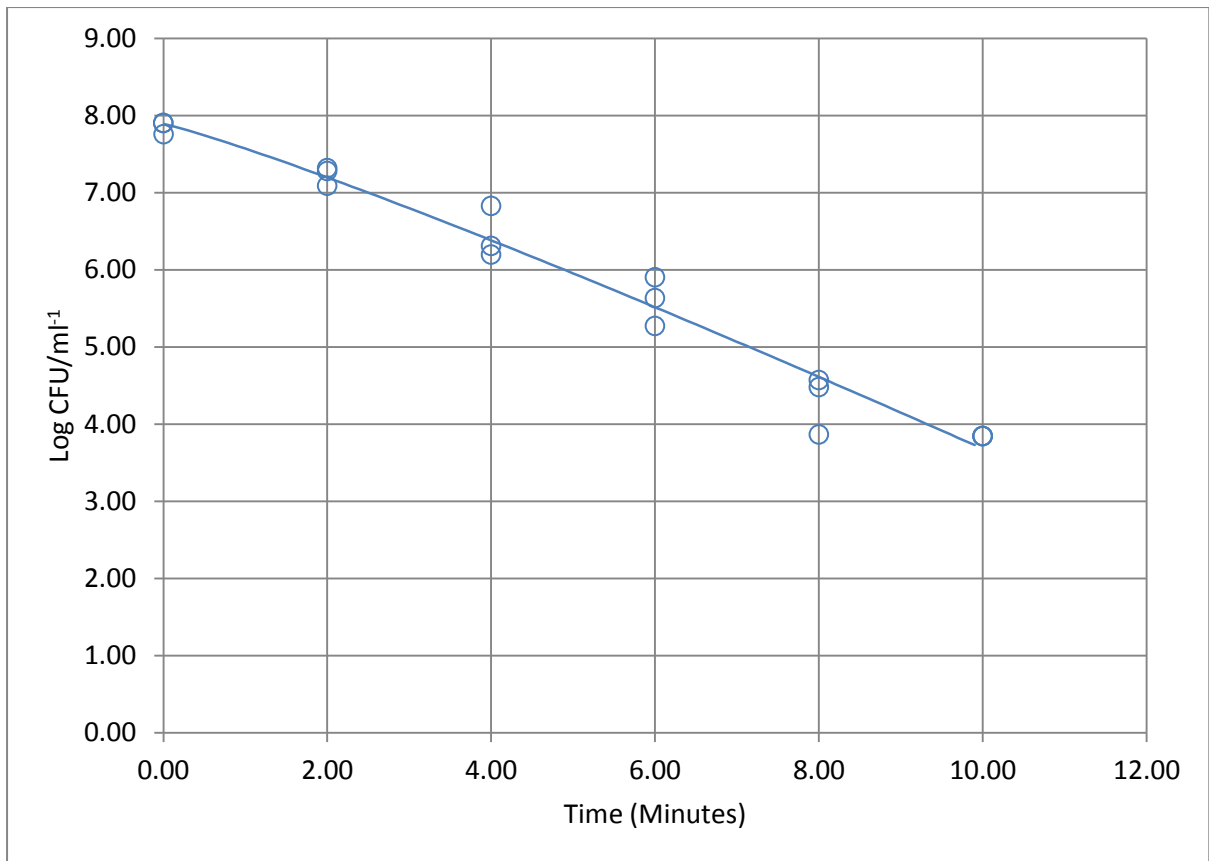


Figure 238. Plot illustrating predicted response curve using a Weibull model for survival of strain 12662 (ST-257, CC-257) following gradual heating at 56°C.

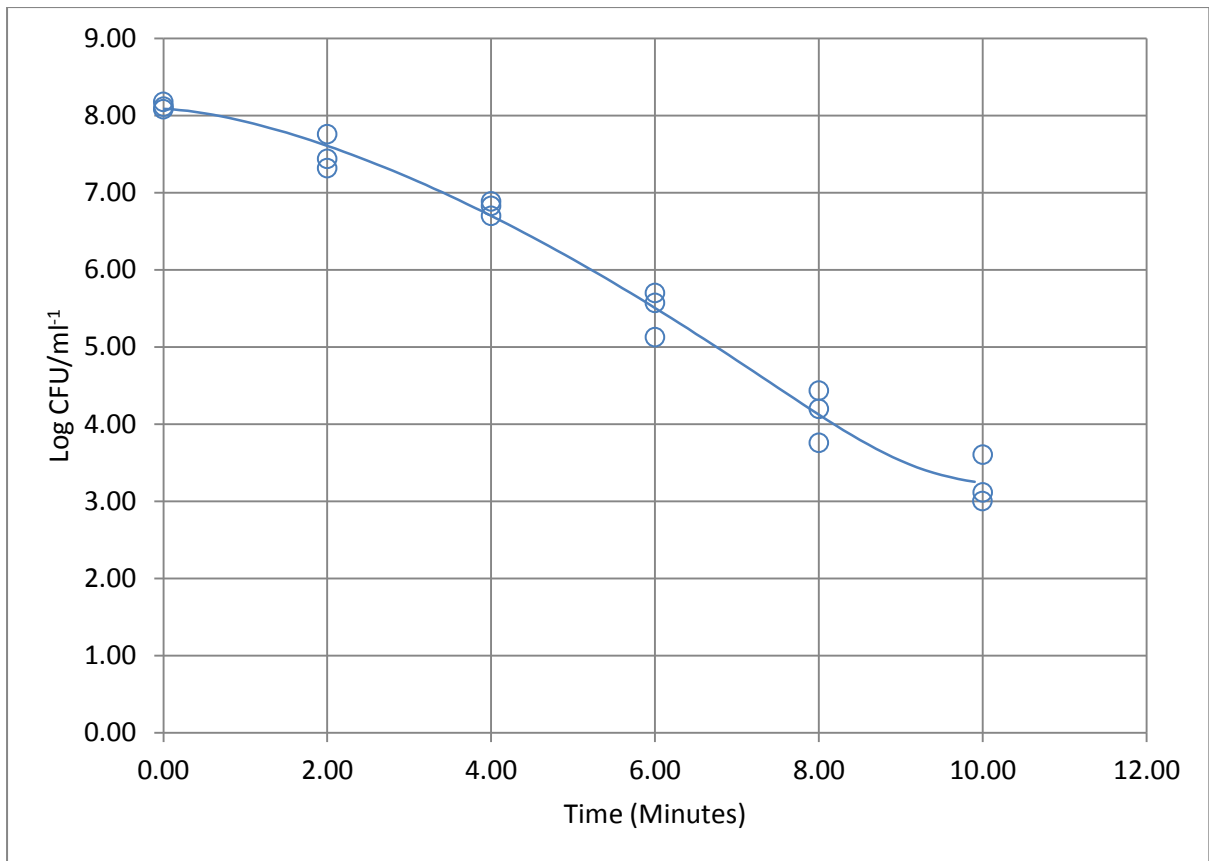


Figure 239. Plot illustrating predicted response curve using a Weibull model incorporating an asymptotic function for strain 12720 (ST-51, CC-443) following heating at 56°C.

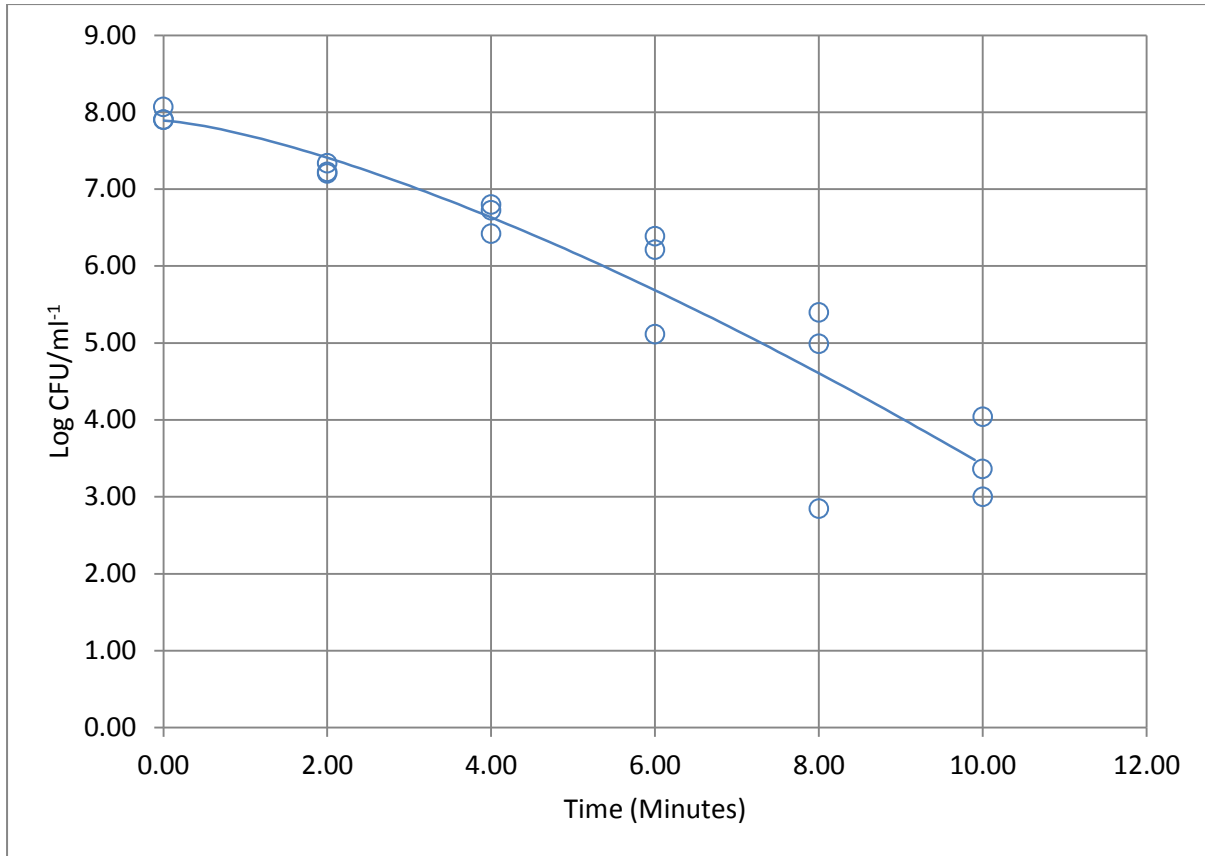


Figure 240. Plot illustrating predicted response curve using a Weibull model for strain 12745 (ST-257, CC-257) following heating at 56°C.

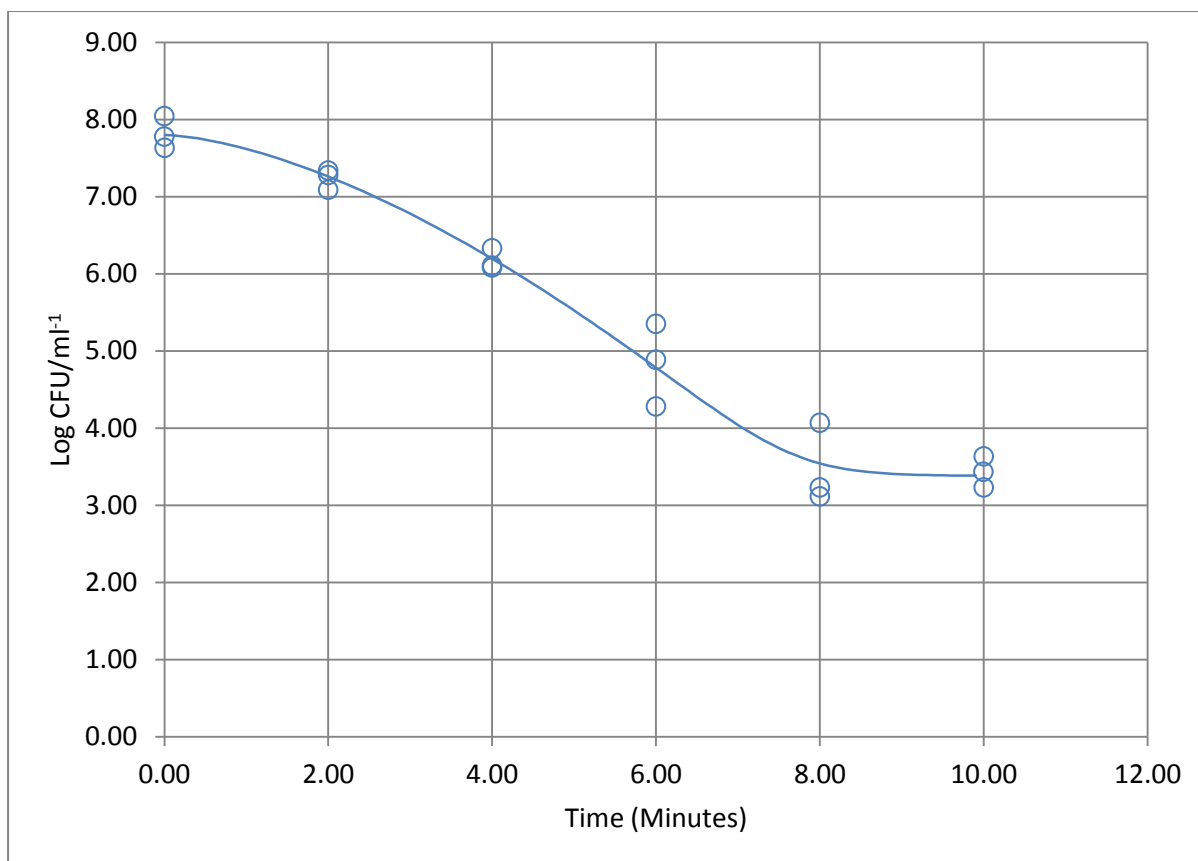


Figure 241. Plot illustrating predicted response curve using a Weibull model incorporating an asymptotic function for strain 12783 (ST-574, CC-574) following heating at 56°C.

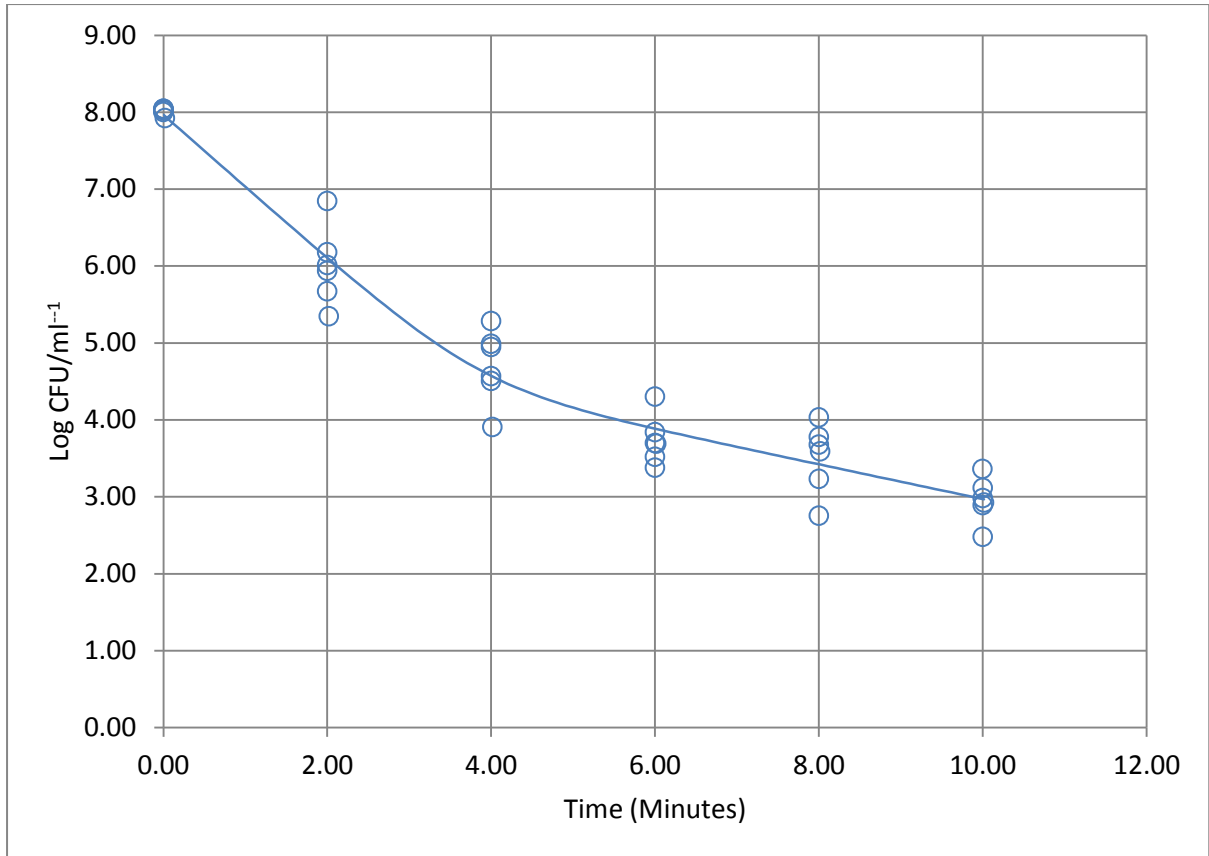


Figure 242. Plot illustrating predicted response curve using a Biphasic model for strain 13121 (ST-45, CC-45) following heating at 56°C.

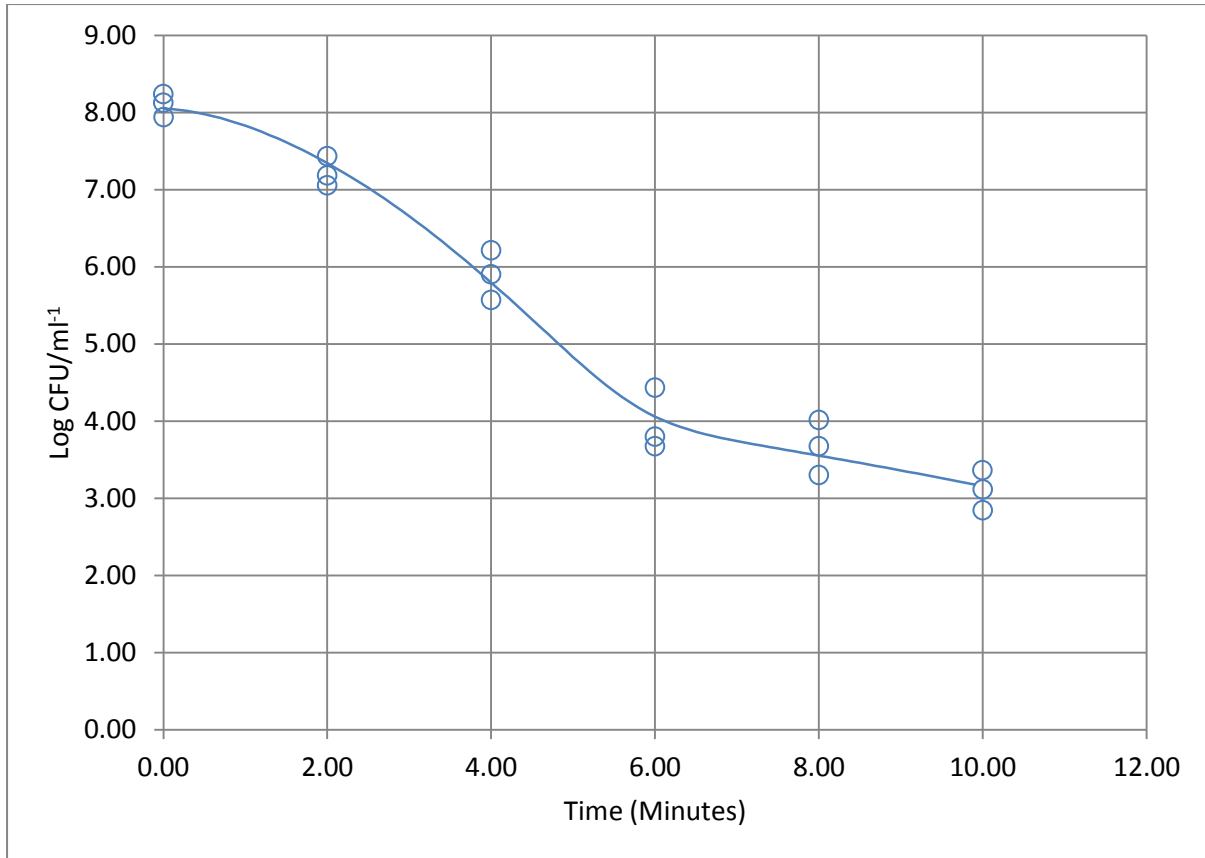


Figure 243. Plot illustrating predicted response curve using a mixed Weibull distribution model incorporating for strain 13126 (ST-21, CC-21) following heating at 56°C.

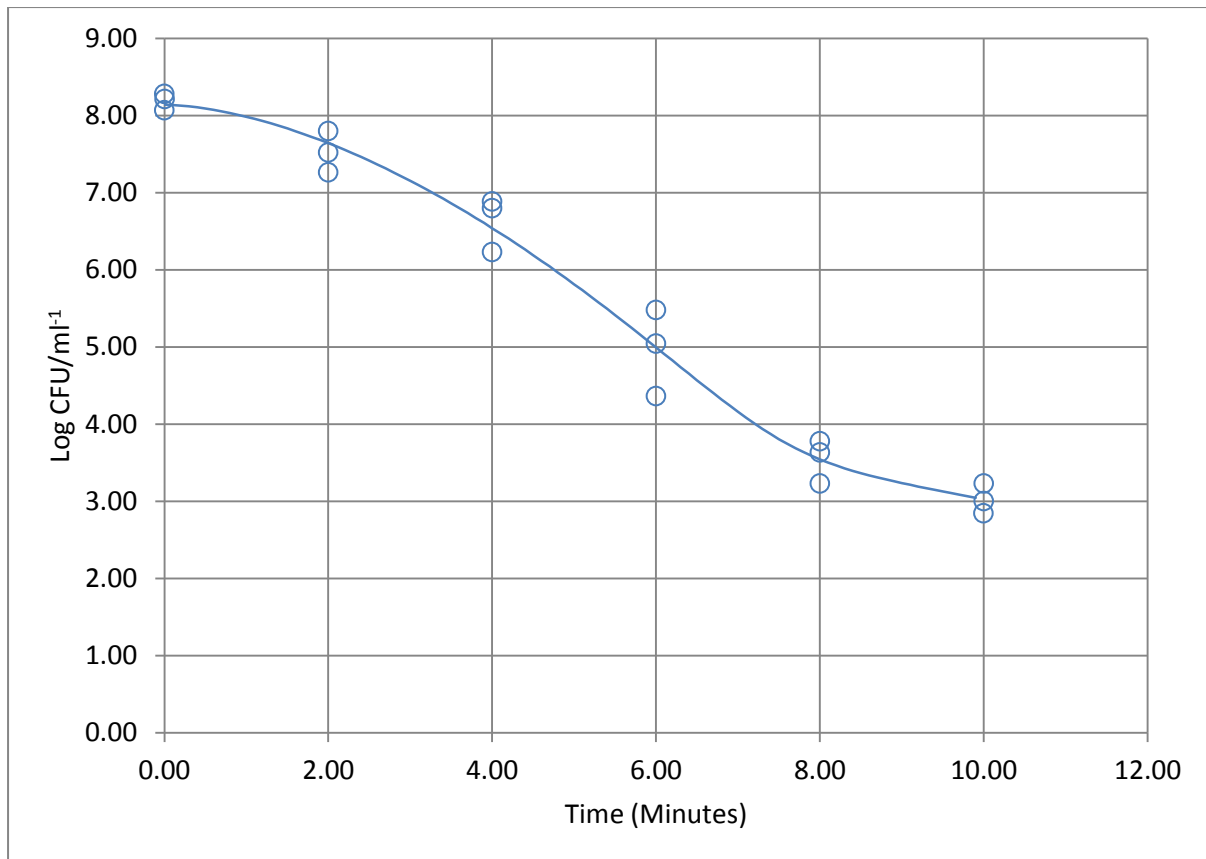


Figure 244. Plot illustrating predicted response curve using a mixed Weibull distribution model incorporating for strain 13136 (ST-45, CC-45) following heating at 56°C.

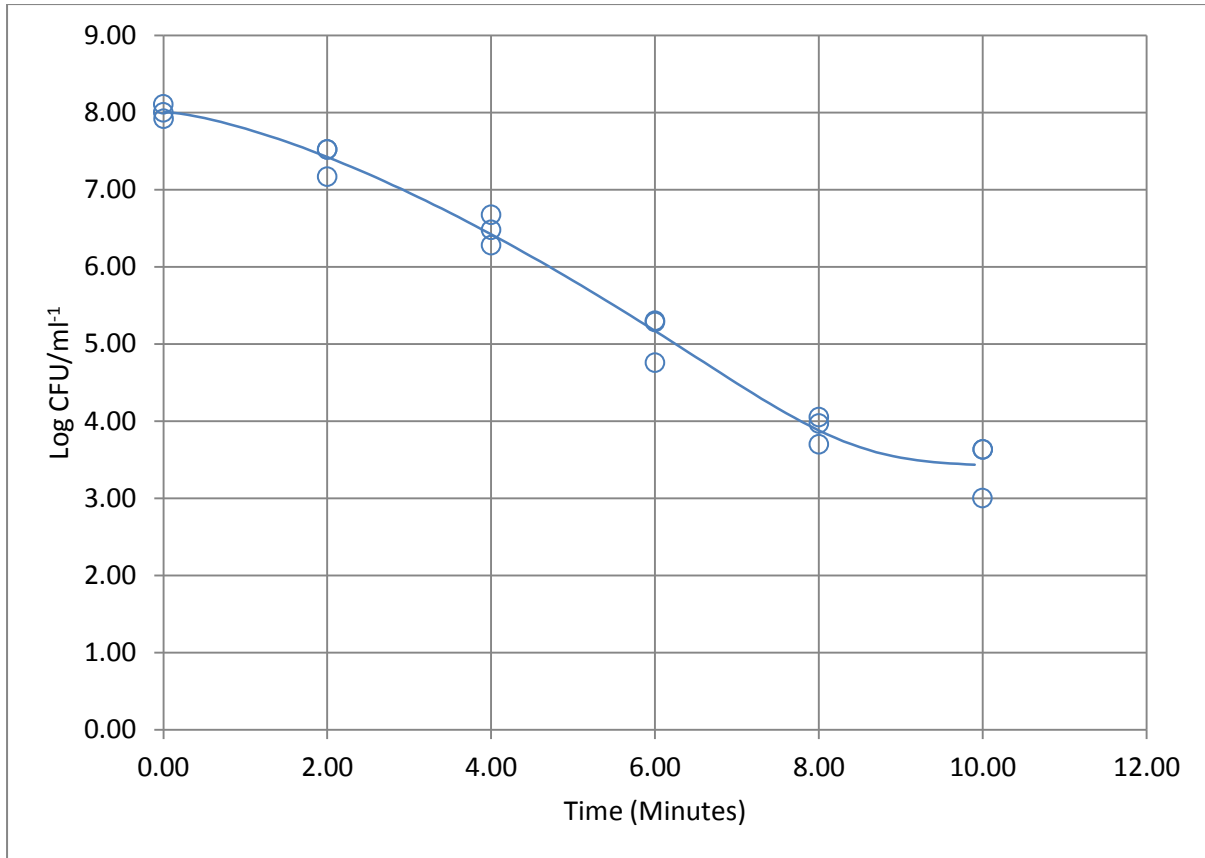


Figure 245. Plot illustrating predicted response curve using a Weibull model incorporating an asymptotic function for strain 13163 (ST-21, CC-21) following heating at 56°C.

2.3.7 Time-temperature Simulations: 60°C

Table 221. Assessment of model fit for individual strains following heating at 60°C.

Strain	RMSE	$R^2_{adjusted}$	D-value
11253 (ST-825, CC-828)	0.235	0.990	1.382
11368 (ST-574, CC-574)	0.321	0.975	1.476
11762 (ST-829, CC-828)	0.577	0.910	0.485
12610 (ST-825, CC-828)	0.509	0.951	0.935
12628 (ST-1773, CC-828)	0.701	0.895	0.691
12645 (ST-51, CC-443)	0.403	0.960	1.341
12662 (ST-257, CC-257)	0.451	0.949	1.080
12720 (ST-51, CC-443)	0.381	0.961	1.215
12745 (ST-257, CC-257)	0.560	0.927	0.927
12783 (ST-574, CC-574)	0.574	0.916	0.915
13121 (ST-45, CC-45)	0.389	0.953	0.475
13126 (ST-21, CC-21)	0.398	0.957	1.277
13136 (ST-45, CC-45)	0.392	0.960	1.017
13163 (ST-21, CC-21)	0.447	0.946	1.393

Table 222. Biphasic model incorporating a shoulder effect for survival of strain 11253 (ST-825, CC-828) following heating at 60°C.

Parameters	Estimates	Standard Error
F	1.000	0.000
Kmax1	5.417	1.151
Kmax2	0.778	0.165
<i>NO</i>	8.011	0.136
SI	0.976	0.151

Table 223. Log-linear model incorporating an asymptotic function and shoulder-effect for survival of strain 11368 (ST-574, CC-574) following heating at 60°C.

Parameters	Estimates	Standard Error
SI	0.931	0.205
Kmax	4.042	0.439
Nres	3.183	0.115
<i>NO</i>	7.972	0.185

Table 224. Biphasic model for survival of strain 11762 (ST-829, CC-828) following heating at 60°C.

Parameters	Estimates	Standard Error
F	0.999	0.001
Kmax1	4.776	0.886
Kmax2	0.724	0.259
<i>NO</i>	8.121	0.333

Table 225. Weibull model incorporating an asymptotic function for survival of strain 12610 (ST-825, CC-828) following heating at 60°C.

Parameters	Estimates	Standard Error
Nres	2.780	0.208
δ	0.935	0.237
ρ	1.357	0.284
<i>NO</i>	8.223	0.294

Table 226. Weibull model incorporating an asymptotic function for survival of strain 12628 (ST-1773, CC-828) following heating at 60°C.

Parameters	Estimates	Standard Error
Nres	2.629	0.371
δ	0.691	0.355
ρ	0.878	0.250
<i>NO</i>	8.122	0.406

Table 227. Mixed Weibull distribution model for survival of strain 12645 (ST-51, CC-443) following heating at 60°C.

Parameters	Estimates	Standard Error
α	4.374	0.482
δ_1	1.341	0.246
ρ	1.738	0.368
<i>NO</i>	8.001	0.241
δ_2	10.464	6.592

Table 228. Mixed Weibull distribution model for survival of strain 12662 (ST-257, CC-257) following heating at 60°C.

Parameters	Estimates	Standard Error
α	3.591	0.446
δ_1	1.080	0.191
ρ	1.344	0.236
N_0	8.088	0.187
δ_2	4.865	1.288

Table 229. Mixed Weibull distribution model for survival of strain 12720 (ST-51, CC-443) following heating at 60°C.

Parameters	Estimates	Standard Error
α	4.038	0.459
δ_1	1.215	0.221
ρ	1.597	0.330
N_0	7.952	0.228
δ_2	8.234	3.554

Table 230. Mixed Weibull distribution model for survival of strain 12745 (ST-257, CC-257) following heating at 60°C.

Parameters	Estimates	Standard Error
α	3.734	0.462
δ_1	1.330	0.292
ρ	1.956	1.007
N_0	8.134	0.335
δ_2	5.844	1.326

Table 231. Mixed Weibull distribution model for survival of strain 12783 (ST-574, CC-574) following heating at 60°C.

Parameters	Estimates	Standard Error
α	4.277	0.619
δ_1	0.915	0.226
ρ	1.204	0.253
N_0	7.943	0.238
δ_2	9.336	7.753

Table 232. Biphasic model for survival of strain 13121 (ST-45, CC-45) following heating at 60°C.

Parameters	Estimates	Standard Error
F	1.000	0.000
Kmax1	4.888	0.534
Kmax2	0.275	0.201
<i>NO</i>	7.932	0.225

Table 233. Mixed Weibull distribution model for survival of strain 13126 (ST-21, CC-21) following heating at 60°C.

Parameters	Estimates	Standard Error
α	3.739	0.391
δ_1	1.277	0.150
ρ	2.509	1.544
<i>NO</i>	8.056	0.165
δ_2	6.472	1.113

Table 234. Mixed Weibull distribution model for survival of strain 13136 (ST-45, CC-45) following heating at 60°C.

Parameters	Estimates	Standard Error
α	3.671	0.294
δ_1	1.017	0.165
ρ	1.423	0.163
<i>NO</i>	8.012	0.163
δ_2	6.521	1.058

Table 235. Weibull model incorporating an asymptotic function for survival of strain 13163 (ST-21, CC-21) following heating at 60°C.

Parameters	Estimates	Standard Error
Nres	3.556	0.169
δ	1.393	0.276
ρ	1.765	0.419
<i>NO</i>	7.975	0.258

2.3.8 Time-temperature Simulations: 60°C

Predicted Response Curves:

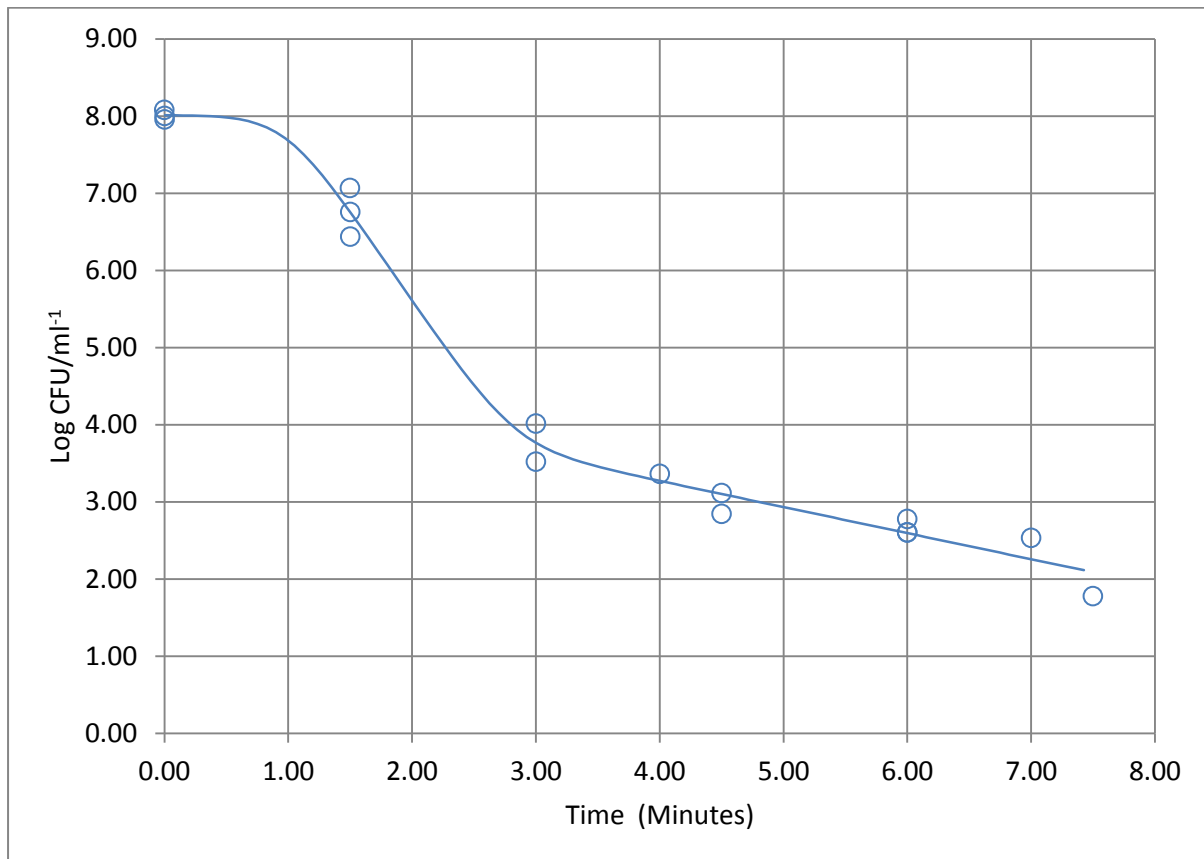


Figure 246. Plot illustrating predicted response curve using a Biphasic model incorporating a shoulder effect for strain 11253 (ST-825, CC-828) following heating at 60°C.

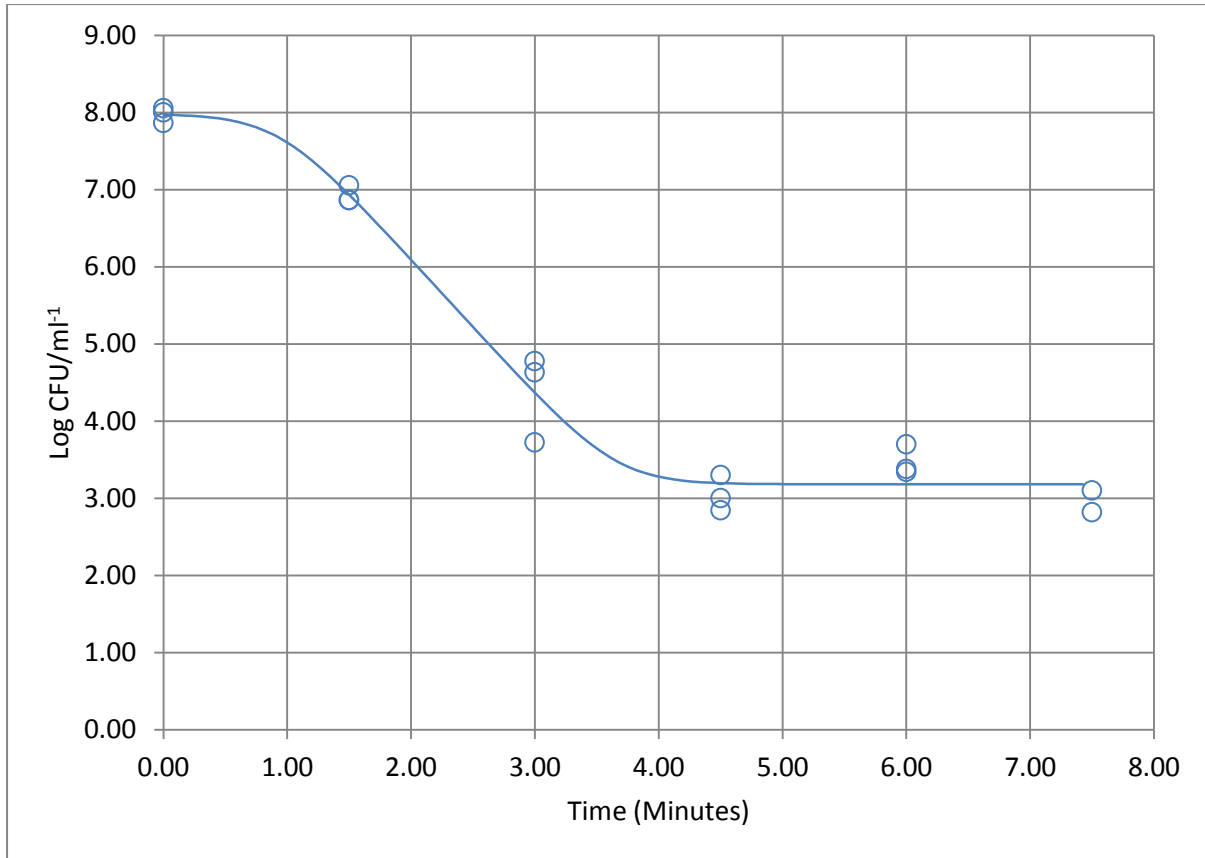


Figure 247. Plot illustrating predicted response curve using a log-linear model incorporating an asymptotic function and shoulder effect for strain 11368 (ST-574, CC-574) following heating at 60°C.

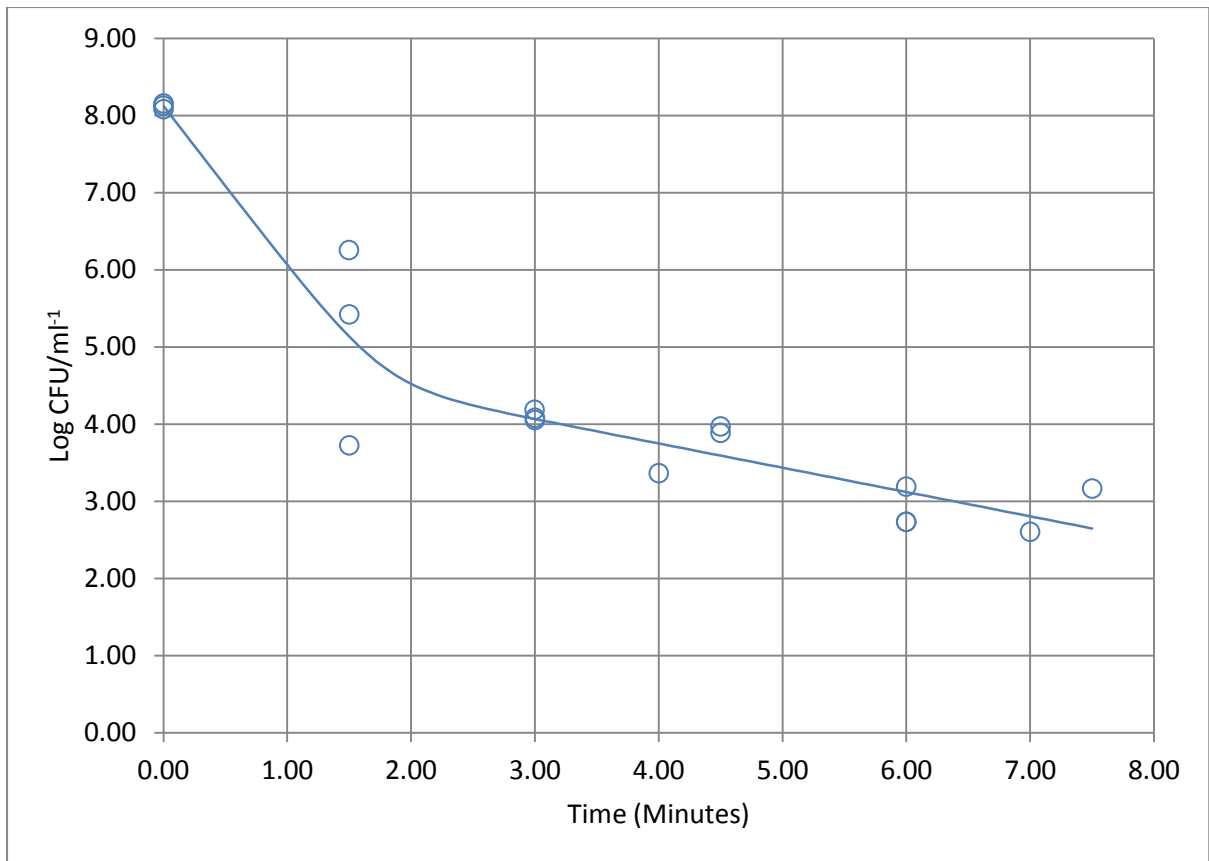


Figure 248. Plot illustrating predicted response curve using a biphasic model for strain 11762 (ST-829, CC-828) following heating at 60°C.

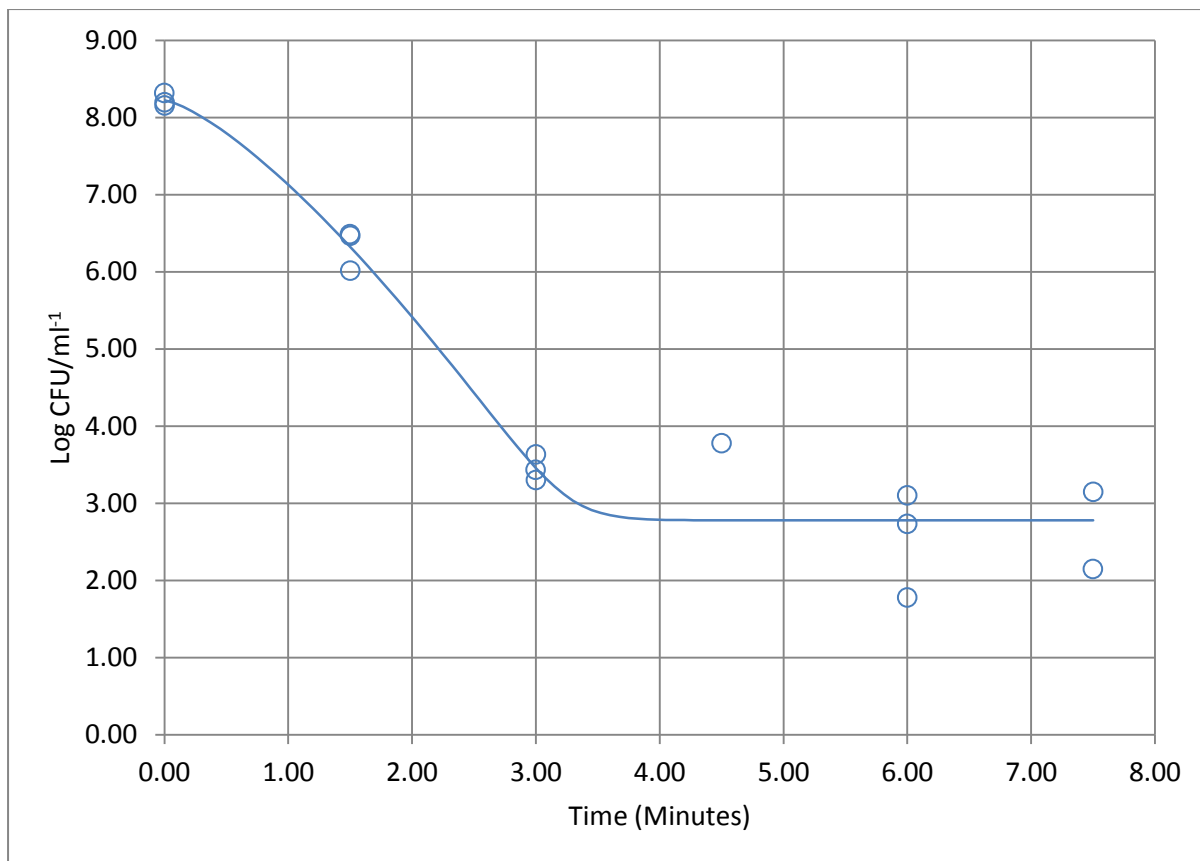


Figure 249. Plot illustrating predicted response curve using a Weibull model incorporating an asymptotic function for strain 12610 (ST-825, CC-828) following heating at 60°C.

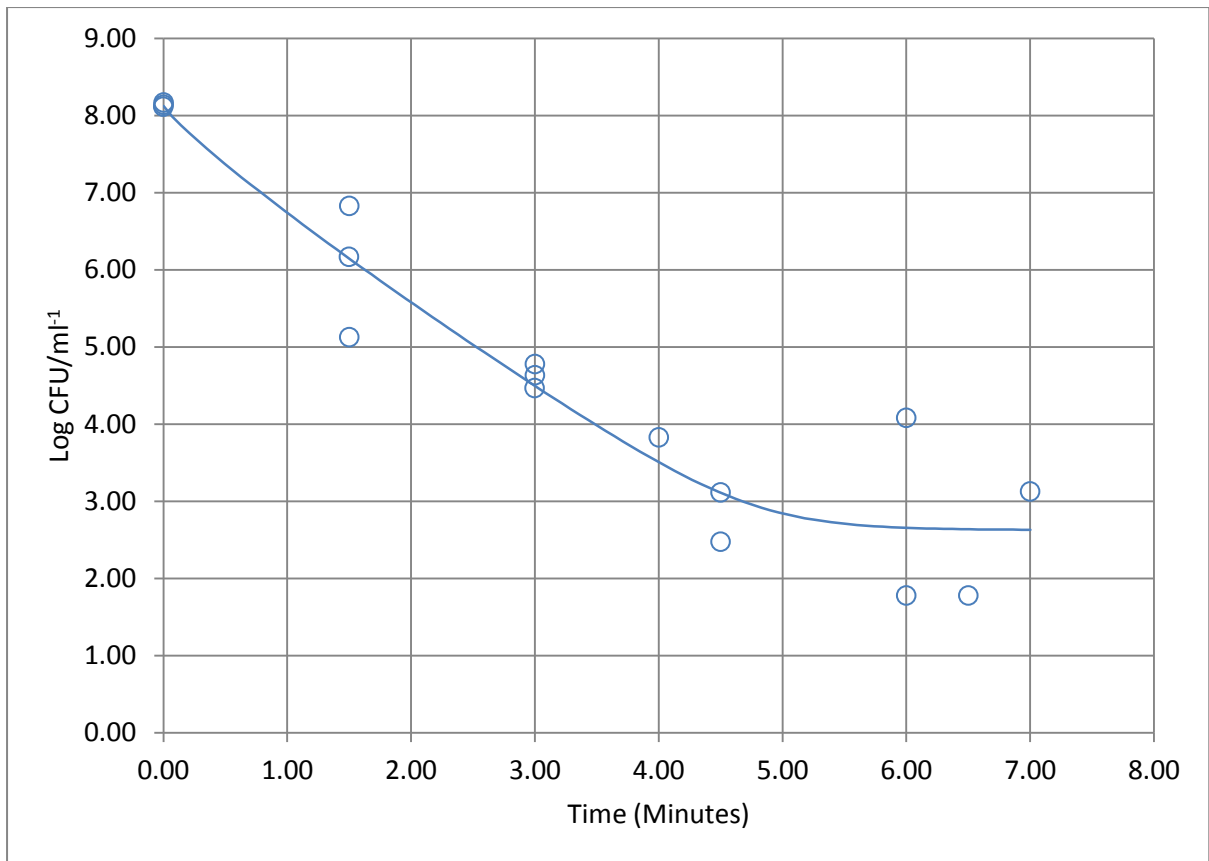


Figure 250. Plot illustrating predicted response curve using a Weibull model incorporating an asymptotic function for strain 12628 (ST-1773, CC-828) following heating at 60°C.

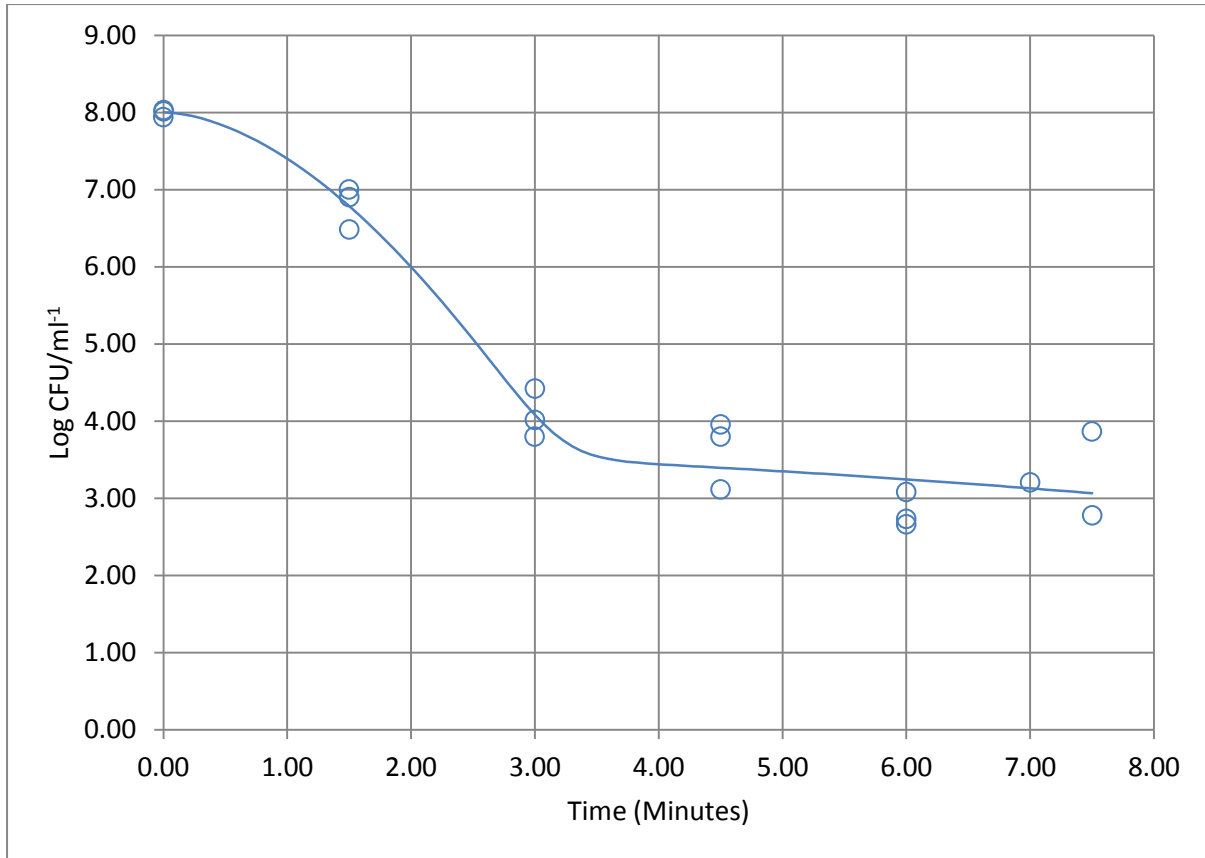


Figure 251. Plot illustrating predicted response curve using a mixed Weibull distribution model incorporating for survival of strain 12645 (ST-51, CC-443) following at 60°C.

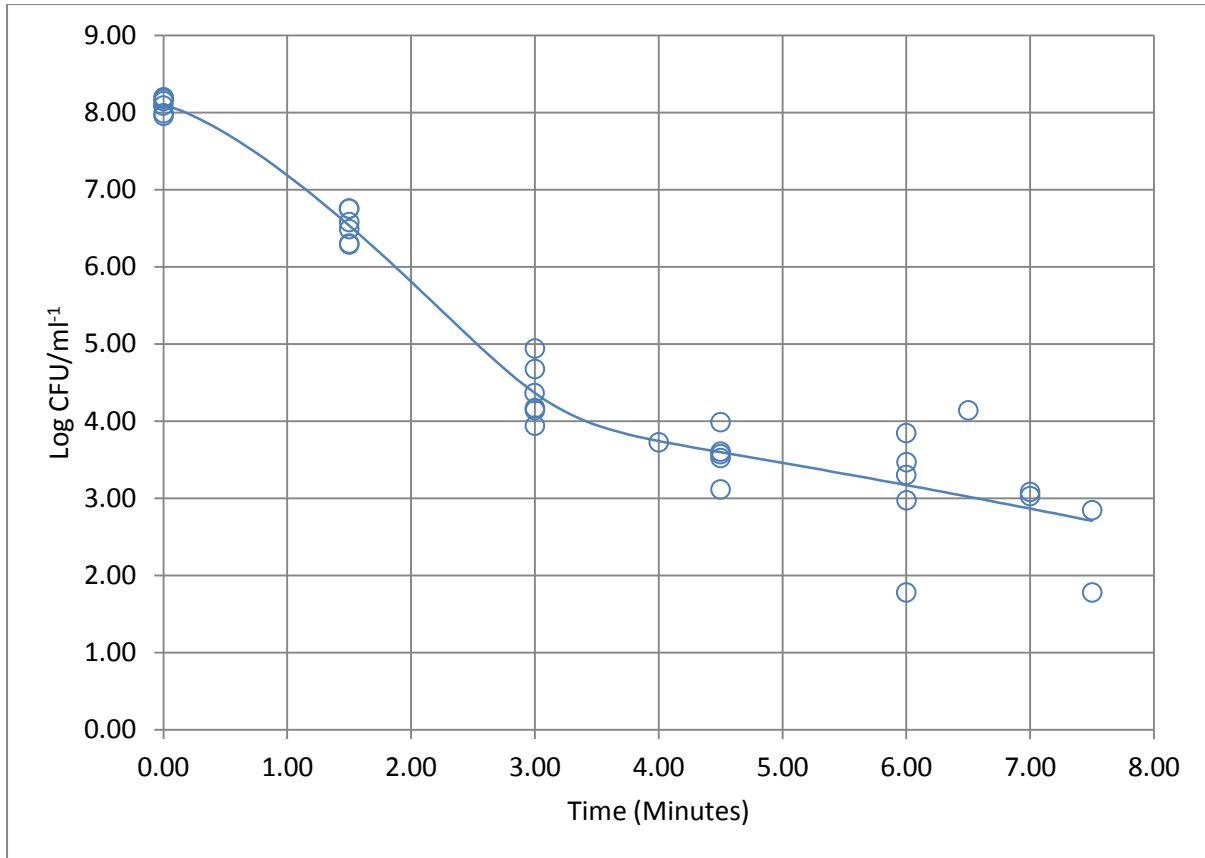


Figure 252. Plot illustrating predicted response curve using a mixed Weibull distribution model for survival of strain 12662 (ST-257, CC-257) following gradual heating at 60°C.

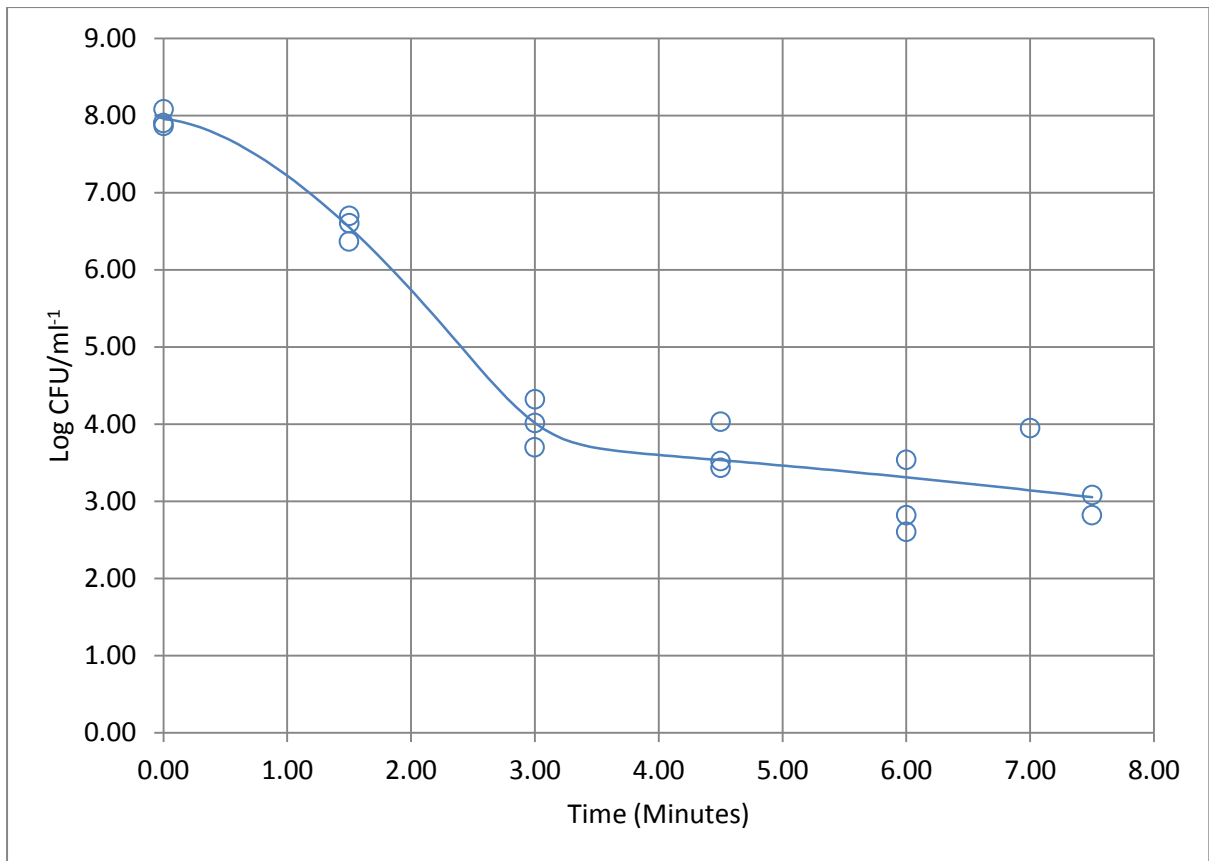


Figure 253. Plot illustrating predicted response curve using a mixed Weibull distribution model for strain 12720 (ST-51, CC-443) following heating at 60°C.

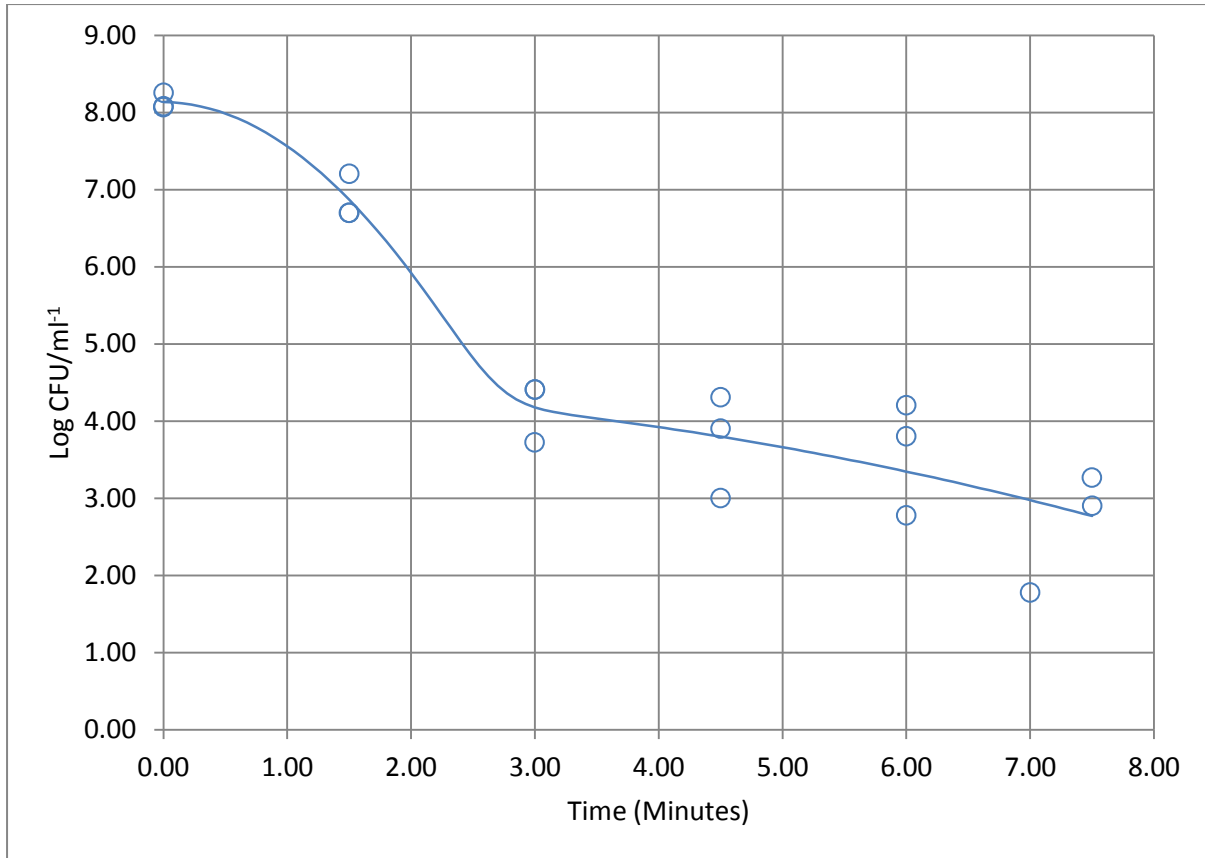


Figure 254. Plot illustrating predicted response curve using a mixed Weibull distribution model for strain 12745 (ST-257, CC-257) following heating at 60°C.

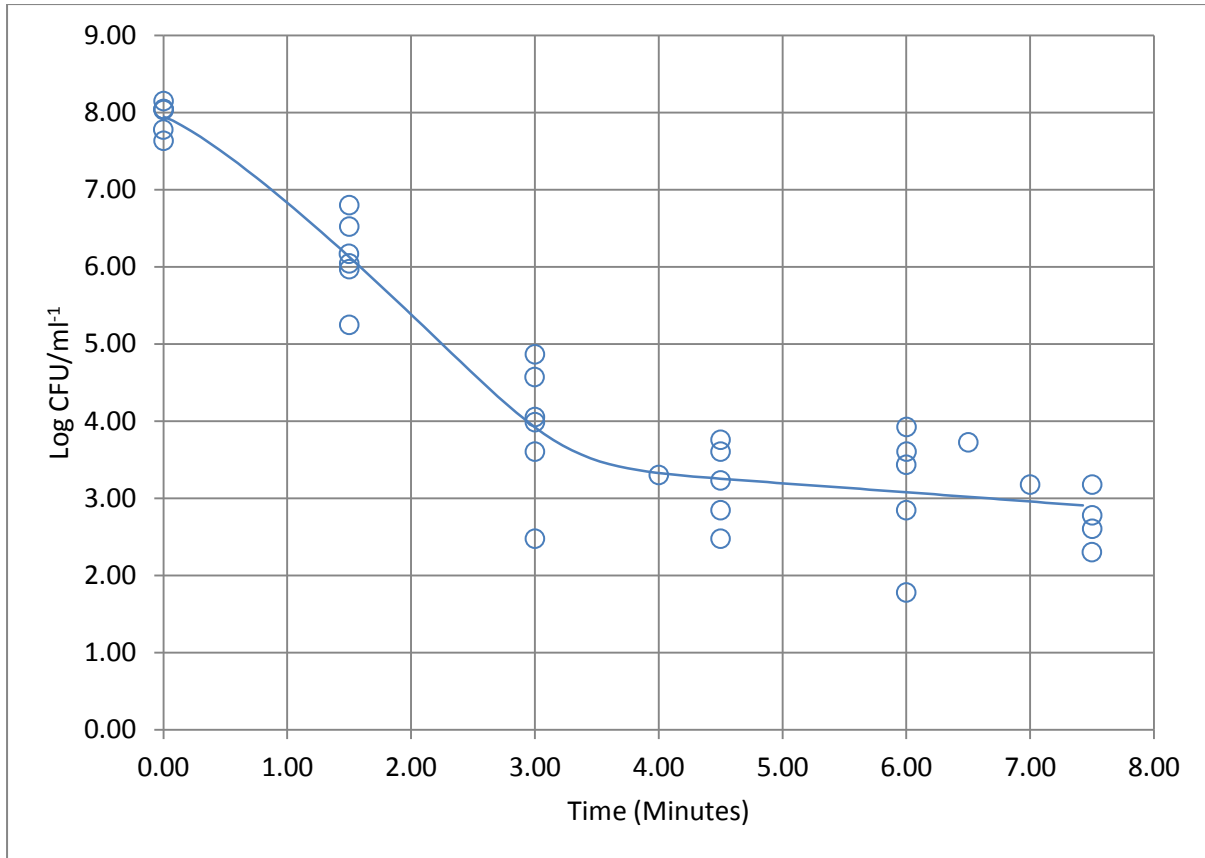


Figure 255. Plot illustrating predicted response curve using a mixed Weibull distribution model for strain 12783 (ST-574, CC-574) following heating at 60°C.

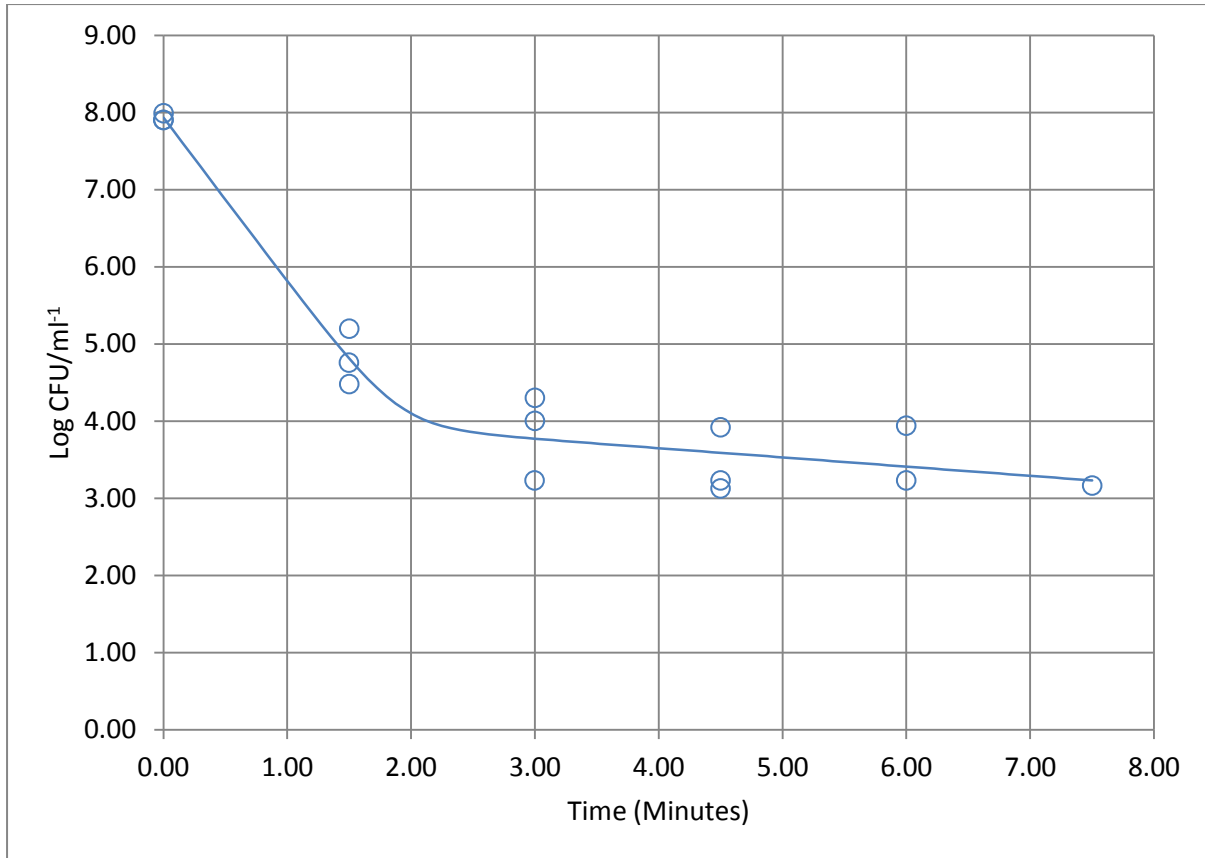


Figure 256. Plot illustrating predicted response curve using a Biphasic model for strain 13121 (ST-45, CC-45) following heating at 60°C.

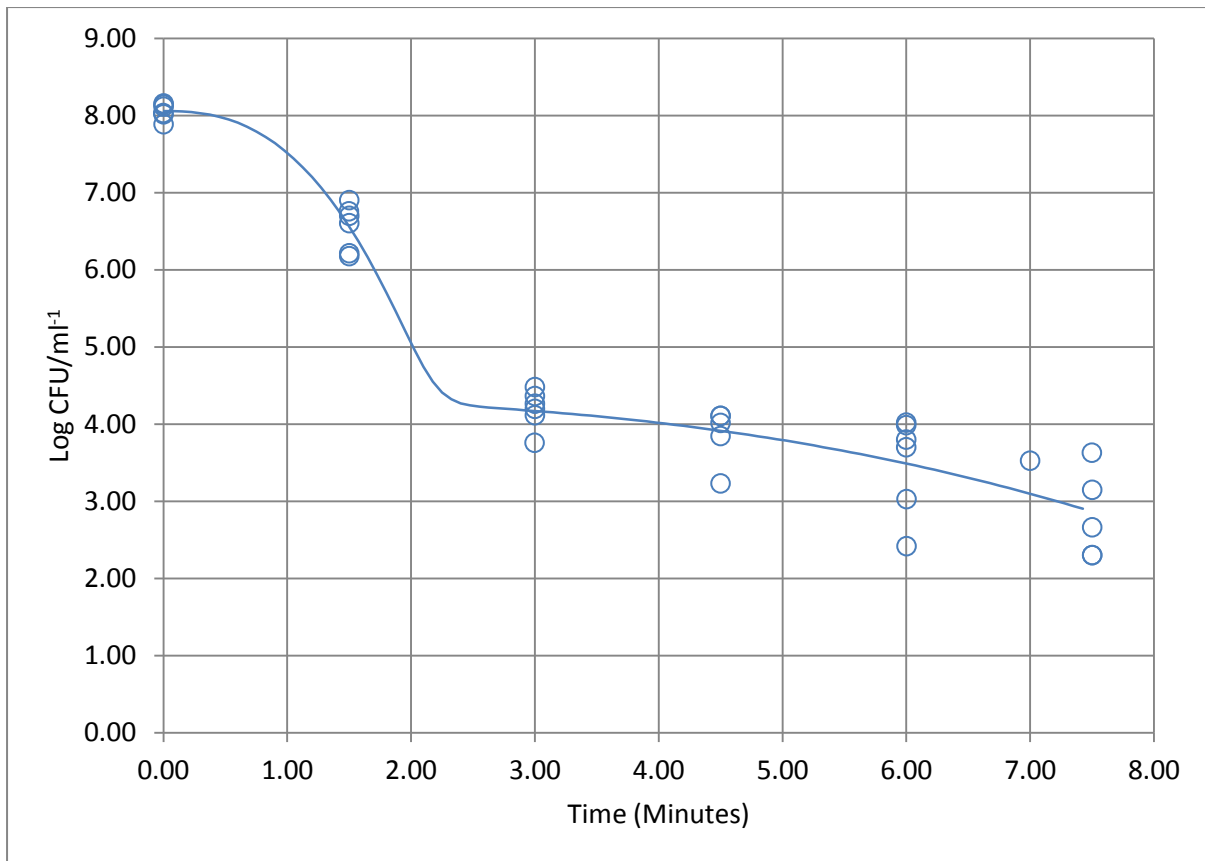


Figure 257. Plot illustrating predicted response curve using a mixed Weibull distribution model incorporating for strain 13126 (ST-21, CC-21) following heating at 60°C.

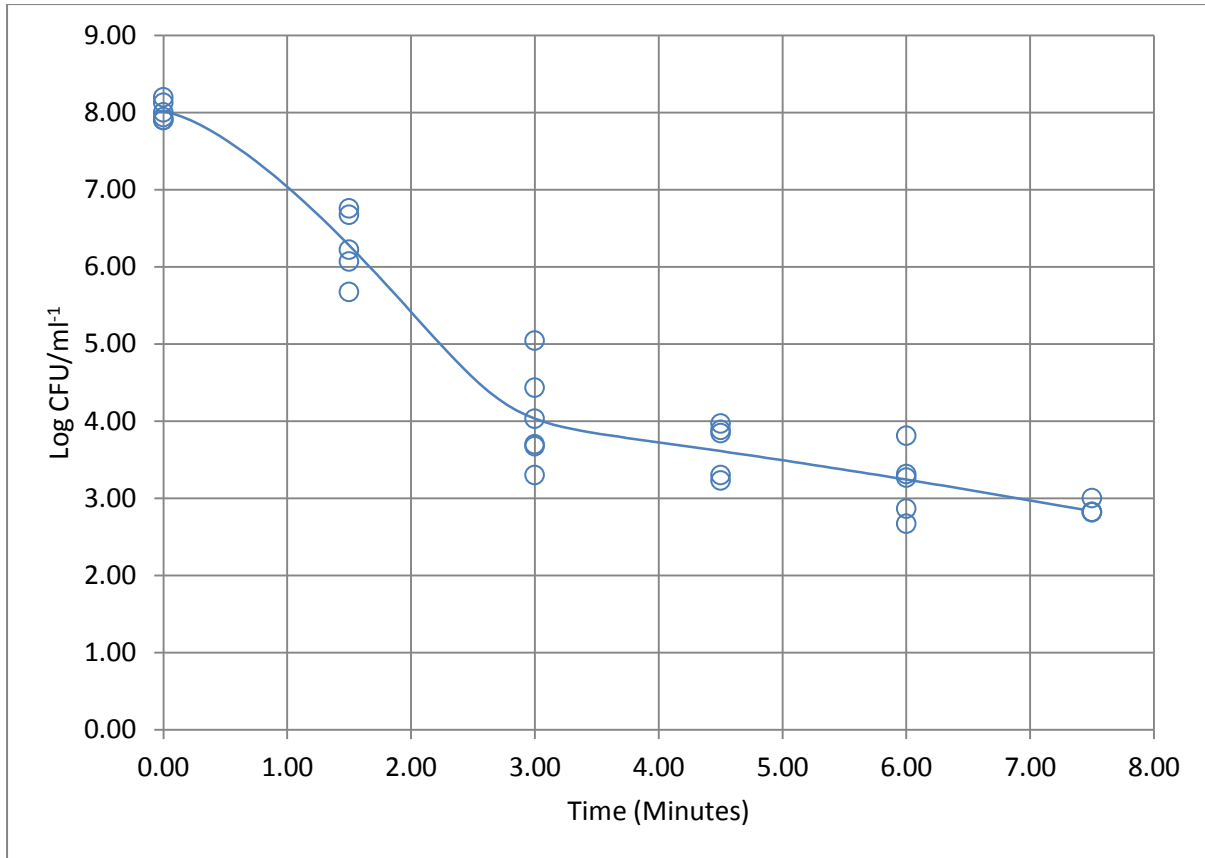


Figure 258. Plot illustrating predicted response curve using a mixed Weibull distribution model incorporating for strain 13136 (ST-45, CC-45) following heating at 60°C.

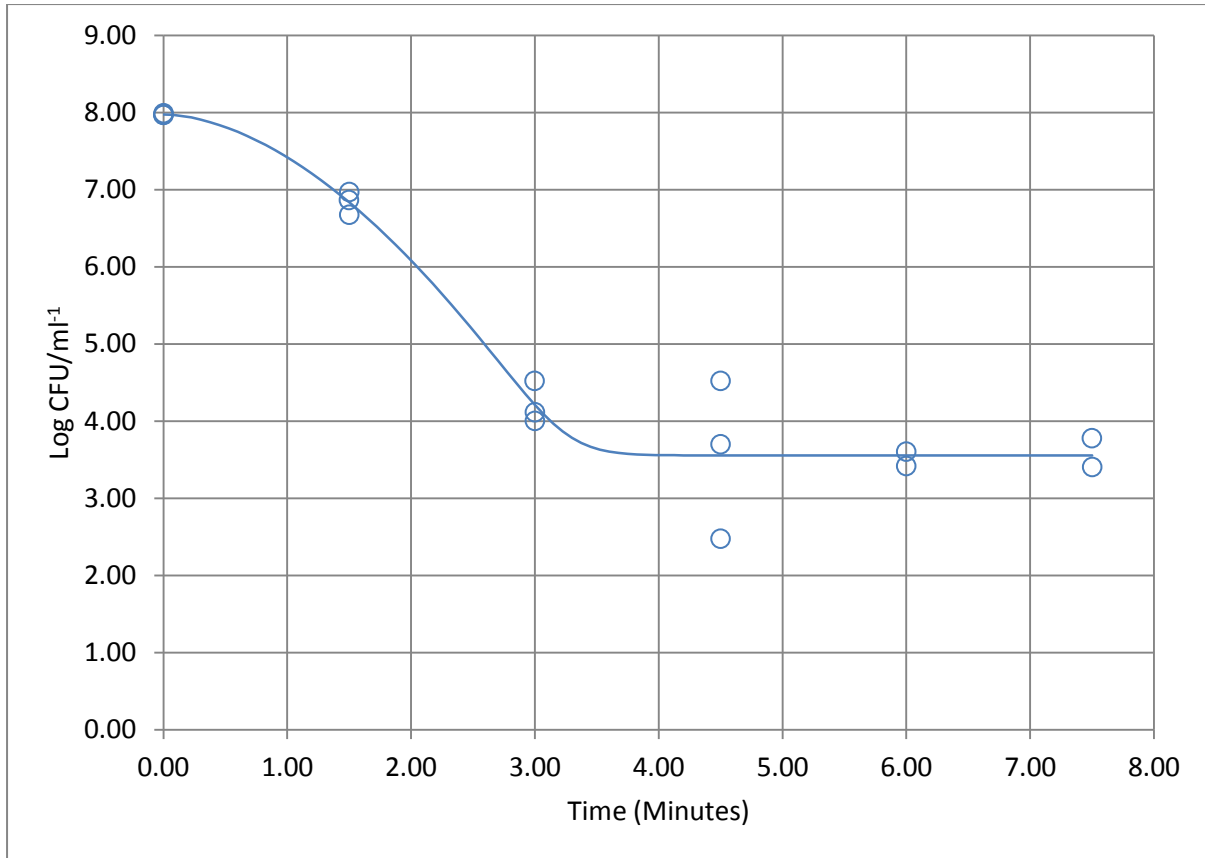


Figure 259. Plot illustrating predicted response curve using a Weibull model incorporating an asymptotic function for strain 13163 (ST-21, CC-21) following heating at 60°C.

2.3.9 Time-temperature Simulations: 64°C

Table 236. Assessment of model fit for individual strains following heating at 64°C.

Strain	RMSE	$R^2_{adjusted}$	D-value
11253 (ST-825, CC-828)	0.399	0.965	0.247
11368 (ST-574, CC-574)	0.502	0.939	0.256
11762 (ST-829, CC-828)	0.643	0.917	0.249
12610 (ST-825, CC-828)	0.578	0.930	0.234
12628 (ST-1773, CC-828)	0.706	0.883	0.600
12645 (ST-51, CC-443)	0.462	0.937	0.290
12662 (ST-257, CC-257)	0.739	0.888	0.249
12720 (ST-51, CC-443)	0.473	0.929	0.283
12745 (ST-257, CC-257)	0.482	0.931	0.119
12783 (ST-574, CC-574)	0.719	0.901	0.247
13121 (ST-45, CC-45)	0.564	0.917	0.204
13126 (ST-21, CC-21)	0.574	0.916	0.259
13136 (ST-45, CC-45)	0.560	0.924	0.244
13163 (ST-21, CC-21)	0.570	0.903	0.231

Table 237. Biphasic model incorporating for survival of strain 11253 (ST-825, CC-828) following heating at 64°C.

Parameters	Estimates	Standard Error
F	1.000	0.000
Kmax1	9.349	0.801
Kmax2	0.418	0.212
<i>NO</i>	8.004	0.230

Table 238. Log-linear model incorporating an asymptotic function for survival of strain 11368 (ST-574, CC-574) following heating at 64°C.

Parameters	Estimates	Standard Error
Kmax	8.990	0.981
Nres	2.940	0.159
<i>NO</i>	7.973	0.290

Table 239. Biphasic model for survival of strain 11762 (ST-829, CC-828) following heating at 64°C.

Parameters	Estimates	Standard Error
F	1.000	0.000
Kmax1	9.246	1.294
Kmax2	0.720	0.275
<i>NO</i>	8.118	0.371

Table 240. Log-linear model incorporating an asymptotic function for survival of strain 12610 (ST-825, CC-828) following heating at 64°C.

Parameters	Estimates	Standard Error
Kmax1	9.858	1.119
Kmax2	2.704	0.174
<i>NO</i>	8.222	0.334

Table 241. Biphasic model for survival of strain 12628 (ST-1773, CC-828) following heating at 64°C.

Parameters	Estimates	Standard Error
F	1.000	0.000
Kmax1	8.683	1.488
Kmax2	0.416	0.388
<i>NO</i>	8.141	0.408

Table 242. Biphasic model for survival of strain 12645 (ST-51, CC-443) following heating at 64°C.

Parameters	Estimates	Standard Error
F	1.000	0.000
Kmax1	7.933	0.919
Kmax2	0.325	0.216
<i>NO</i>	7.995	0.267

Table 243. Biphasic model for survival of strain 12662 (ST-257, CC-257) following heating at 64°C.

Parameters	Estimates	Standard Error
F	1.000	0.001
Kmax1	9.246	2.873
<i>Kmax2</i>	1.164	0.332
<i>NO</i>	8.176	.0427

Table 244. Biphasic model for survival of strain 12720 (ST-51, CC-443) following heating at 64°C.

Parameters	Estimates	Standard Error
F	0.999	0.001
Kmax1	8.176	2.171
Kmax2	0.982	0.215
<i>NO</i>	7.948	0.273

Table 245. Biphasic model for survival of strain 12745 (ST-257, CC-257) following heating at 64°C.

Parameters	Estimates	Standard Error
F	1.000	0.000
Kmax1	19.372	1026.404
Kmax2	0.692	0.157
<i>NO</i>	8.141	0.464

Table 246. Biphasic for survival of strain 12783 (ST-574, CC-574) following heating at 64°C.

Parameters	Estimates	Standard Error
F	1.000	0.000
Kmax1	9.330	1.693
Kmax2	0.819	0.411
<i>NO</i>	8.072	0.415

Table 247. Log-linear model with asymptotic function for survival of strain 13121 (ST-45, CC-45) following heating at 64°C.

Parameters	Estimates	Standard Error
Kmax	11.302	1.143
Nres	3.046	0.118
<i>NO</i>	8.022	0.230

Table 248. Biphasic model for survival of strain 13126 (ST-21, CC-21) following heating at 64°C.

Parameters	Estimates	Standard Error
F	1.000	0.000
Kmax1	8.899	0.970
Kmax2	0.627	0.196
<i>NO</i>	8.056	0.234

Table 249. Biphasic model for survival of strain 13136 (ST-45, CC-45) following heating at 64°C.

Parameters	Estimates	Standard Error
F	1.000	0.000
Kmax1	9.457	1.202
Kmax2	0.539	0.217
<i>NO</i>	8.010	0.229

Table 250. Log-linear model incorporating an asymptotic function for survival of strain 13163 (ST-21, CC-21) following heating at 64°C.

Parameters	Estimates	Standard Error
Kmax	9.960	1.373
Nres	3.341	0.164
<i>NO</i>	7.975	0.329

2.3.10 Time-Temperature Simulations: 64°C

Predicted Response Curves:

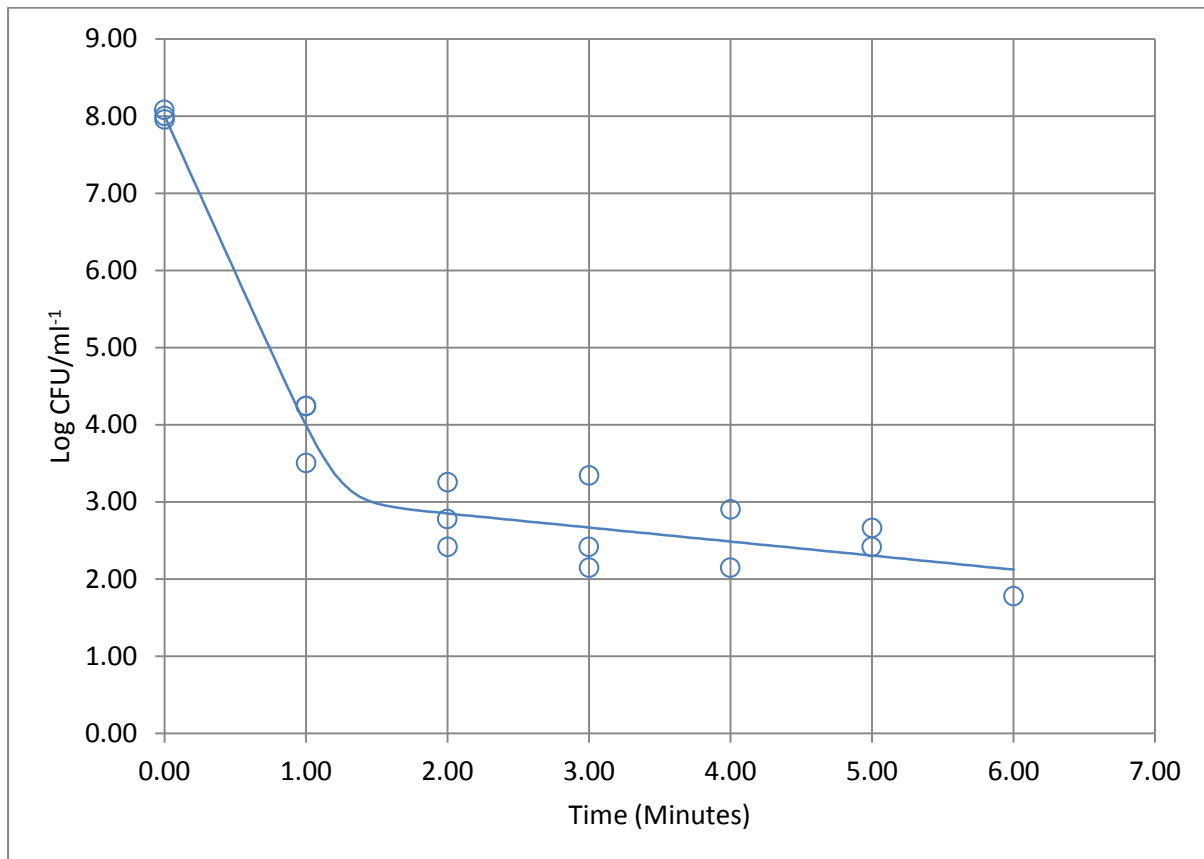


Figure 260. Plot illustrating predicted response curve using a Biphasic model for strain 11253 (ST-825, CC-828) following heating at 64°C.

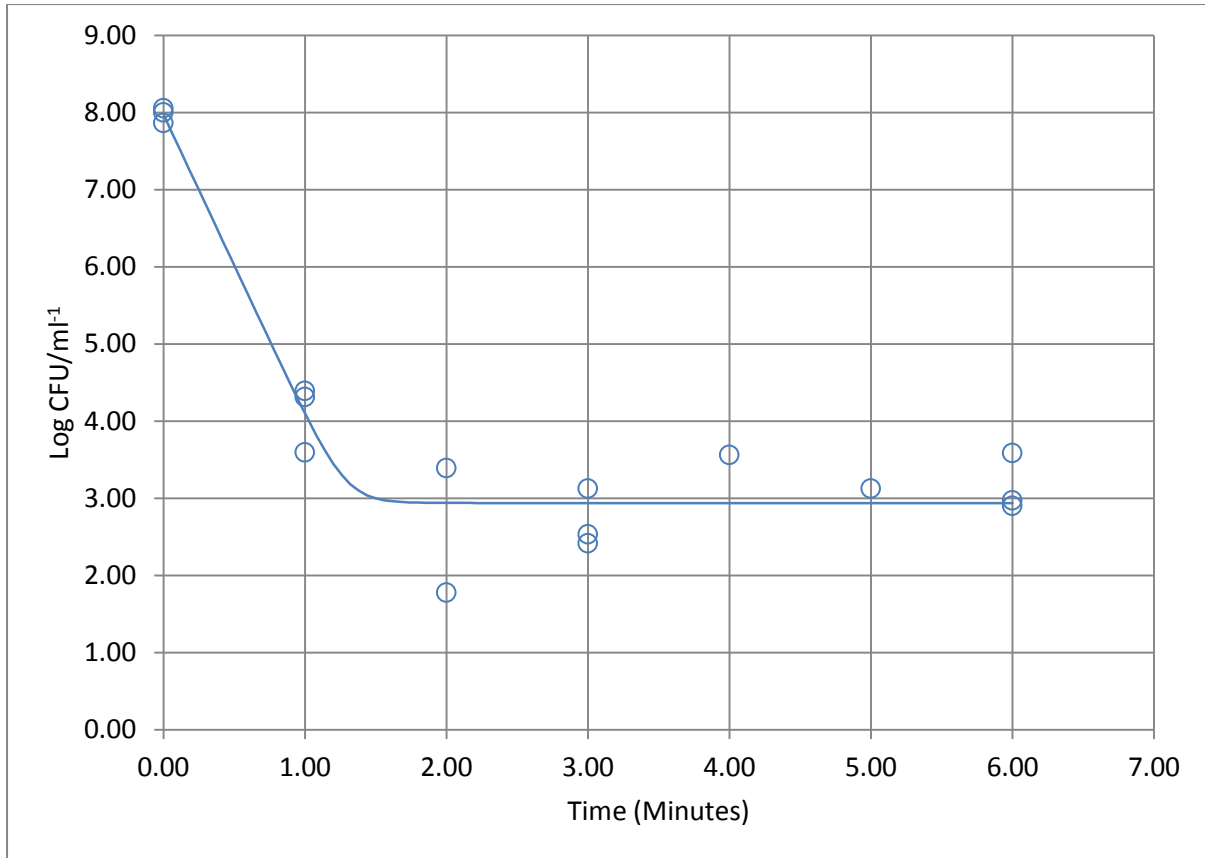


Figure 261. Plot illustrating predicted response curve using a Log-linear model incorporating an asymptotic function for strain 11368 (ST-574, CC-574) following heating at 64°C.

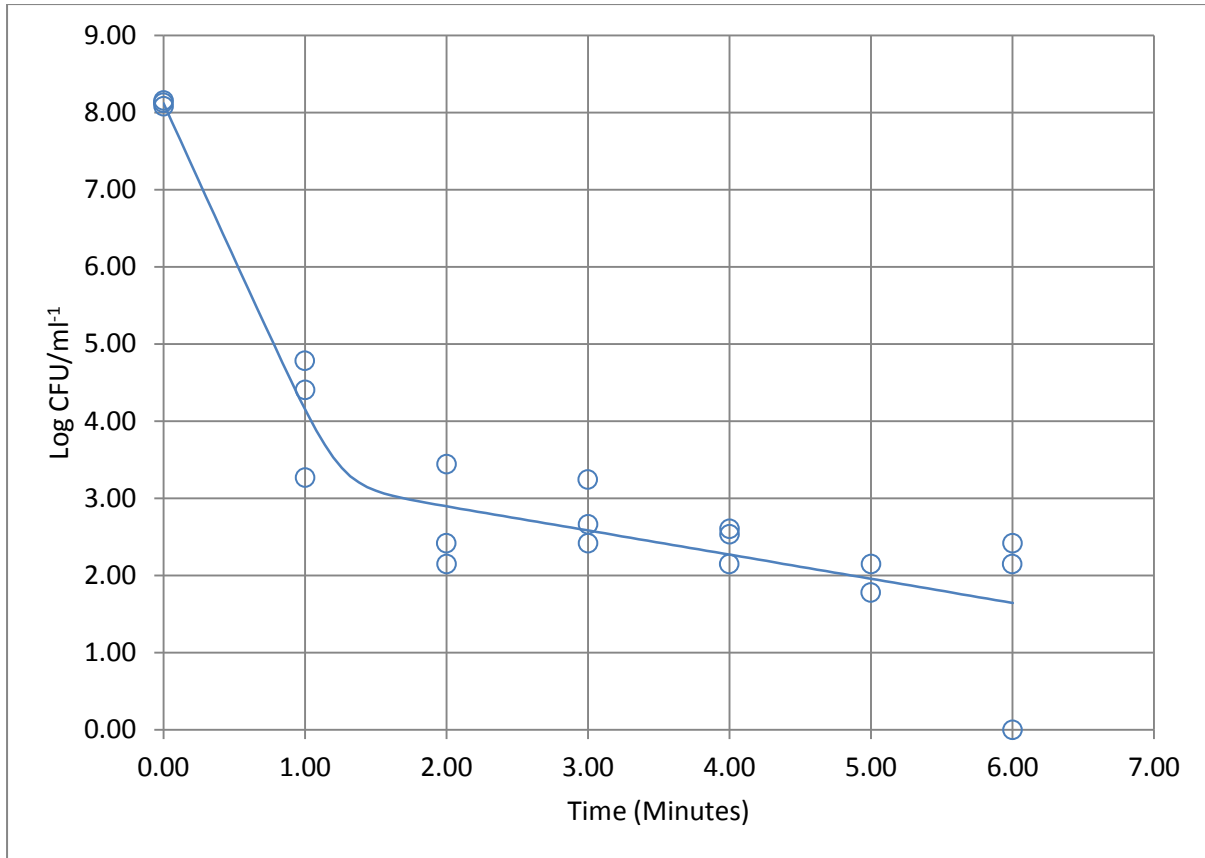


Figure 262. Plot illustrating predicted response curve using a Biphasic model for strain 11762 (ST-829, CC-828) following heating at 64°C.

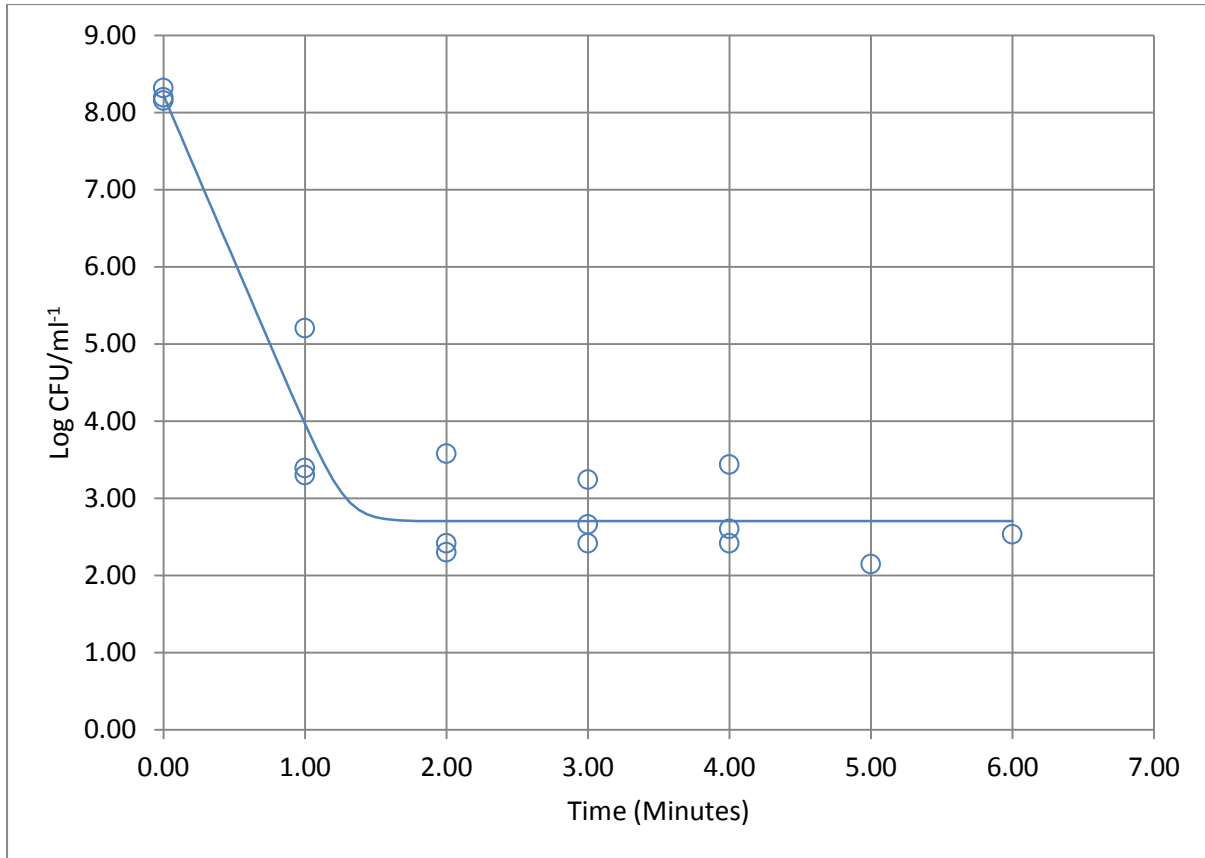


Figure 263. Plot illustrating predicted response curve using a Log-linear model incorporating an asymptotic function for strain 12610 (ST-825, CC-828) following heating at 64°C.

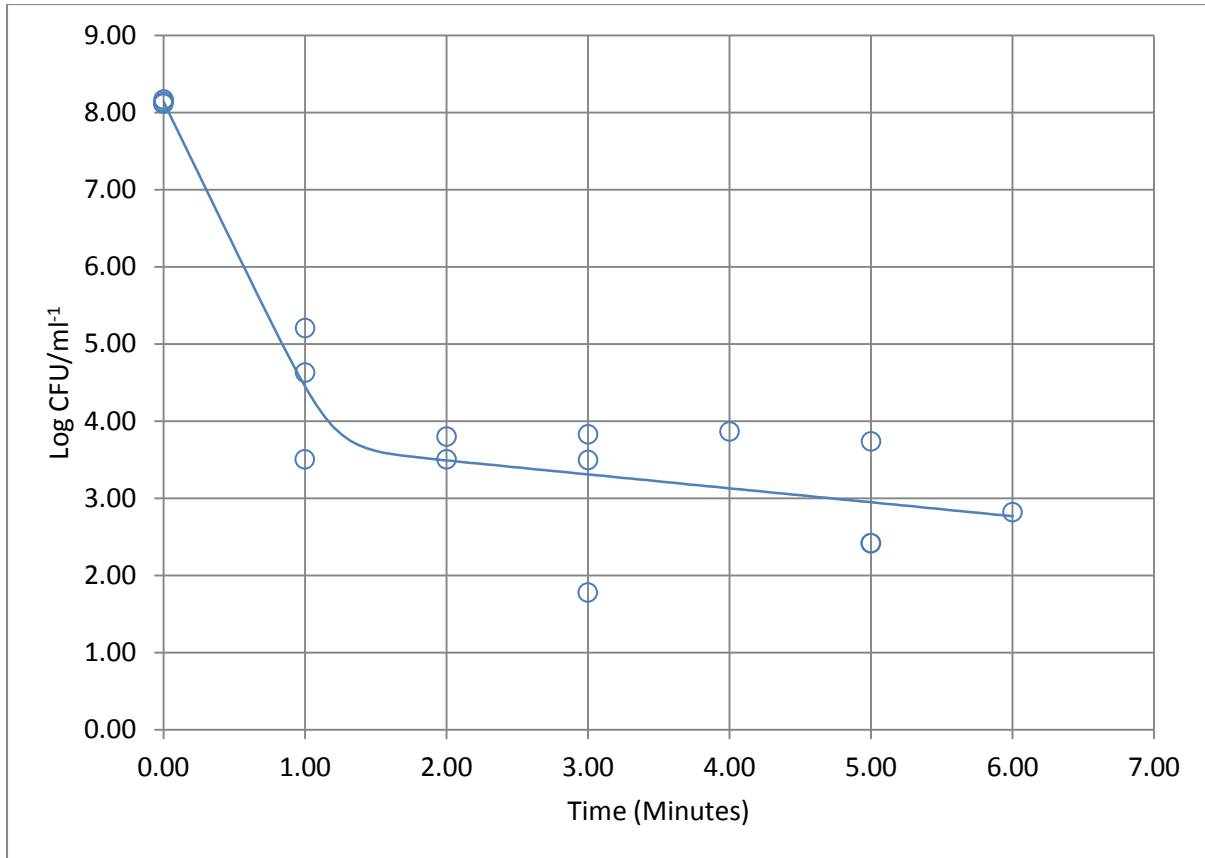


Figure 264. Plot illustrating predicted response curve using a Biphasic model for strain 12628 (ST-1773, CC-828) following heating at 64°C.

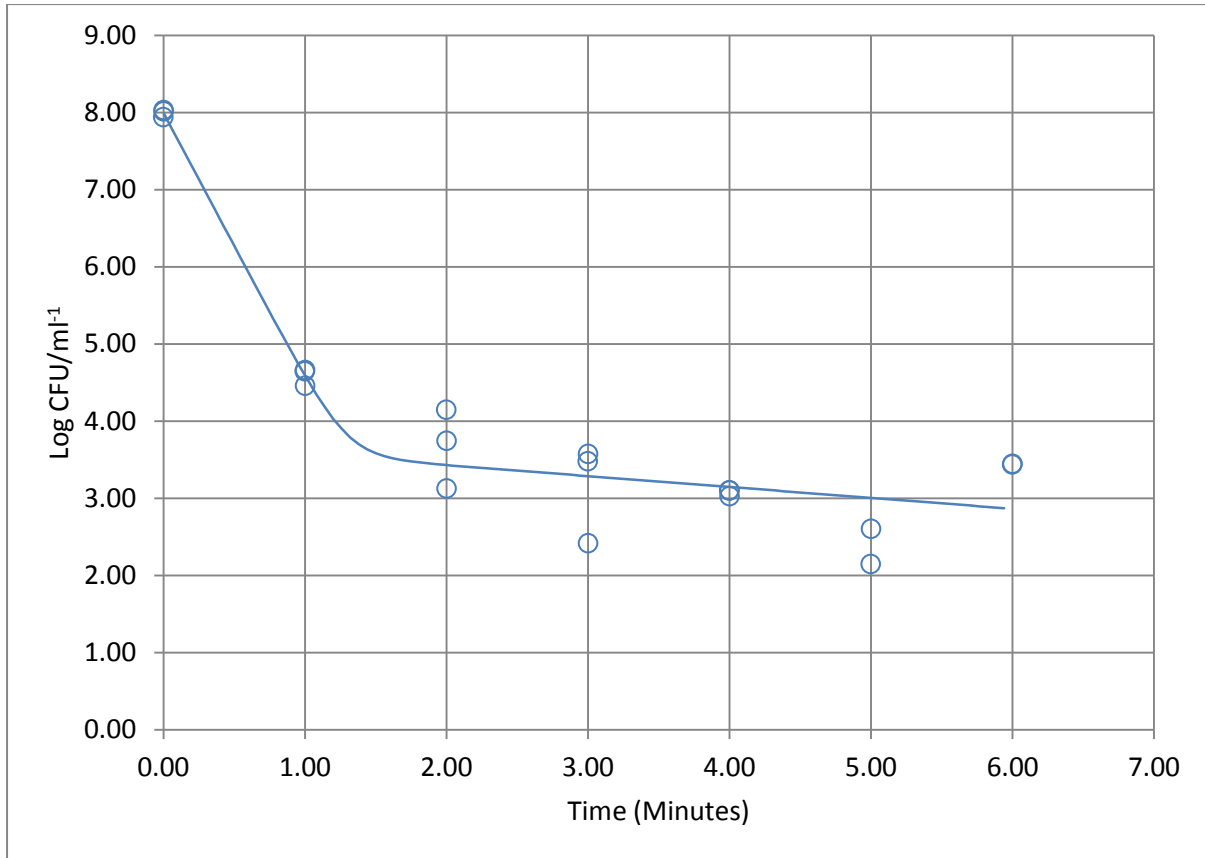


Figure 265. Plot illustrating predicted response curve using a Biphasic model for strain 12645 (ST-51, CC-443) following heating at 64°C.

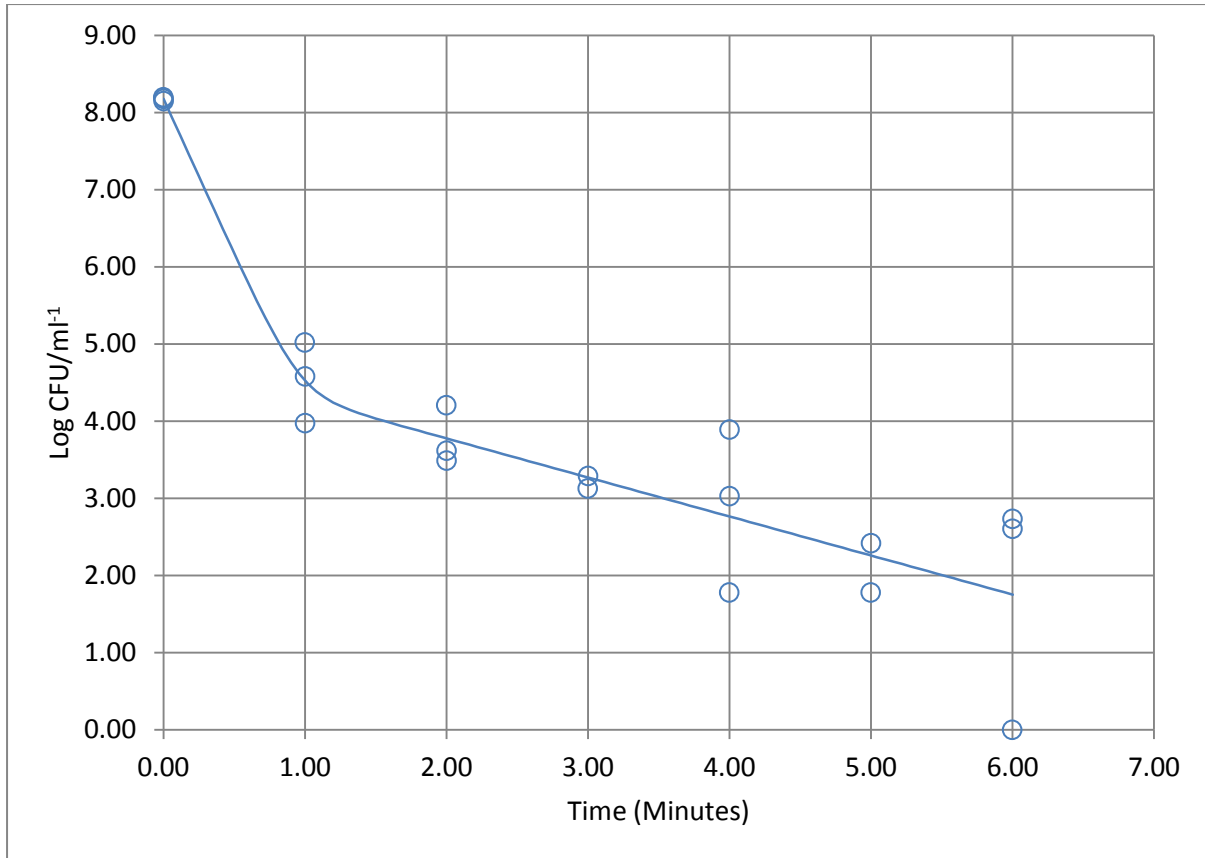


Figure 266. Plot illustrating predicted response curve using a Biphasic model for strain 12662 (ST-257, CC-257) following heating at 64°C.

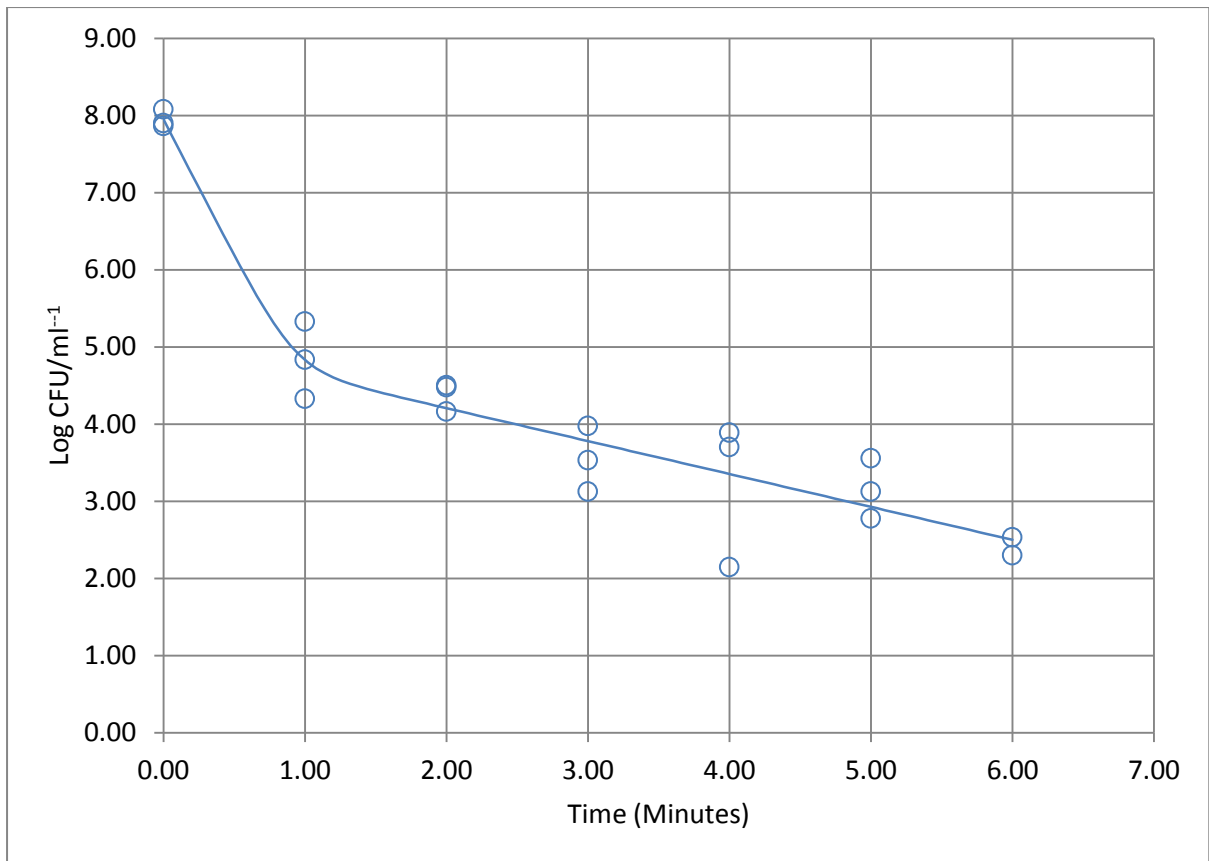


Figure 267. Plot illustrating predicted response curve using a Biphasic model for strain 12720 (ST-51, CC-443) following heating at 64°C.

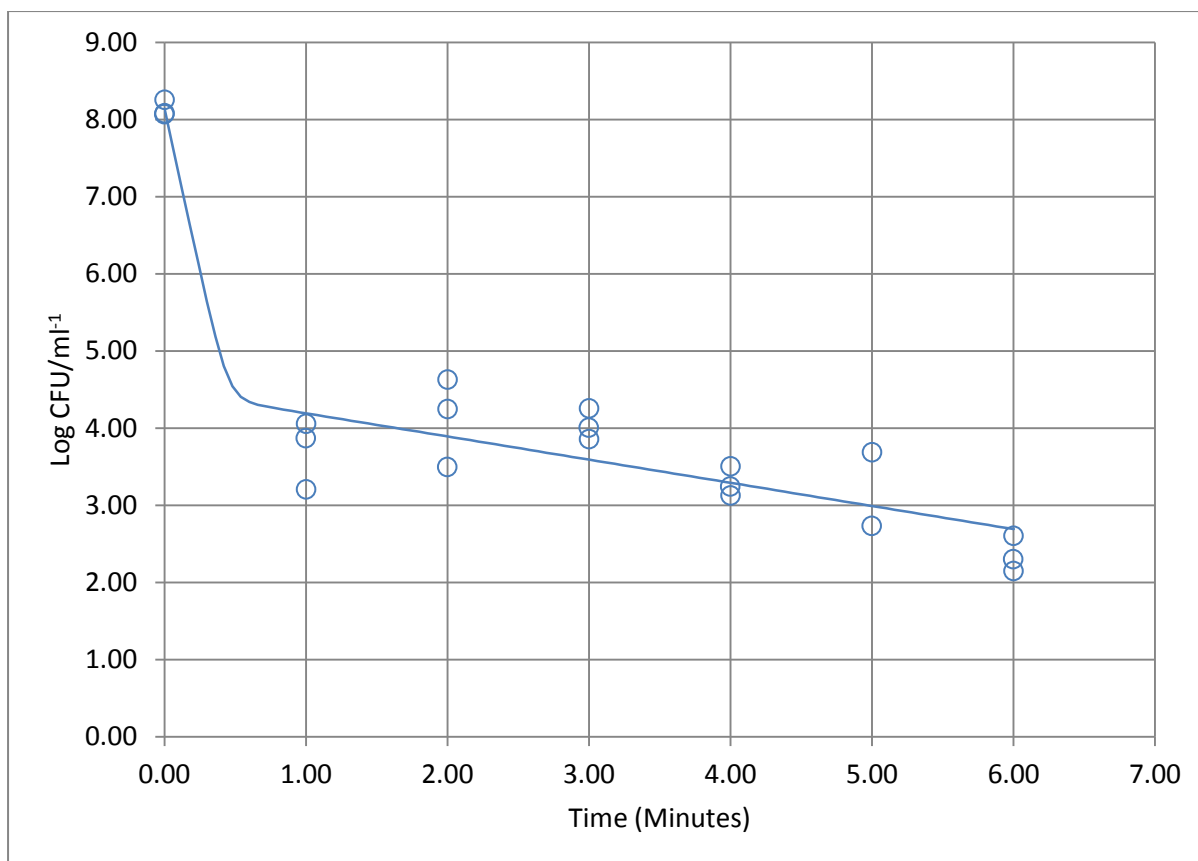


Figure 268. Plot illustrating predicted response curve using a Biphasic model for strain 12745 (ST-257, CC-257) following heating at 64°C.

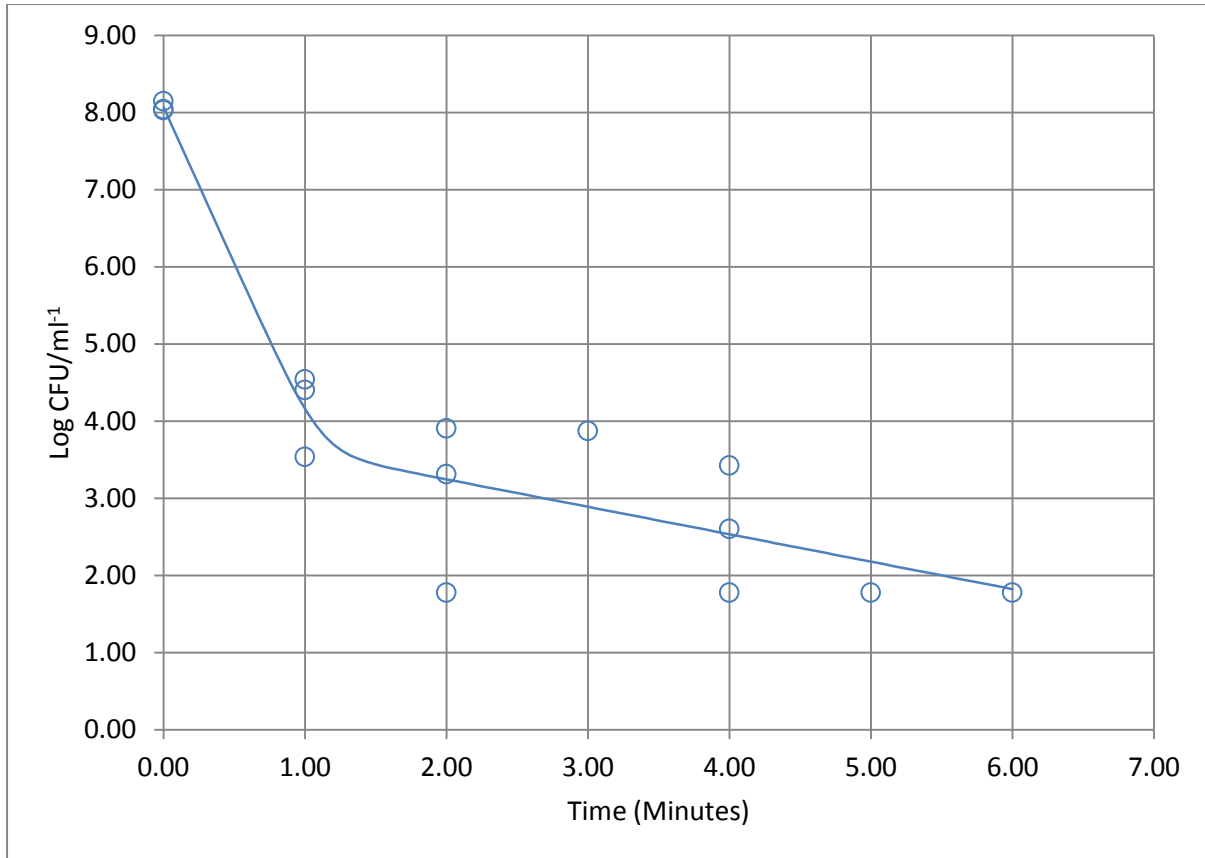


Figure 269. Plot illustrating predicted response curve using a Biphasic model for strain 12783 (ST-574, CC-574) following heating at 64°C.

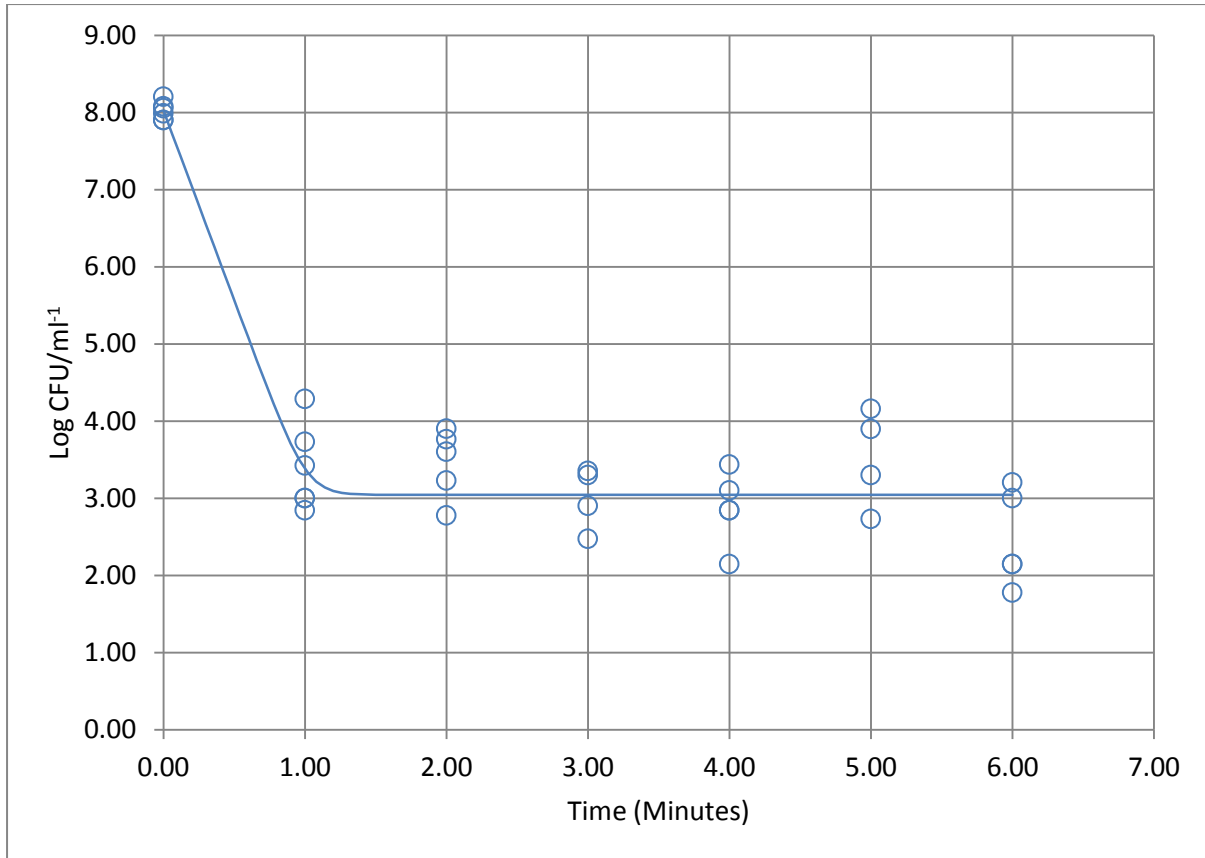


Figure 270. Plot illustrating predicted response curve using a Log-linear model incorporating an asymptotic function for strain 13121 (ST-45, CC-45) following heating at 64°C.

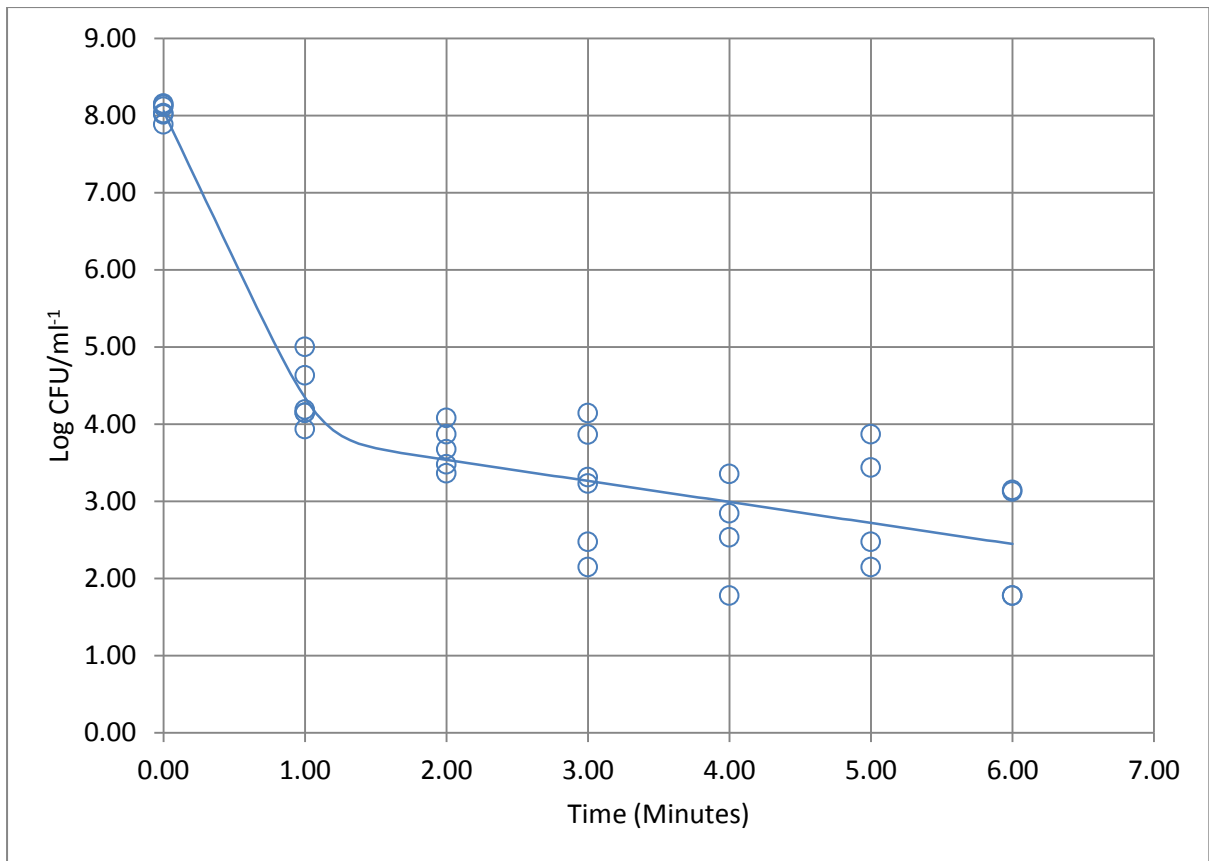


Figure 271. Plot illustrating predicted response curve using a Biphasic model for strain 13126 (ST-21, CC-21) following heating at 64°C.

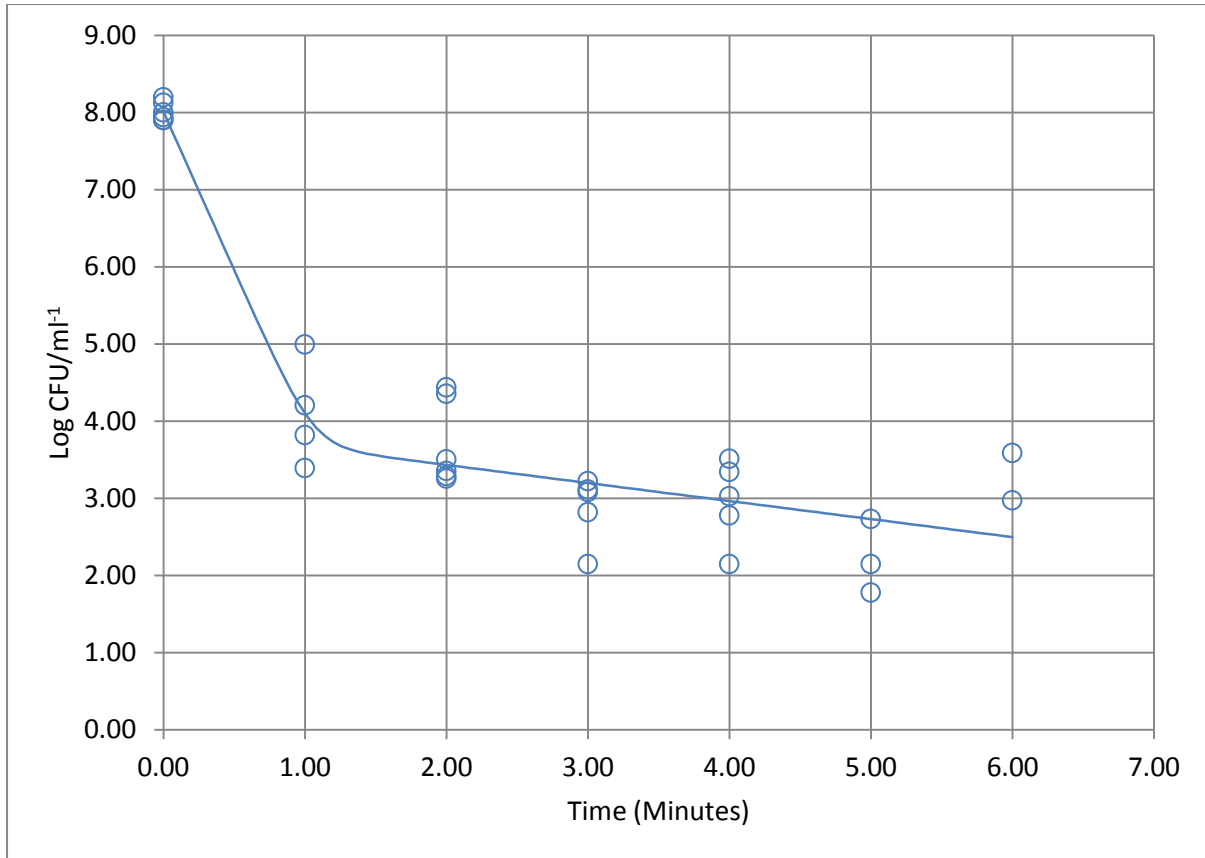


Figure 272. Plot illustrating predicted response curve using a Biphasic model for strain 13136 (ST-45, CC-458) following heating at 64°C.

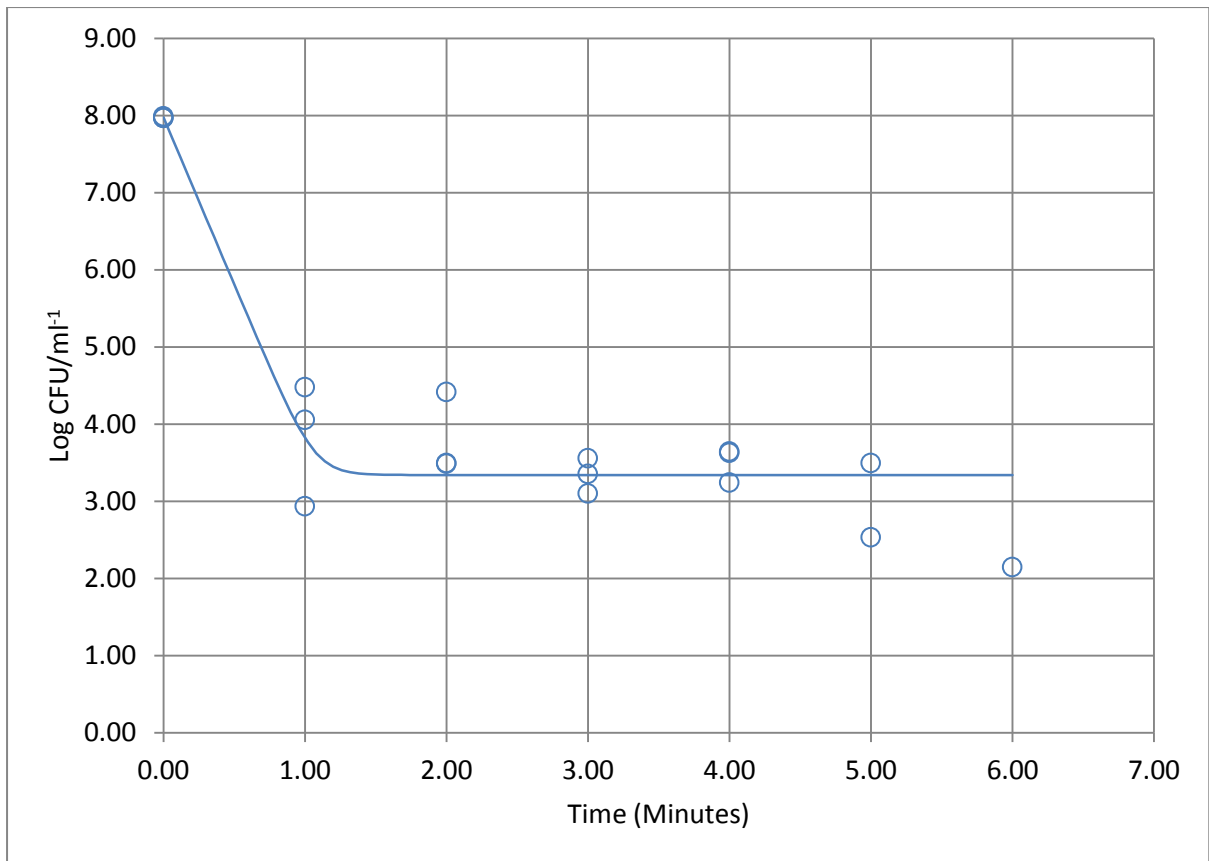


Figure 273. Plot illustrating predicted response curve using a Biphasic model for strain 13163 (ST-21, CC-21) following heating at 64°C.

2.3.11 pH and Time-Temperature Simulation: 56°C

Table 251. Assessment of model fit for individual strains following exposure to pH and heating at 56°C.

Strain	pH	RMSE	$R^2_{adjusted}$	D-value
12628 (ST-1773, CC-828)	4.5	0.417	0.965	0.450
12628 (ST-1773, CC-828)	5.5	0.708	0.905	3.661
12628 (ST-1773, CC-828)	6.5	0.262	0.981	3.192
12628 (ST-1773, CC-828)	7.5	0.314	0.976	2.270
12628 (ST-1773, CC-828)	8.5	0.479	0.938	1.809
12662 (ST-257, CC-257)	4.5	0.627	0.901	0.550
12662 (ST-257, CC-257)	5.5	0.265	0.963	5.624
12662 (ST-257, CC-257)	6.5	0.228	0.969	5.492
12662 (ST-257, CC-257)	7.5	0.273	0.967	3.687
12662 (ST-257, CC-257)	8.5	0.432	0.950	1.496
13126 (ST-21, CC-21)	4.5	0.590	0.913	0.471
13126 (ST-21, CC-21)	5.5	0.321	0.960	4.531
13126 (ST-21, CC-21)	6.5	0.242	0.979	4.136
13126 (ST-21, CC-21)	7.5	0.353	0.952	2.455
13126 (ST-21, CC-21)	8.5	0.324	0.963	1.811
13136 (ST-45, CC-45)	4.5	0.723	0.870	0.510
13136 (ST-45, CC-45)	5.5	0.203	0.987	4.309
13136 (ST-45, CC-45)	6.5	0.251	0.973	3.537
13136 (ST-45, CC-45)	7.5	0.301	0.978	3.100
13136 (ST-45, CC-45)	8.5	0.436	0.945	1.658

Table 252. Biphasic model for survival of strain 12628 (ST-1773, CC-828) following exposure to pH 4.5 and heating at 56°C.

Parameters	Estimates	Standard Error
F	1.000	0.000
Kmax1	5.089	0.413
Kmax2	0.173	0.106
N0	8.068	0.240

Table 253. Mixed Weibull distribution model for survival of strain 12628 (ST-1773, CC-828) following exposure to pH 5.5 and heating at 56°C.

Parameters	Estimates	Standard Error
α	4.096	0.614
δ_1	3.661	0.671
ρ	2.910	1.050
N_0	8.090	0.350
δ_2	10.866	2.432

Table 254. Mixed Weibull distribution model for survival of strain 12628 (ST-1773, CC-828) following exposure to pH 6.5 and heating at 56°C.

Parameters	Estimates	Standard Error
α	3.573	0.515
δ_1	3.192	0.379
ρ	1.664	0.270
N_0	8.100	0.147
δ_2	10.384	2.870

Table 255. Mixed Weibull distribution model for survival of strain 12628 (ST-1773, CC-828) following exposure to pH 7.5 and heating at 56°C.

Parameters	Estimates	Standard Error
α	3.119	1.663
δ_1	2.270	0.427
ρ	1.179	0.207
N_0	8.118	0.183
δ_2	5.618	3.098

Table 256. Mixed Weibull distribution model for survival of strain 12628 (ST-1773, CC-828) following exposure to pH 8.5 and heating at 56°C.

Parameters	Estimates	Standard Error
α	2.811	0.584
δ_1	1.809	0.515
ρ	1.364	0.440
N_0	8.141	0.284
δ_2	6.120	2.290

Table 257. Biphasic model for survival of strain 12662 (ST-257, CC-257) following exposure to pH 4.5 and heating at 56°C.

Parameters	Estimates	Standard Error
F	1.000	0.000
Kmax1	4.241	0.648
Kmax2	0.311	0.132
N0	8.089	0.362

Table 258. Weibull model incorporating an asymptotic function for survival of strain 12662 (ST-257, CC-257) following exposure to pH 5.5 and heating at 56°C.

Parameters	Estimates	Standard Error
Nres	4.510	0.146
δ	5.624	0.448
ρ	2.263	0.386
N0	7.902	0.121

Table 259. Weibull model for survival of strain 12662 (ST-257, CC-257) following exposure to pH 6.5 and heating at 56°C.

Parameters	Estimates	Standard Error
δ	5.492	0.455
ρ	1.646	0.162
N0	7.918	0.108

Table 260. Weibull model incorporating an asymptotic function for survival of strain 12662 (ST-257, CC-257) following exposure to pH 7.5 and heating at 56°C.

Parameters	Estimates	Standard Error
Nres	3.676	0.260
δ	3.687	0.503
ρ	1.316	0.179
N0	7.910	0.147

Table 261. Mixed Weibull distribution model for survival of strain 12662 (ST-257, CC-257) following exposure to pH 8.5 and heating at 56°C.

Parameters	Estimates	Standard Error
α	3.571	0.459
δ_1	1.496	0.369
ρ	1.335	0.323
N_0	7.965	0.257
δ_2	7.756	2.282

Table 262. Biphasic model for survival of strain 13126 (ST-21, CC-21) following exposure to pH 4.5 and heating at 56°C.

Parameters	Estimates	Standard Error
F	1.000	0.000
Kmax1	4.893	1.137
Kmax2	0.419	0.126
N_0	7.972	0.341

Table 263. Weibull model incorporating an asymptotic function for survival of strain 13126 (ST-21, CC-21) following exposure to pH 5.5 and heating at 56°C.

Parameters	Estimates	Standard Error
α	3.910	0.148
δ_1	4.531	0.521
ρ	1.952	0.360
N_0	7.798	0.159

Table 264. Mixed Weibull distribution model for survival of strain 13126 (ST-21, CC-21) following exposure to pH 6.5 and heating at 56°C.

Parameters	Estimates	Standard Error
α	3.595	0.778
δ_1	4.136	0.405
ρ	1.807	0.267
N_0	7.794	0.128
δ_2	15.999	12.720

Table 265. Mixed Weibull distribution model incorporating an asymptotic function for survival of strain 13126 (ST-21, CC-21) following exposure to pH 7.5 and heating at 56°C.

Parameters	Estimates	Standard Error
α	3.579	0.699
δ_1	2.455	0.491
ρ	1.327	0.289
N_0	7.804	0.206
δ_2	20.253	25.151

Table 266. Biphasic model incorporating a shoulder-effect for survival of strain 13126 (ST-21, CC-21) following exposure to pH 8.5 and heating at 56°C.

Parameters	Estimates	Standard Error
F	1.000	0.000
Kmax1	3.632	1.643
Kmax2	0.191	0.096
N_0	7.825	0.187
SI	1.205	0.417

Table 267. Biphasic model for survival of strain 13136 (ST-45, CC-45) following exposure to pH 4.5 and heating at 56°C.

Parameters	Estimates	Standard Error
F	1.000	0.000
Kmax1	4.483	0.844
Kmax2	0.290	0.152
N_0	7.910	0.417

Table 268. Weibull model incorporating an asymptotic function for survival of strain 13136 (ST-45, CC-45) following exposure to pH 5.5 and heating at 56°C.

Parameters	Estimates	Standard Error
Nres	3.635	0.095
δ	4.309	0.306
ρ	1.938	0.202
N_0	8.026	0.101

Table 269. Mixed Weibull distribution model incorporating an asymptotic function for survival of strain 13136 (ST-45, CC-45) following exposure to pH 6.5 and heating at 56°C.

Parameters	Estimates	Standard Error
α	2.951	0.541
δ_1	3.357	0.416
ρ	1.770	0.361
N_0	7.977	0.143
δ_2	9.614	2.503

Table 270. Mixed Weibull distribution model incorporating an asymptotic function for survival of strain 13136 (ST-45, CC-45) following exposure to pH 7.5 and heating at 56°C.

Parameters	Estimates	Standard Error
α	3.290	0.401
δ_1	3.100	0.397
ρ	1.815	0.325
N_0	7.969	0.168
δ_2	8.131	1.419

Table 271. Mixed Weibull distribution model incorporating an asymptotic function for survival of strain 13136 (ST-45, CC-45) following exposure to pH 8.5 and heating at 56°C.

Parameters	Estimates	Standard Error
α	3.805	0.439
δ_1	1.658	0.390
ρ	1.449	0.361
N_0	8.003	0.259
δ_2	10.802	3.644

2.3.12 pH Time-temperature Simulations: 56°C

Predicted Response Curves:

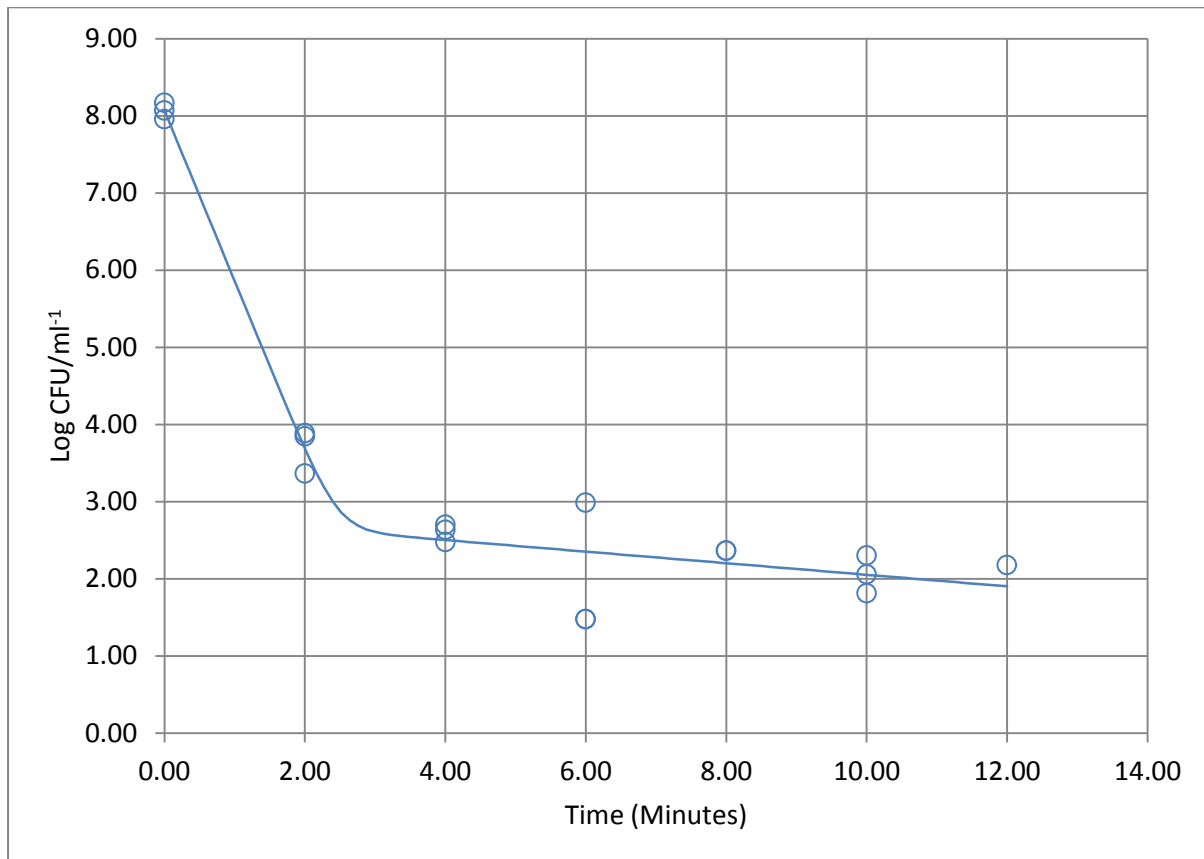


Figure 274. Plot illustrating predicted response using a biphasic model for strain 12628 (ST-1773, CC-828) following exposure to pH 4.5 and heating at 56°C.

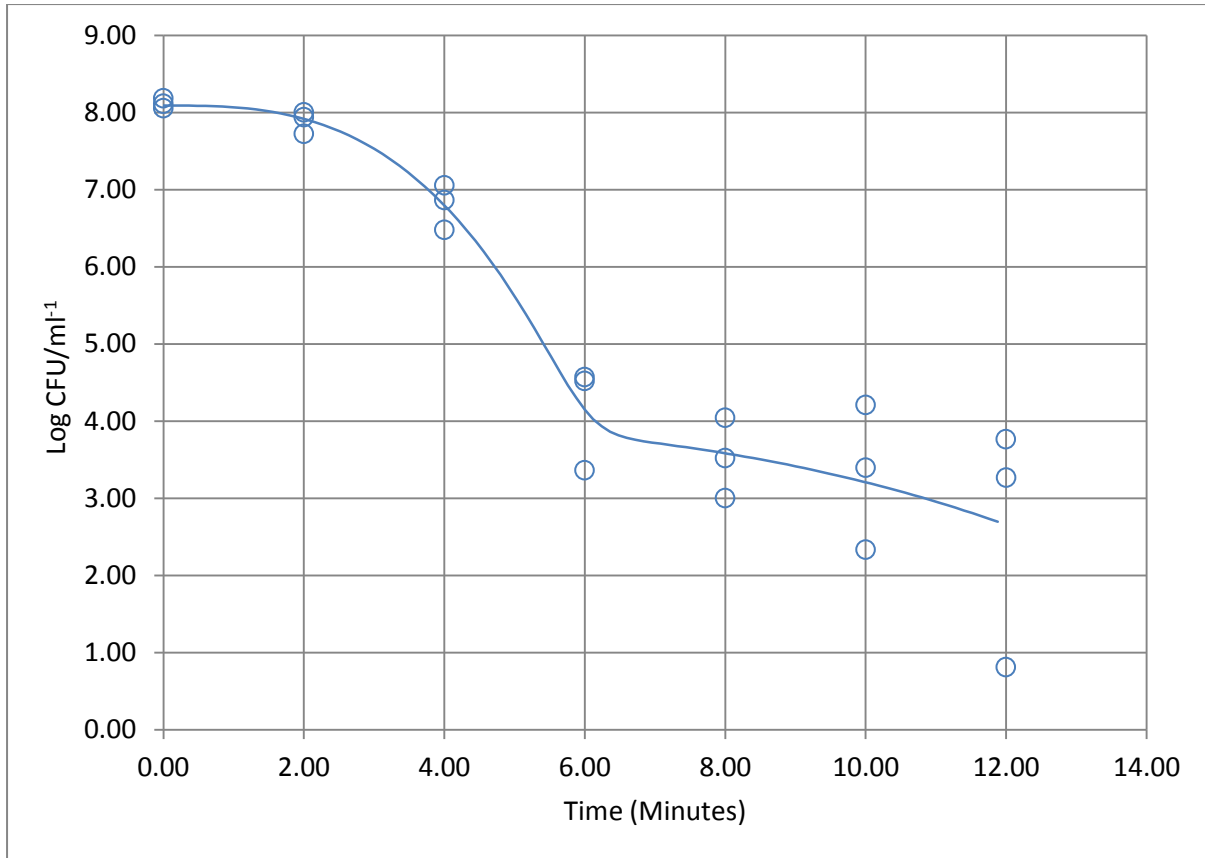


Figure 275. Plot illustrating predicted response using a mixed Weibull distribution model for strain 12628 (ST-1773, CC-828) following exposure to pH 5.5 and heating at 56°C.

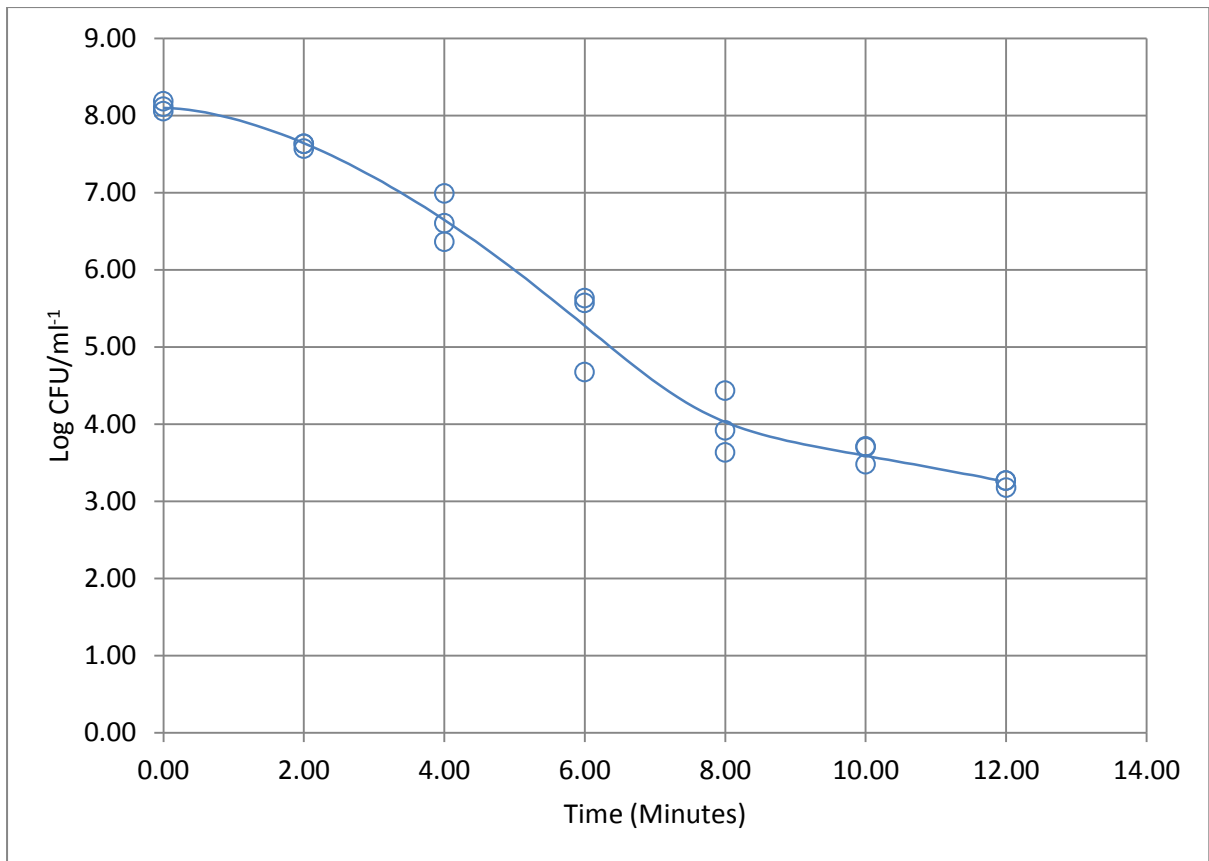


Figure 276. Plot illustrating predicted response using a mixed Weibull distribution model for strain 12628 (ST-1773, CC-828) following exposure to pH 6.5 and heating at 56°C.

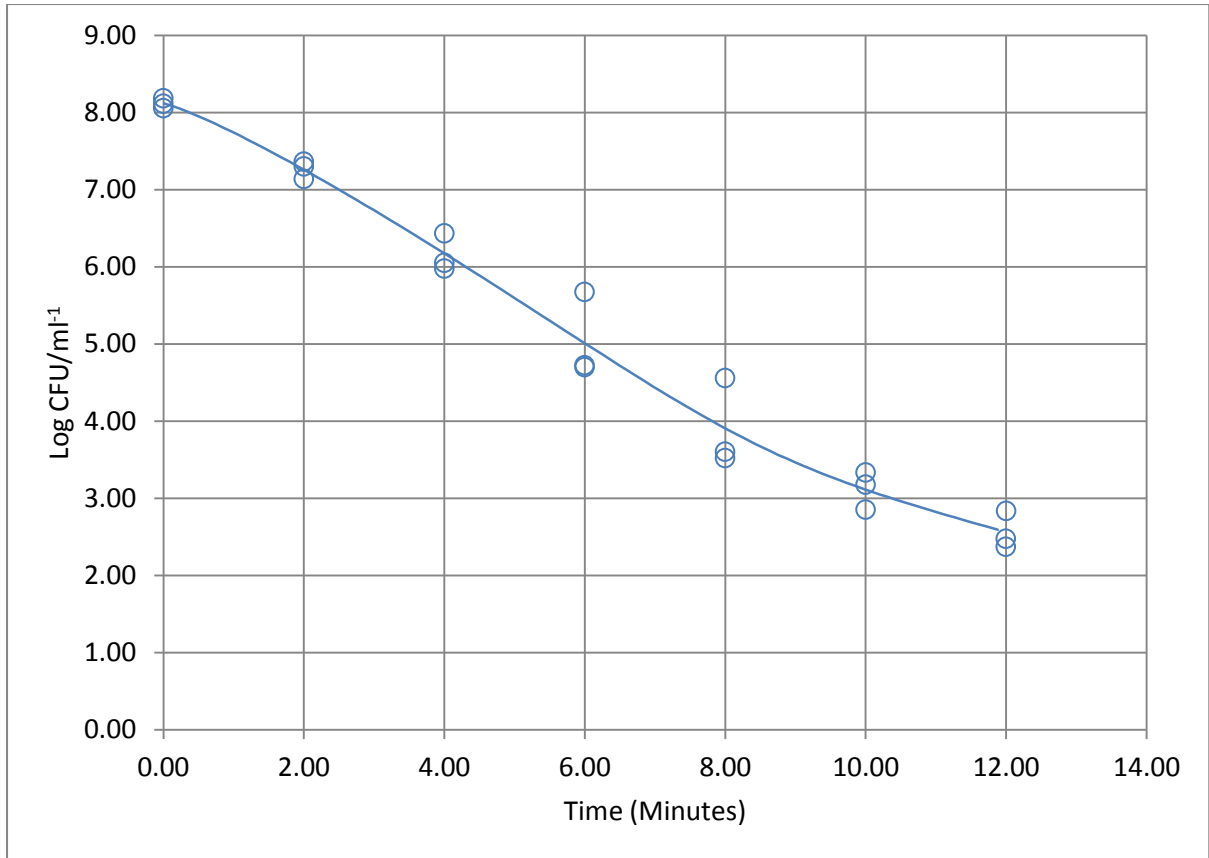


Figure 277. Plot illustrating predicted response using a mixed Weibull distribution model for strain 12628 (ST-1773, CC-828) following exposure to pH 7.5 and heating at 56°C.

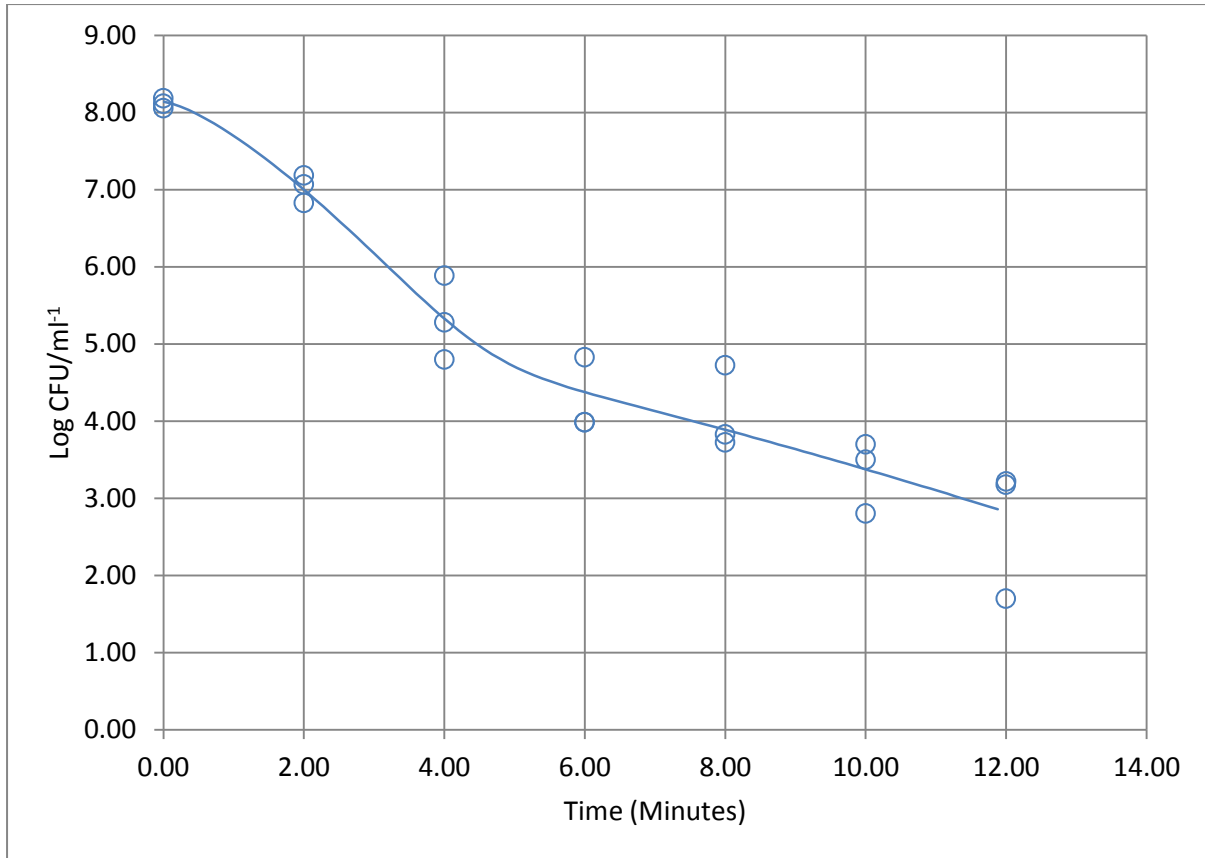


Figure 278. Plot illustrating predicted response using a mixed Weibull distribution model for strain 12628 (ST-1773, CC-828) following exposure to pH 8.5 and heating at 56°C.

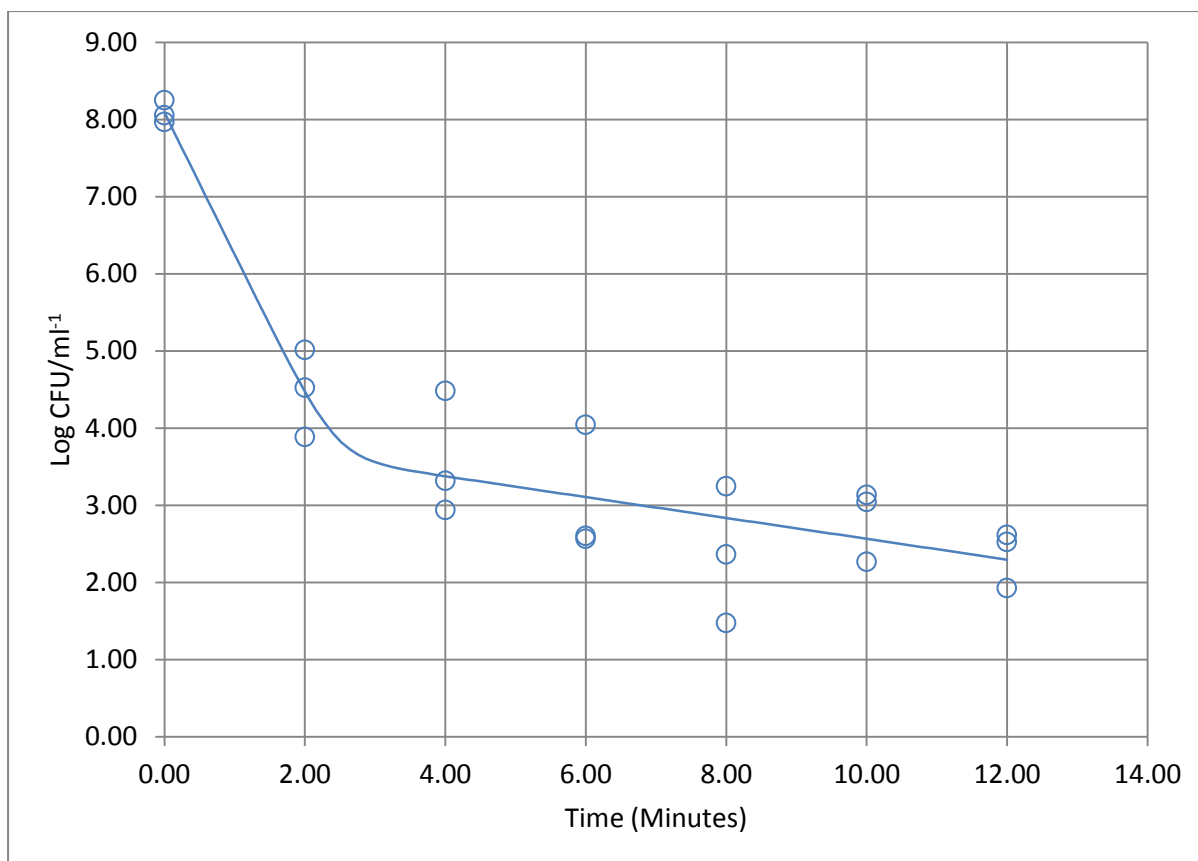


Figure 279. Plot illustrating predicted response using a biphasic model for strain 12662 (ST-257, CC-257) following exposure to pH 4.5 and heating at 56°C.

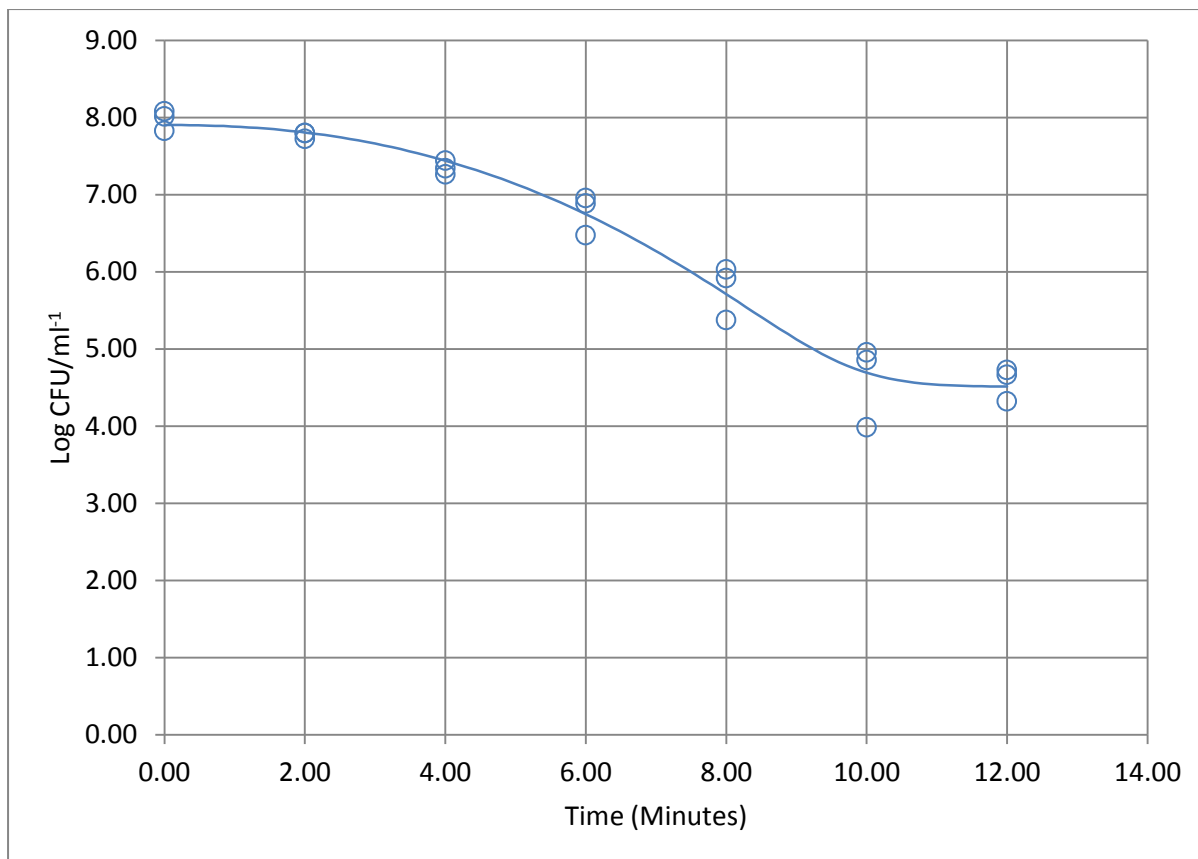


Figure 280. Plot illustrating predicted response using a Weibull model incorporating an asymptotic function strain 12662 (ST-257, CC-257) following exposure to pH 5.5 and heating at 56°C.

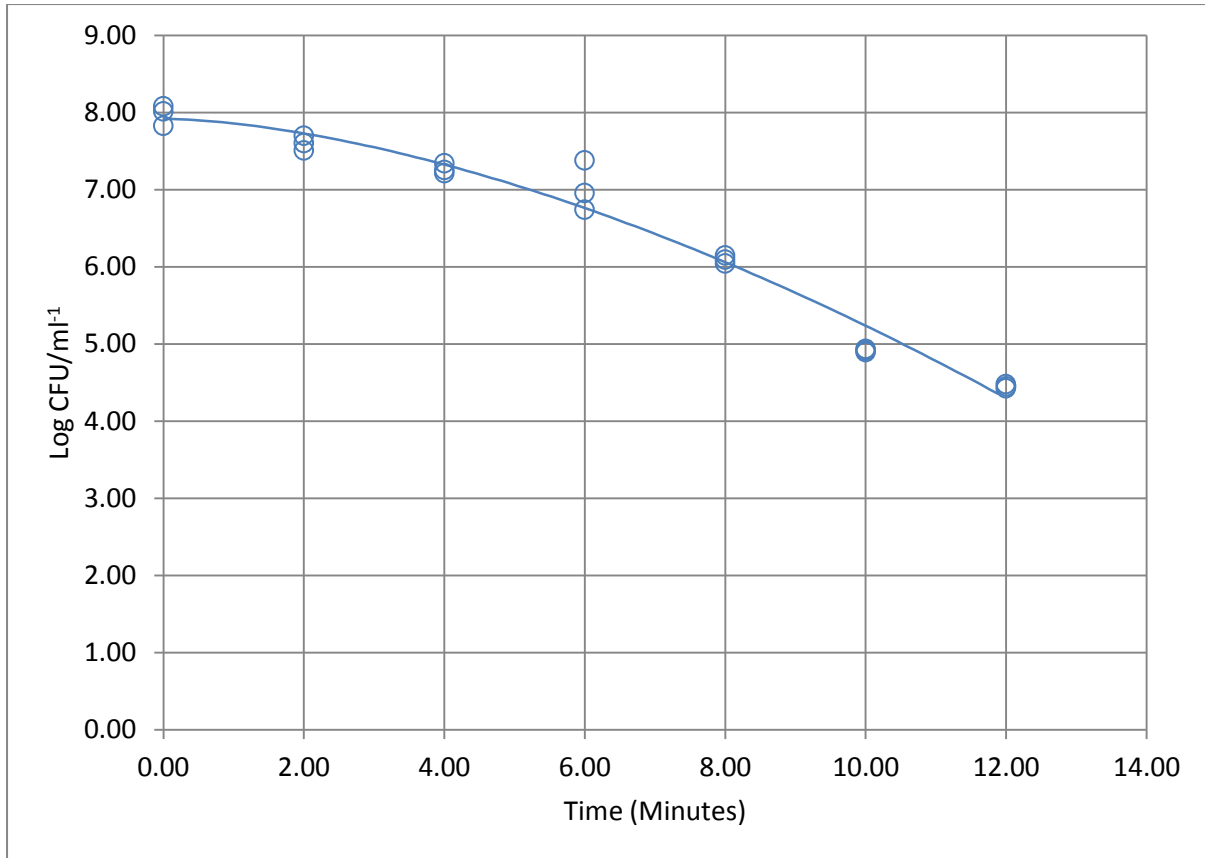


Figure 281. Plot illustrating predicted response using a Weibull model for strain 12662 (ST-257, CC-257) following exposure to pH 6.5 and heating at 56°C.

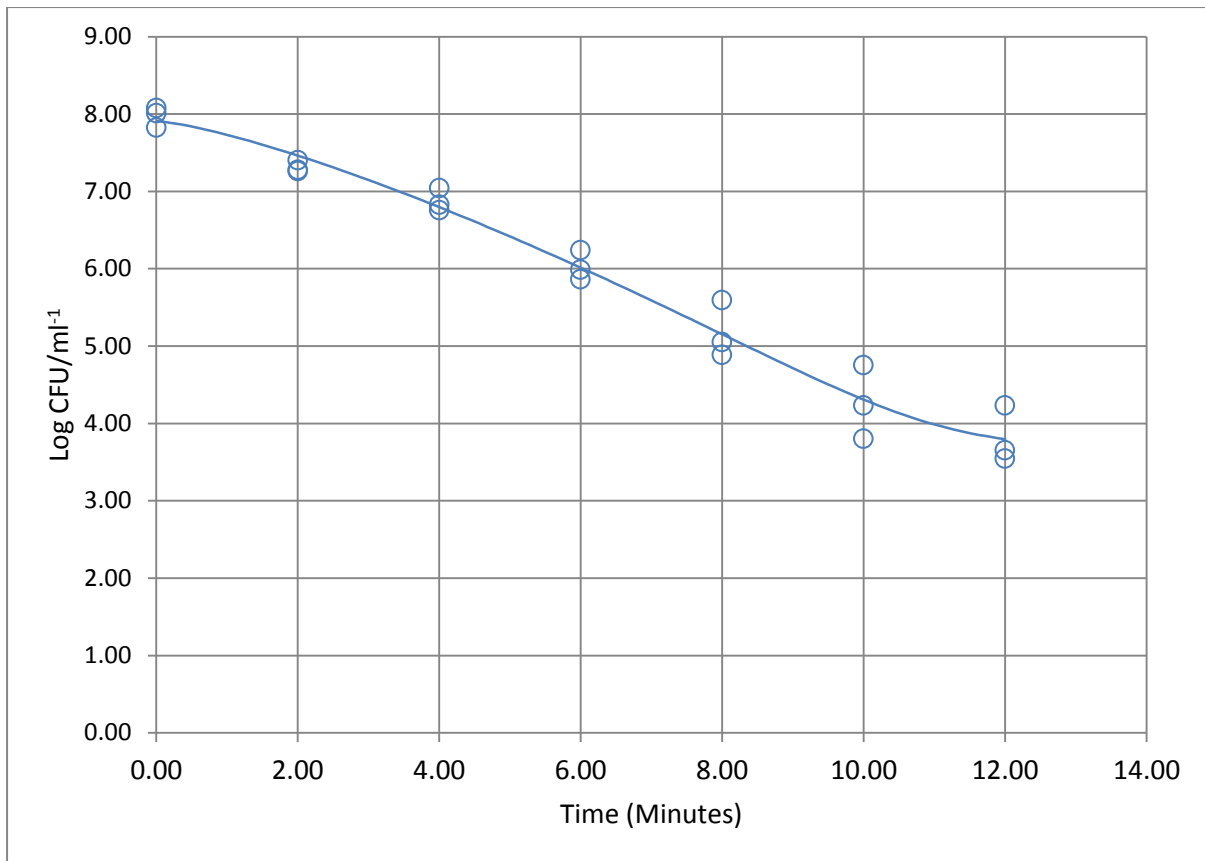


Figure 282. Plot illustrating predicted response using a Weibull model incorporating an asymptotic function for strain 12662 (ST-257, CC-257) following exposure to pH 7.5 and heating at 56°C.

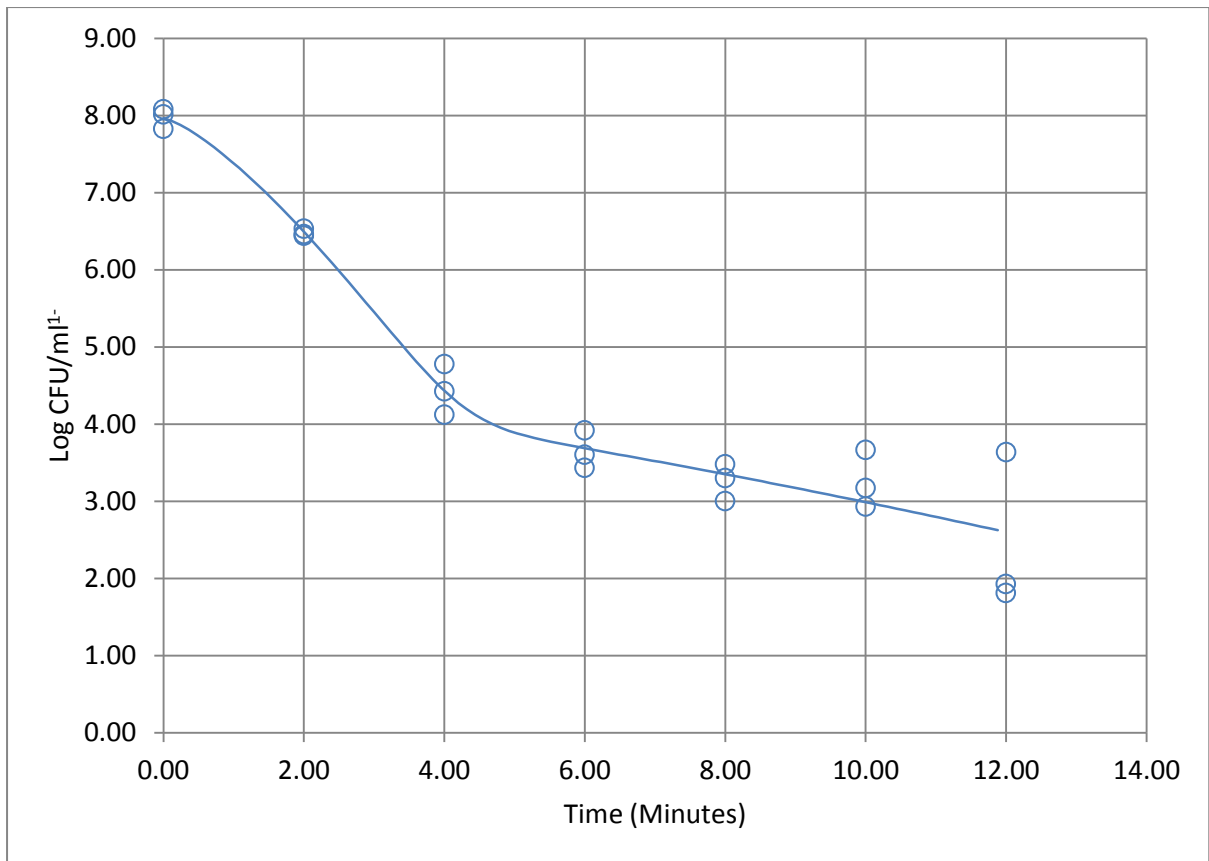


Figure 283. Plot illustrating predicted response using a mixed Weibull distribution model for strain 12662 (ST-257, CC-257) following exposure to pH 8.5 and heating at 56°C.

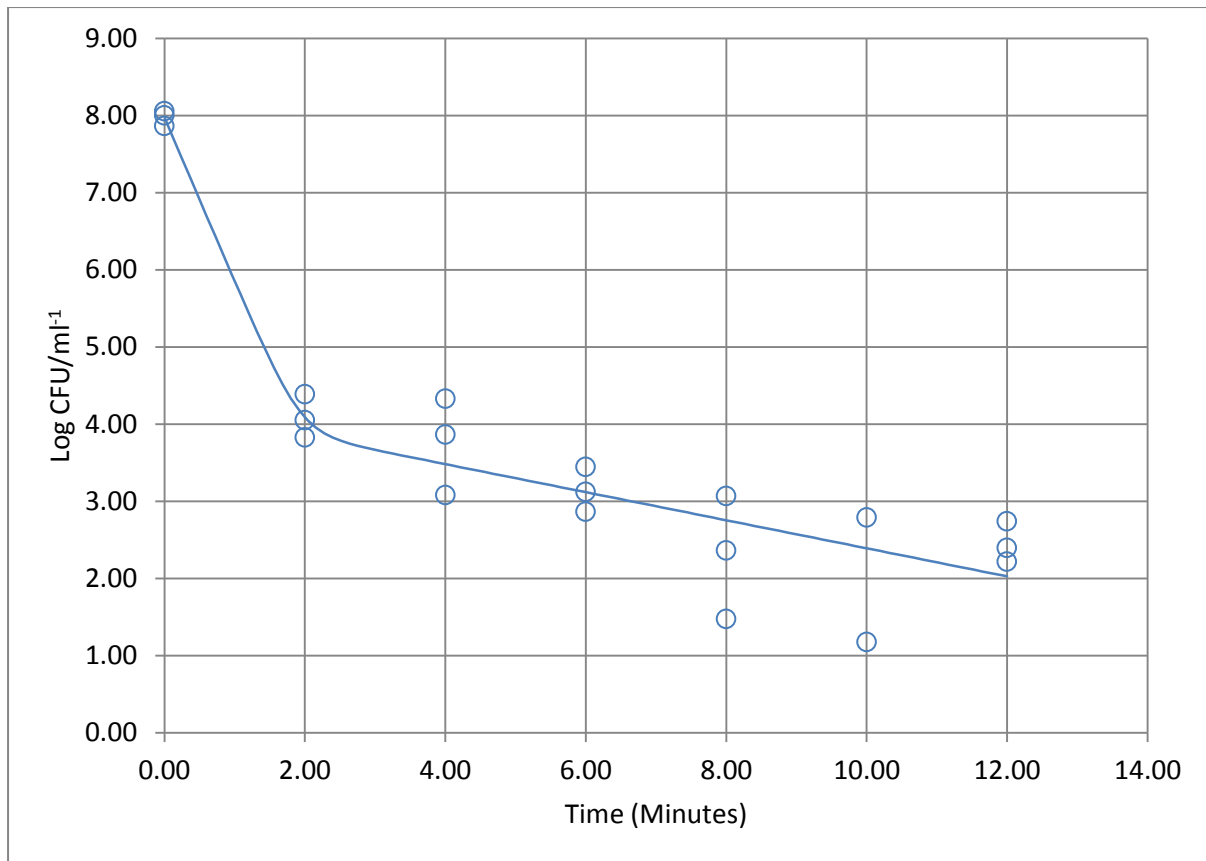


Figure 284. Plot illustrating predicted response using a Biphasic model for strain 13126 (ST-21, CC-21) following exposure to pH 4.5 and heating at 56°C.

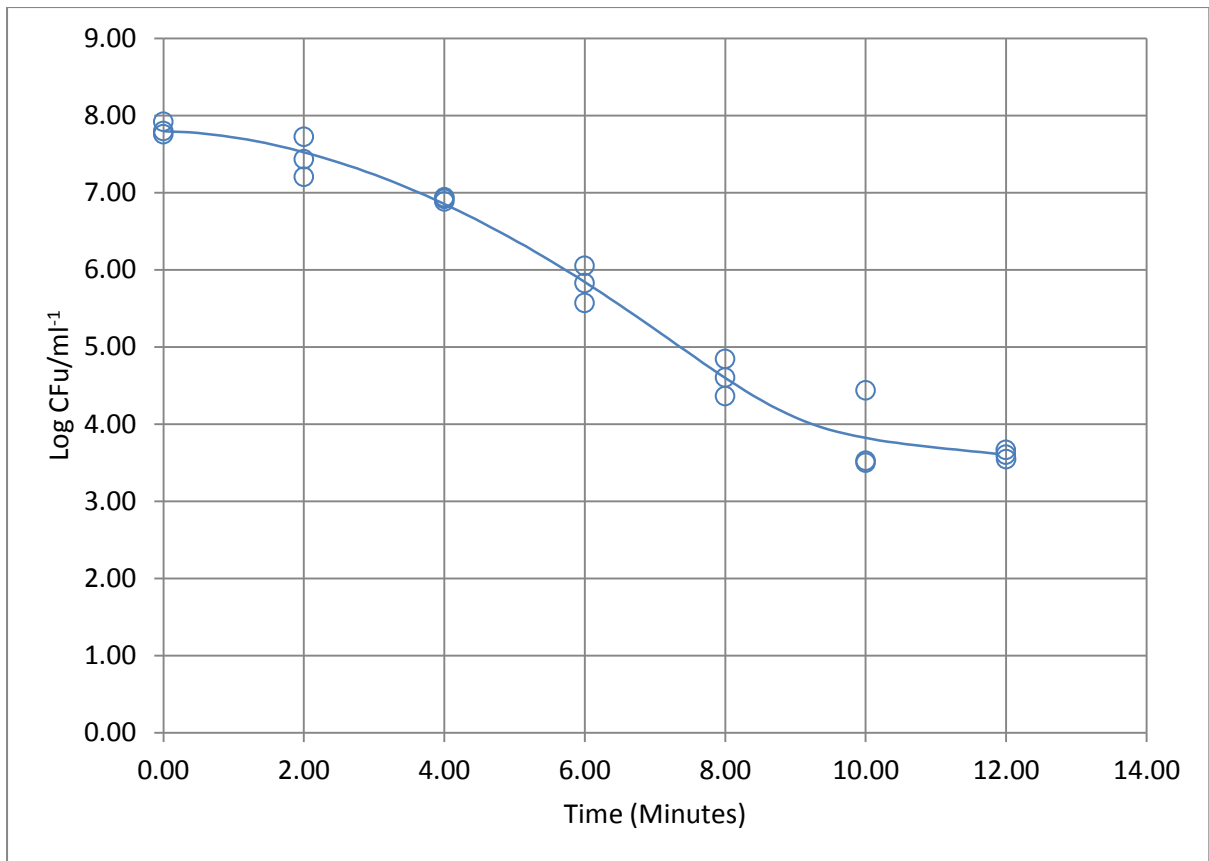


Figure 285. Plot illustrating predicted response using a mixed Weibull distribution model for strain 13126 (ST-21, CC-21) following exposure to pH 5.5 and heating at 56°C.

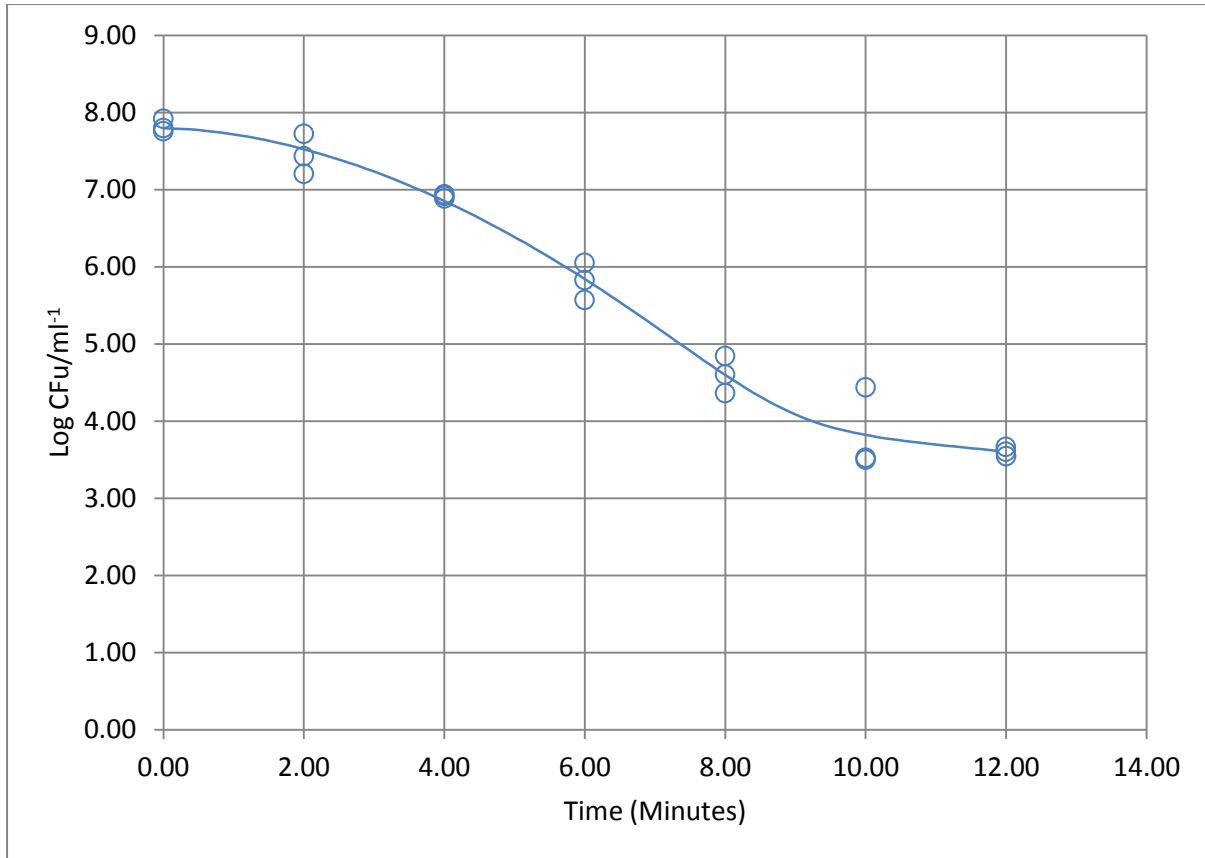


Figure 286. Plot illustrating predicted response using a mixed Weibull distribution model for strain 13126 (ST-21, CC-21) following exposure to pH 6.5 and heating at 56°C.

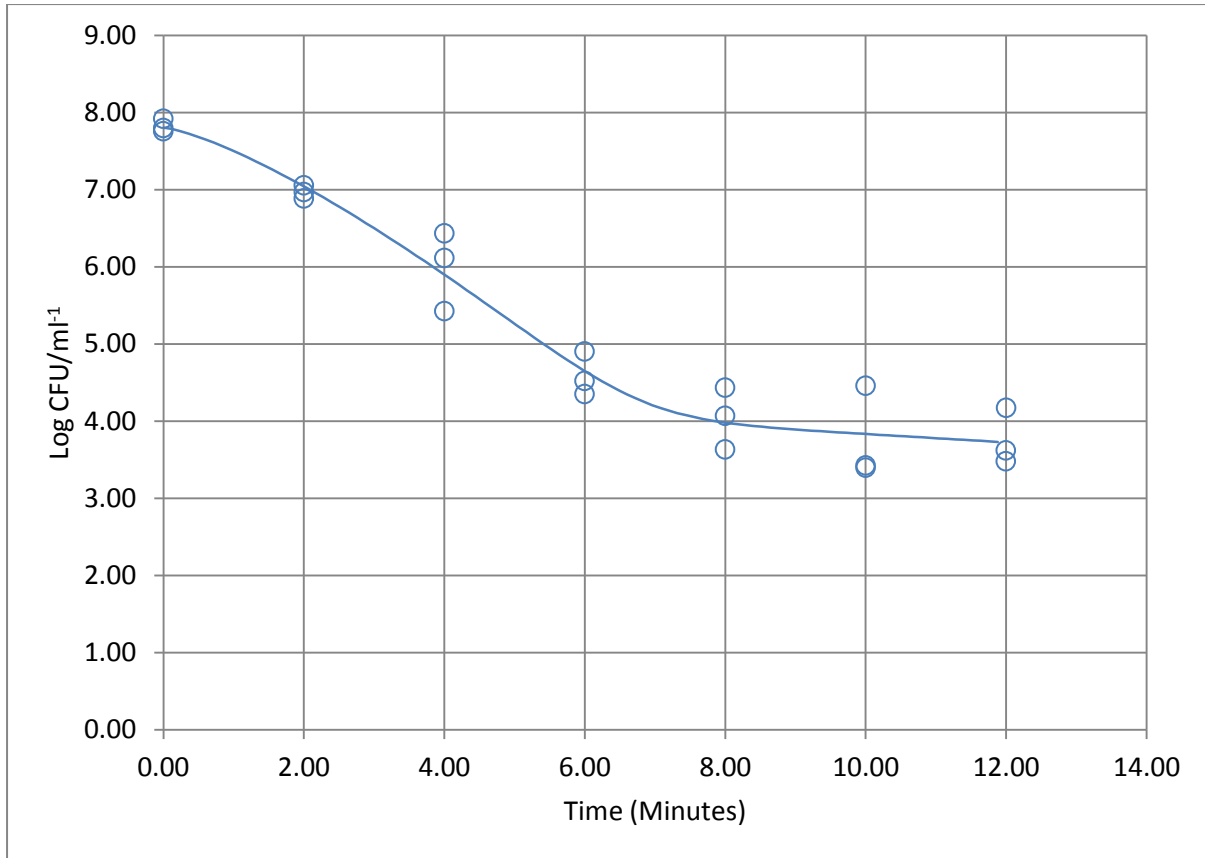


Figure 287. Plot illustrating predicted response using a mixed Weibull distribution model for strain 13126 (ST-21, CC-21) following exposure to pH 7.5 and heating at 56°C.

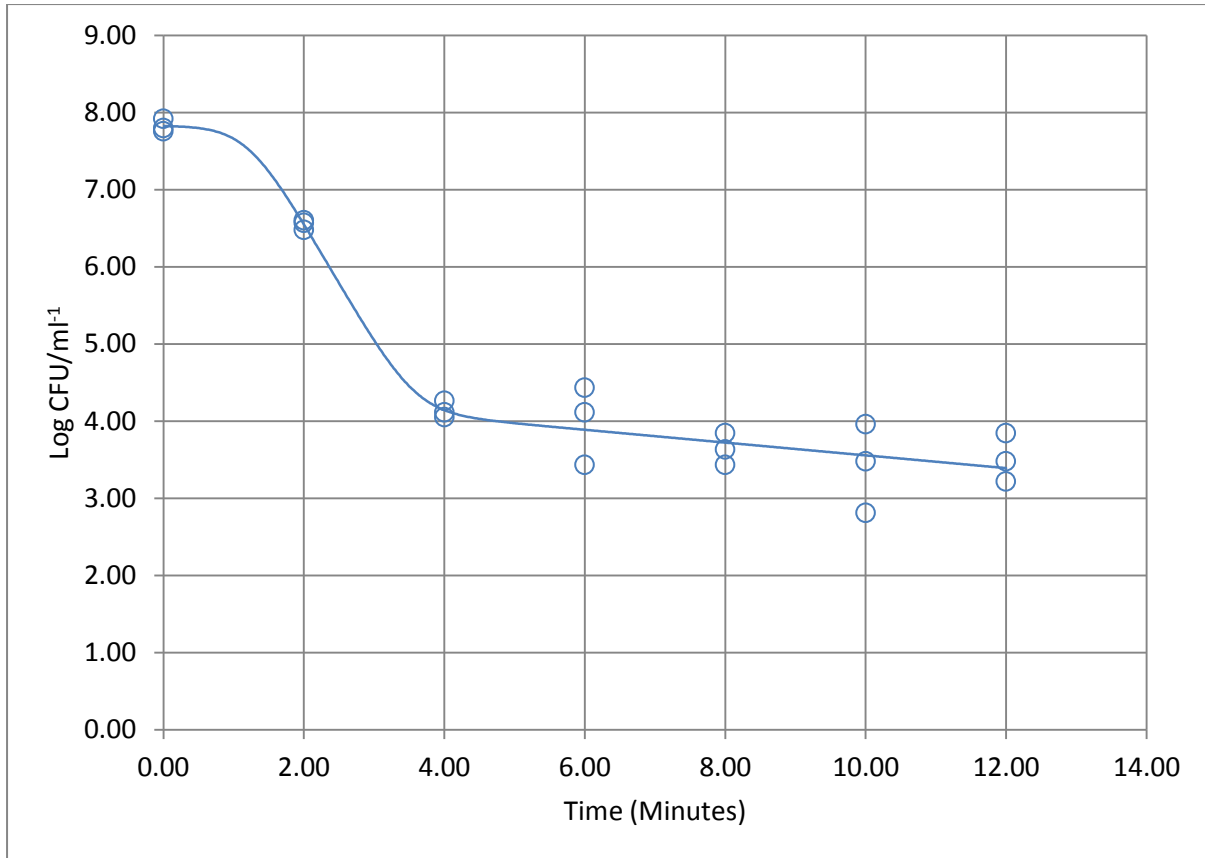


Figure 288. Plot illustrating predicted response using a mixed Weibull distribution model for strain 13126 (ST-21, CC-21) following exposure to pH 8.5 and heating at 56°C.

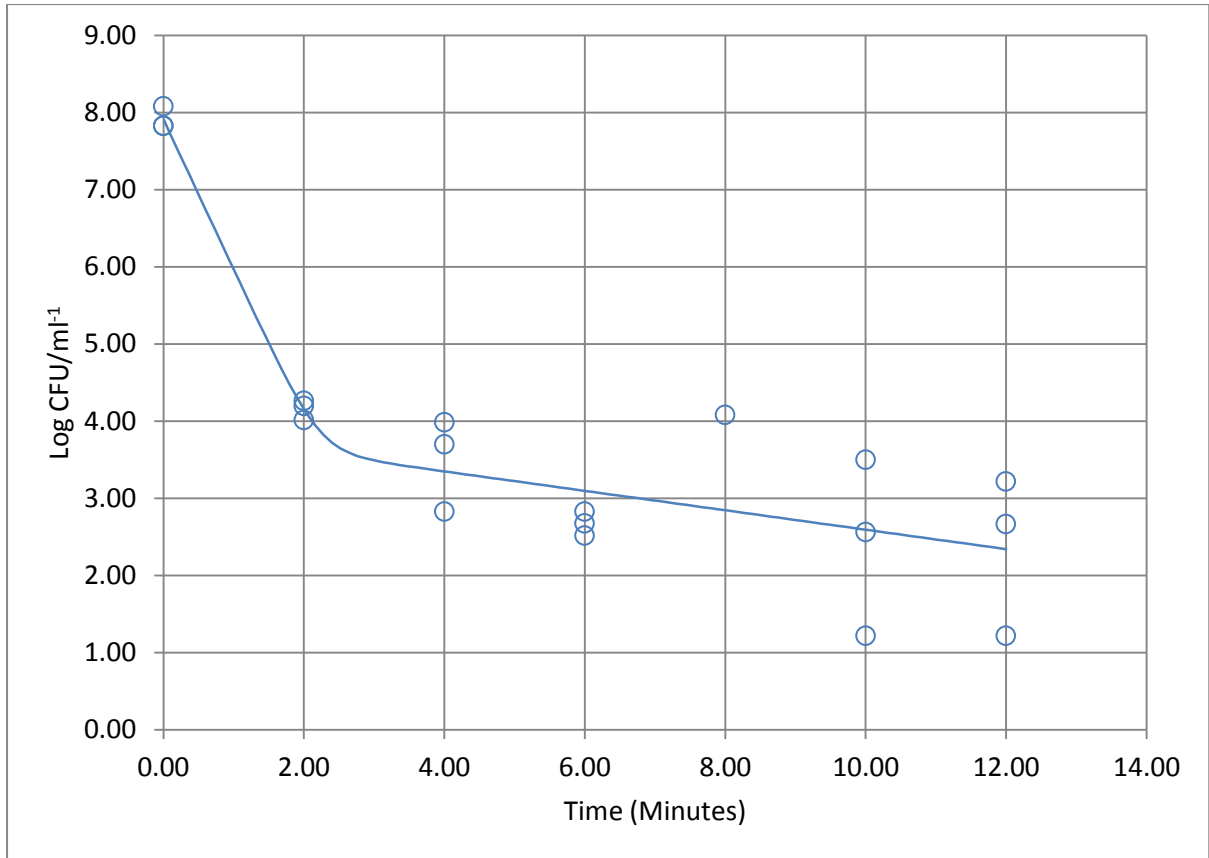


Figure 289. Plot illustrating predicted response using a biphasic model for strain 13136 (ST-45, CC-45) following exposure to pH 4.5 and heating at 56°C.

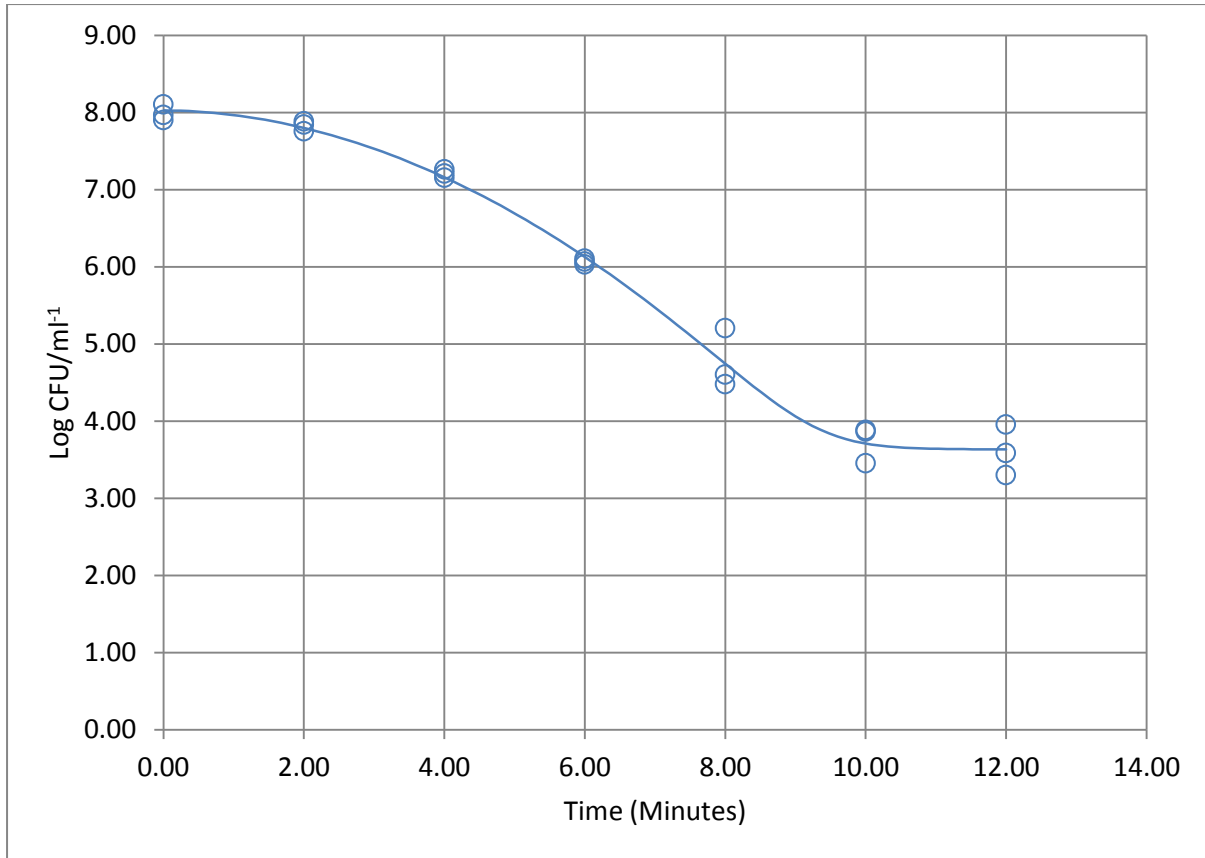


Figure 290. Plot illustrating predicted response using a Weibull model incorporating an asymptotic function for strain 13136 (ST-45, CC-45) following exposure to pH 5.5 and heating at 56°C.

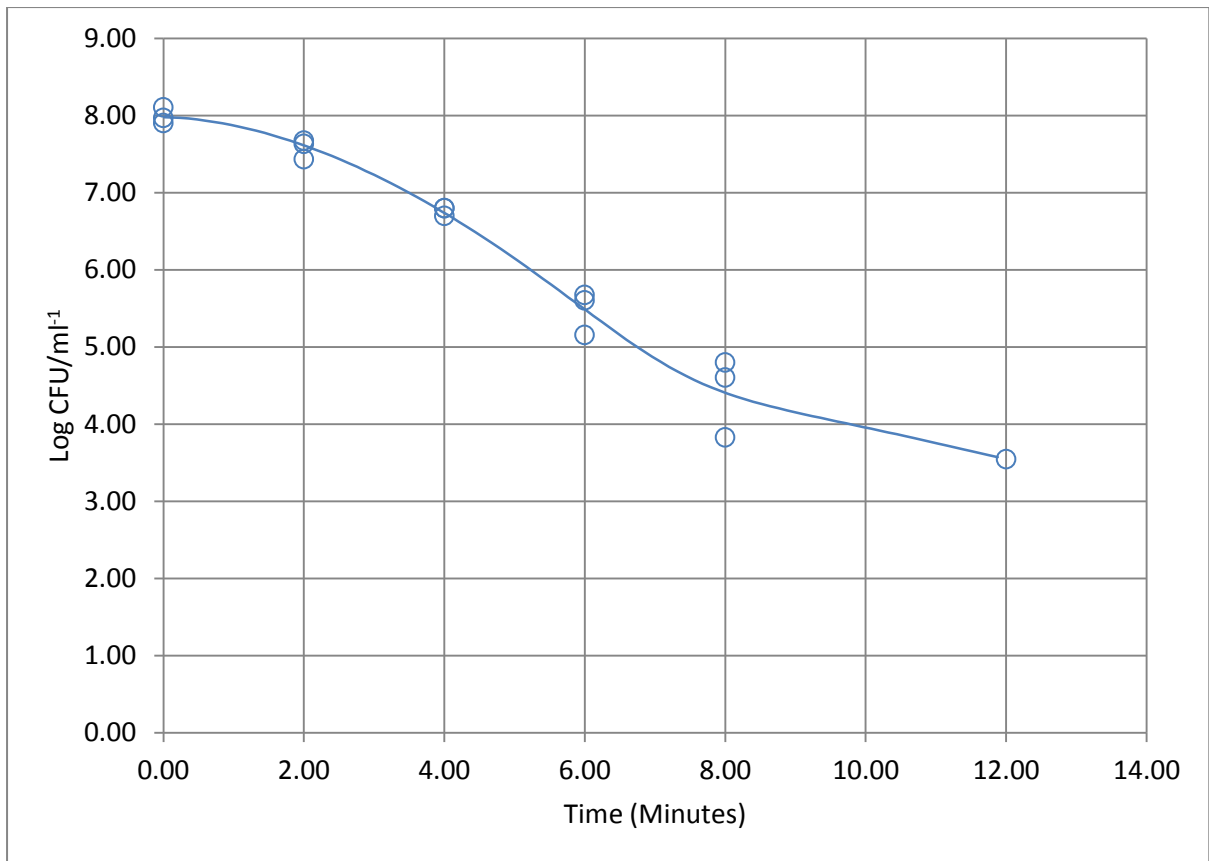


Figure 291. Plot illustrating predicted response using a mixed Weibull distribution model for strain 13136 (ST-45, CC-45) following exposure to pH 6.5 and heating at 56°C.

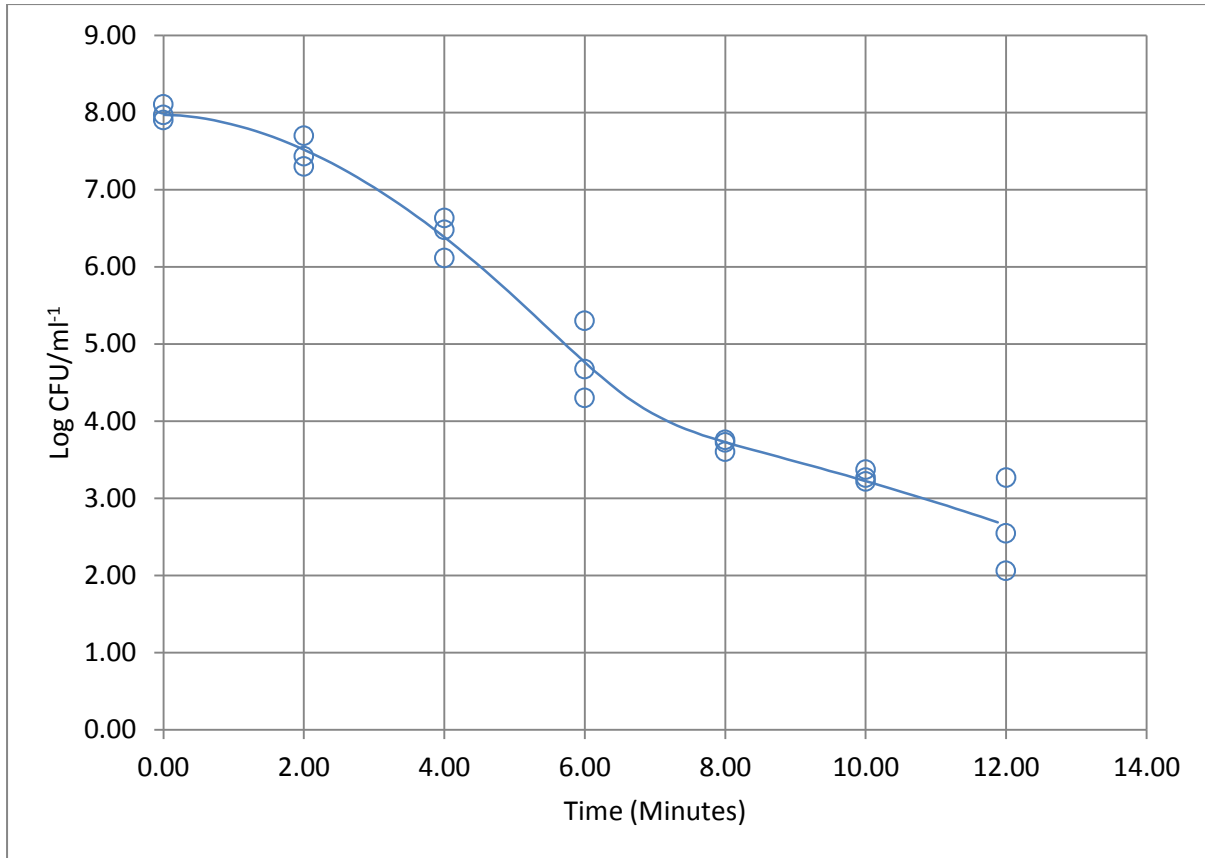


Figure 292. Plot illustrating predicted response using a mixed Weibull distribution model for strain 13136 (ST-45, CC-45) following exposure to pH 7.5 and heating at 56°C.

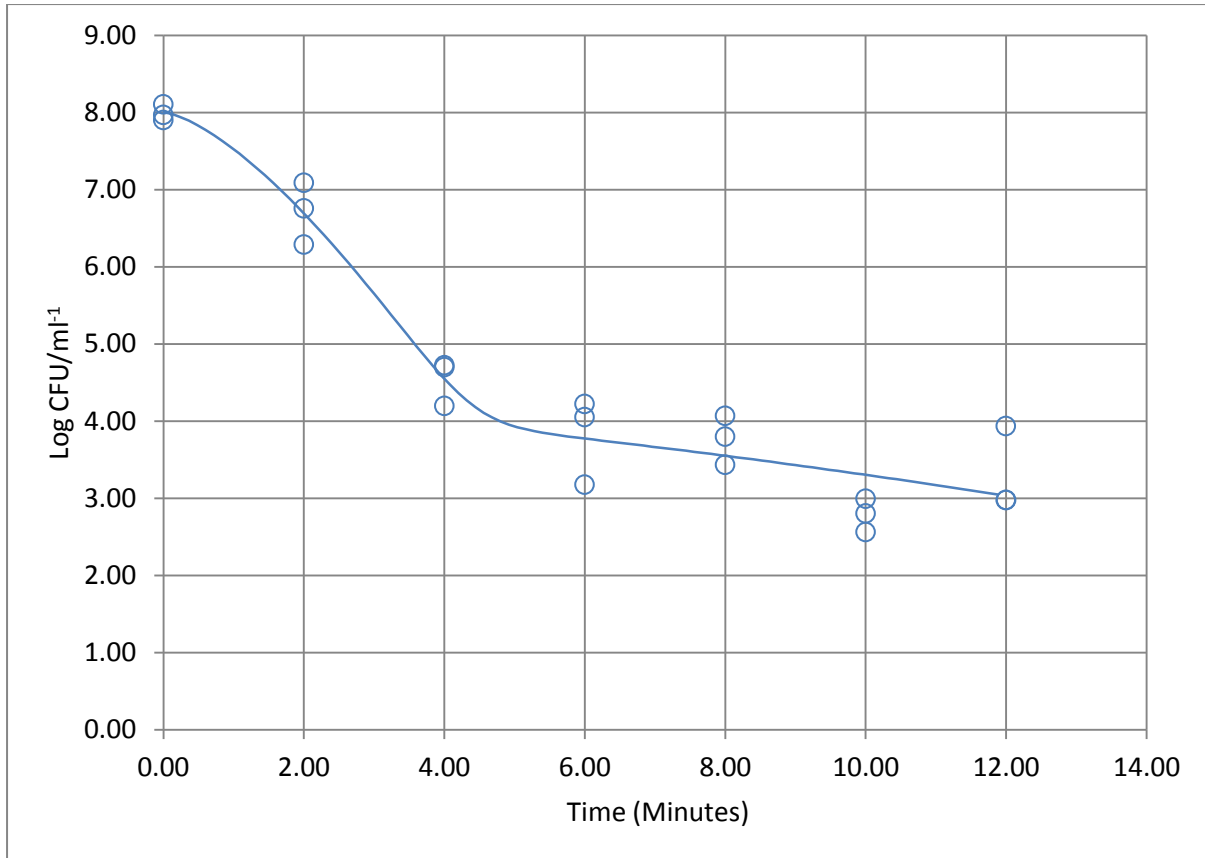


Figure 293. Plot illustrating predicted response using a mixed Weibull distribution model for strain 13136 (ST-45, CC-45) following exposure to pH 8.5 and heating at 56°C.

2.3.13 pH and Time-Temperature Simulations: 60°C

Table 272. Assessment of model fit for individual strains following exposure to pH and heating at 60°C.

Strain	pH	RMSE	$R^2_{adjusted}$	D-value
12628 (ST-1773, CC-828)	4.5			
12628 (ST-1773, CC-828)	5.5	0.502	0.949	1.533
12628 (ST-1773, CC-828)	6.5	0.363	0.960	0.477
12628 (ST-1773, CC-828)	7.5	0.349	0.962	1.036
12628 (ST-1773, CC-828)	8.5	0.535	0.929	0.415
12662 (ST-257, CC-257)	4.5	0.478	0.934	0.388
12662 (ST-257, CC-257)	5.5	0.586	0.925	1.769
12662 (ST-257, CC-257)	6.5	0.367	0.967	1.494
12662 (ST-257, CC-257)	7.5	0.478	0.948	1.138
12662 (ST-257, CC-257)	8.5	0.401	0.958	0.473
13126 (ST-21, CC-21)	4.5	0.301	0.935	0.425
13126 (ST-21, CC-21)	5.5	0.405	0.963	1.487
13126 (ST-21, CC-21)	6.5	0.482	0.939	1.433
13126 (ST-21, CC-21)	7.5	0.518	0.926	1.330
13126 (ST-21, CC-21)	8.5	0.411	0.946	0.553
13136 (ST-45, CC-45)	4.5	0.537	0.929	0.004
13136 (ST-45, CC-45)	5.5	0.426	0.950	1.538
13136 (ST-45, CC-45)	6.5	0.439	0.950	1.048
13136 (ST-45, CC-45)	7.5	0.588	0.951	0.588
13136 (ST-45, CC-45)	8.5	0.424	0.936	0.043

Table 273. Mixed Weibull distribution model for survival of strain 12628 (ST-1773, CC-828) following exposure to pH 5.5 and heating at 60°C.

Parameters	Estimates	Standard Error
α	4.845	0.411
δ_1	1.533	0.299
p	2.207	0.583
N_0	8.040	0.298
δ_2	10.497	3.392

Table 274. Mixed Weibull distribution model for survival of strain 12628 (ST-1773, CC-828) following exposure to pH 6.5 and heating at 60°C.

Parameters	Estimates	Standard Error
α	3.254	0.637
δ_1	0.477	0.225
ρ	0.750	0.222
N_0	8.040	0.220
δ_2	3.578	2.063

Table 275. Mixed Weibull distribution model for survival of strain 12628 (ST-1773, CC-828) following exposure to pH 7.5 and heating at 60°C.

Parameters	Estimates	Standard Error
α	3.363	0.520
δ_1	1.036	0.224
ρ	1.935	1.045
N_0	8.034	0.208
δ_2	6.218	1.844

Table 276. Biphasic model for survival of strain 12628 (ST-1773, CC-828) following exposure to pH 8.5 and heating at 60°C.

Parameters	Estimates	Standard Error
F	1.000	0.000
Kmax1	5.553	0.925
Kmax2	0.521	0.150
N_0	8.034	0.309

Table 277. Biphasic model for survival of strain 12662 (ST-257, CC-257) following exposure to pH 4.5 and heating at 60°C.

Parameters	Estimates	Standard Error
F	1.000	0.000
Kmax1	5.941	0.681
Kmax2	0.259	0.145
N_0	8.089	0.276

Table 278. Mixed Weibull distribution model for survival of strain 12662 (ST-257, CC-257) following exposure to pH 5.5 and heating at 60°C.

Parameters	Estimates	Standard Error
α	4.232	0.479
δ_1	1.769	0.453
ρ	2.137	0.904
N_0	7.969	0.347
δ_2	8.404	2.263

Table 279. Mixed Weibull distribution model for survival of strain 12662 (ST-257, CC-257) following exposure to pH 6.5 and heating at 60°C.

Parameters	Estimates	Standard Error
α	3.892	0.345
δ_1	1.494	0.277
ρ	1.548	0.362
N_0	7.966	0.206
δ_2	8.523	2.247

Table 280. Log-linear model incorporating an asymptotic function for survival of strain 12662 (ST-257, CC-257) following exposure to pH 7.5 and heating at 60°C.

Parameters	Estimates	Standard Error
Kmax	2.025	0.180
Nres	2.649	0.189
N_0	7.784	0.227

Table 281. Biphasic model for survival of strain 12662 (ST-257, CC-257) following exposure to pH 8.5 and heating at 60°C.

Parameters	Estimates	Standard Error
f	1.000	0.000
Kmax1	4.874	0.546
Kmax2	0.575	0.113
N_0	7.963	0.231

Table 282. Mixed Weibull distribution model for survival of strain 13126 (ST-21, CC-21) following exposure to pH 4.5 and heating at 60°C.

Parameters	Estimates	Standard Error
α	5.212	1.910
δ_1	0.425	2.348
ρ	1.204	5.243
N_0	7.973	0.329
δ_2	10.518	11.525

Table 283. Mixed Weibull distribution model for survival of strain 13126 (ST-21, CC-21) following exposure to pH 5.5 and heating at 60°C.

Parameters	Estimates	Standard Error
α	4.035	0.419
δ_1	1.486	0.317
ρ	1.969	0.537
N_0	8.065	0.301
δ_2	7.107	1.468

Table 284. Mixed Weibull distribution model for survival of strain 13126 (ST-21, CC-21) following exposure to pH 6.5 and heating at 60°C.

Parameters	Estimates	Standard Error
α	4.082	0.360
δ_1	1.433	0.262
ρ	2.117	0.637
N_0	8.028	0.287
δ_2	9.101	2.028

Table 285. Mixed Weibull distribution model for survival of strain 13126 (ST-21, CC-21) following exposure to pH 7.5 and heating at 60°C.

Parameters	Estimates	Standard Error
α	4.365	0.491
δ_1	1.330	0.316
ρ	1.711	0.466
N_0	7.965	0.308
δ_2	16.431	16.132

Table 286. Mixed Weibull distribution model for survival of strain 13126 (ST-21, CC-21) following exposure to pH 8.5 and heating at 60°C.

Parameters	Estimates	Standard Error
α	3.657	1.560
δ_1	0.553	0.982
ρ	1.228	2.101
N_0	8.093	0.306
δ_2	6.060	8.336

Table 287. Weibull model for survival of strain 13136 (ST-45, CC-45) following exposure to pH 4.5 and heating at 60°C.

Parameters	Estimates	Standard Error
δ	0.004	0.007
ρ	0.230	0.050
N_0	7.916	0.310

Table 288. Mixed Weibull distribution model for survival of strain 13136 (ST-45, CC-45) following exposure to pH 5.5 and heating at 60°C.

Parameters	Estimates	Standard Error
α	3.897	0.432
δ_1	1.538	0.349
ρ	1.547	0.455
N_0	7.990	0.252
δ_2	8.885	3.070

Table 289. Mixed Weibull distribution model for survival of strain 13136 (ST-45, CC-45) following exposure to pH 6.5 and heating at 60°C.

Parameters	Estimates	Standard Error
α	3.715	0.416
δ_1	1.048	0.246
ρ	1.378	0.340
N_0	7.977	0.261
δ_2	6.025	1.542

Table 290. Mixed Weibull distribution model for survival of strain 13136 (ST-45, CC-45) following exposure to pH 7.5 and heating at 60°C.

Parameters	Estimates	Standard Error
α	3.583	0.672
δ_1	0.588	0.248
ρ	0.826	0.230
NO	7.970	0.243
δ_2	5.139	3.227

Table 291. Weibull model for survival of strain 13136 (ST-45, CC-45) following exposure to pH 8.5 and heating at 60°C.

Parameters	Estimates	Standard Error
δ	0.043	0.038
ρ	0.303	0.050
NO	7.984	0.245

2.3.14 pH and Time-Temperature Simulations: 60°C

Predicted Response Curves:

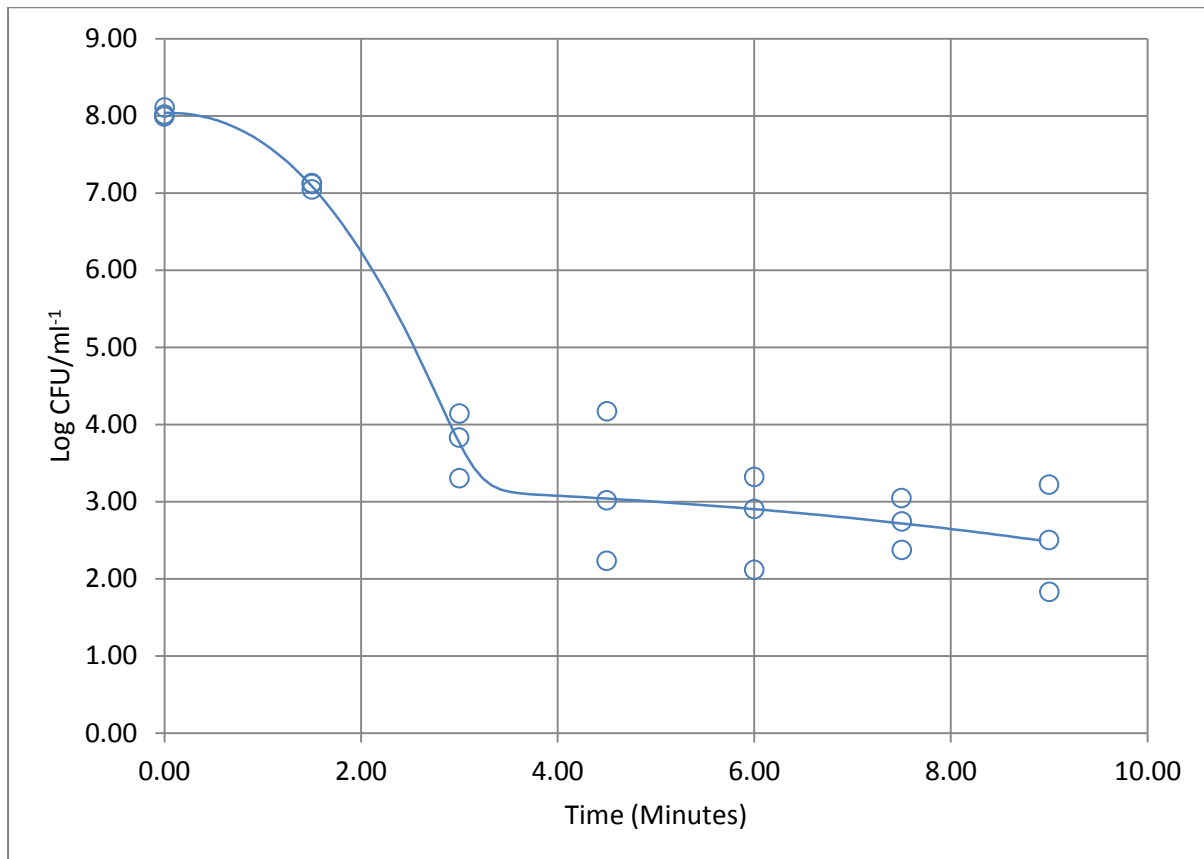


Figure 294. Plot illustrating predicted response using a mixed Weibull distribution model for strain 12628 (ST-1773, CC-828) following exposure to pH 5.5 and heating at 60°C.

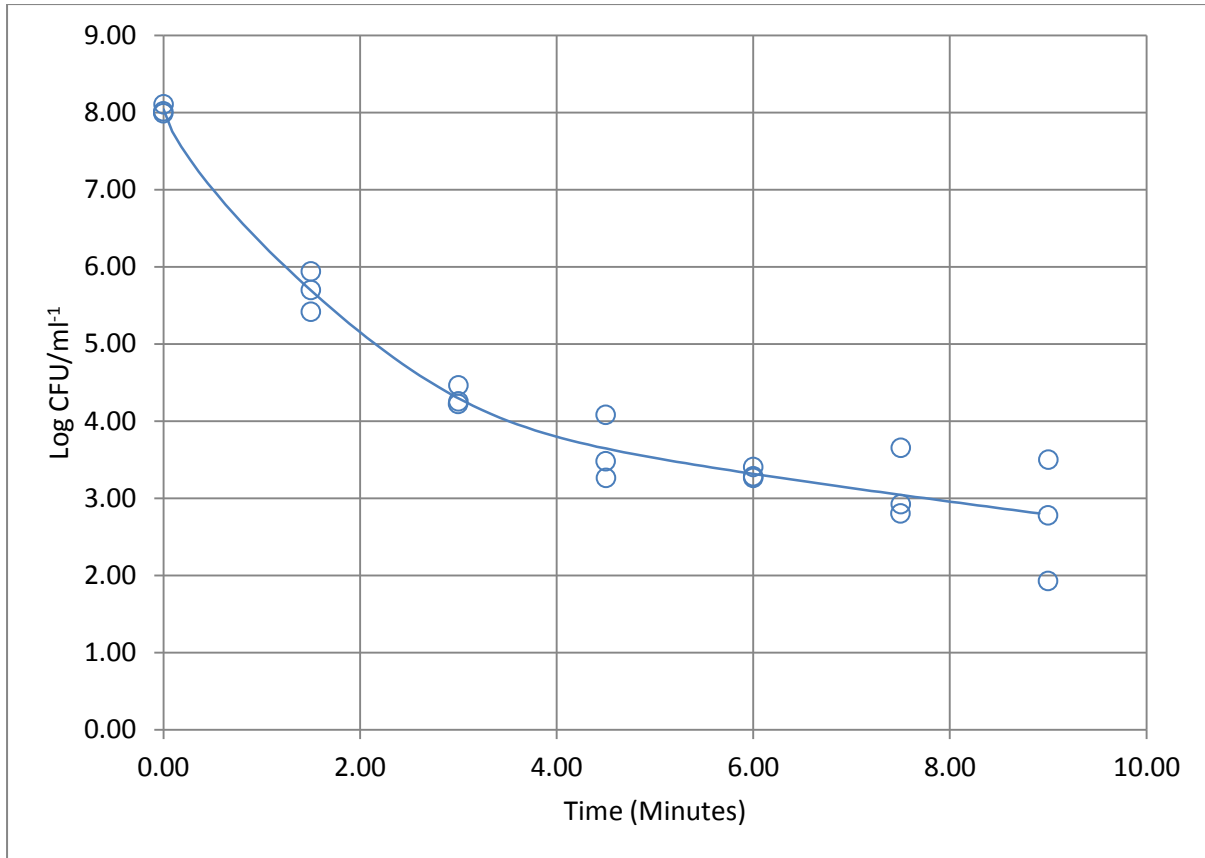


Figure 295. Plot illustrating predicted response using a mixed Weibull distribution model for strain 12628 (ST-1773, CC-828) following exposure to pH 6.5 and heating at 60°C.

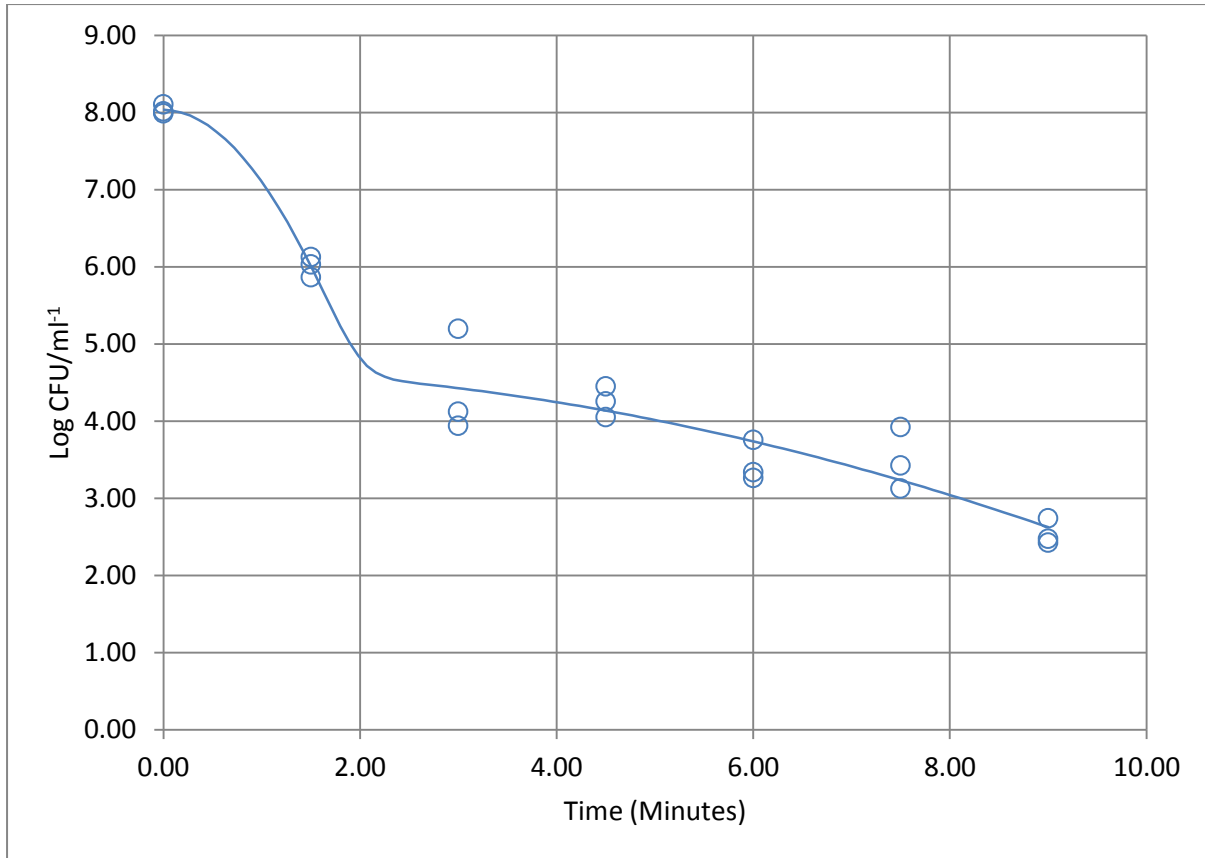


Figure 296. Plot illustrating predicted response using a mixed Weibull distribution model for strain 12628 (ST-1773, CC-828) following exposure to pH 7.5 and heating at 60°C.

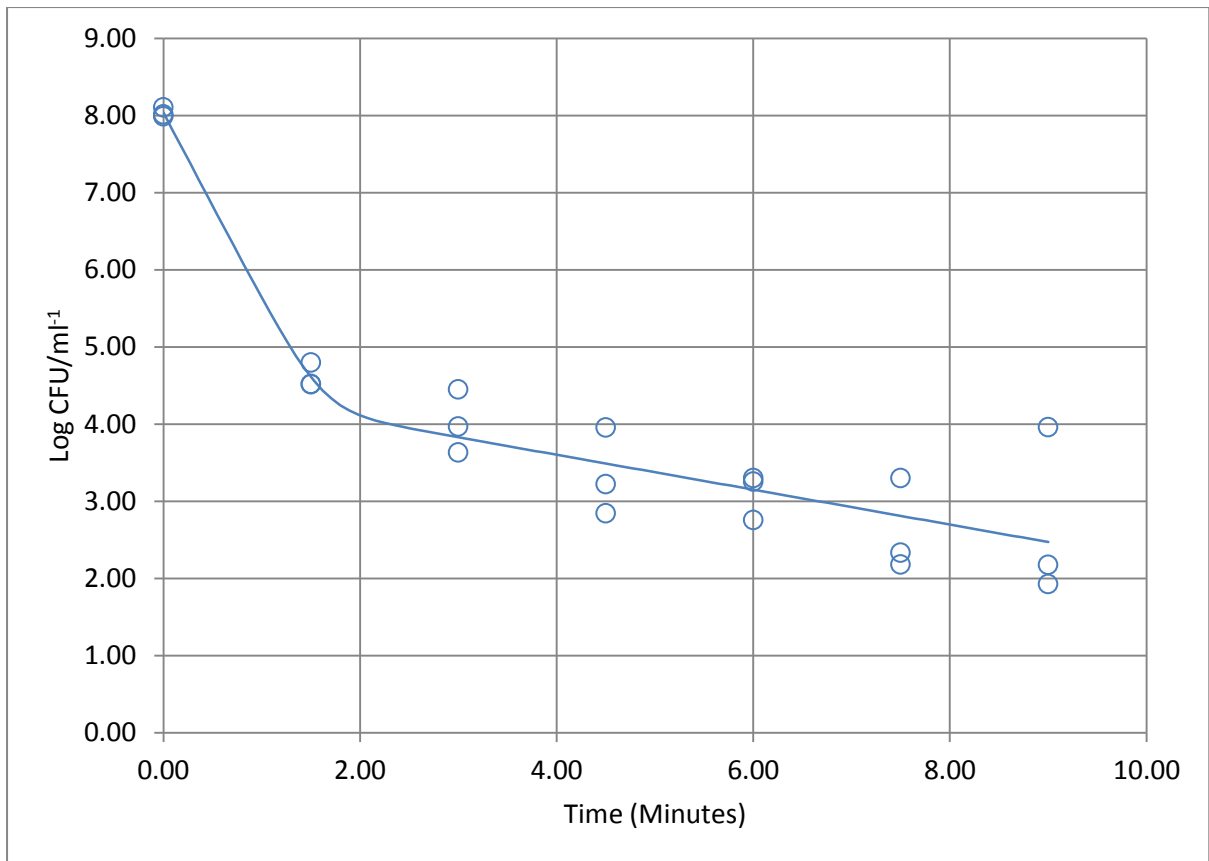


Figure 297. Plot illustrating predicted response using a biphasic model for strain 12628 (ST-1773, CC-828) following exposure to pH 8.5 and heating at 60°C.

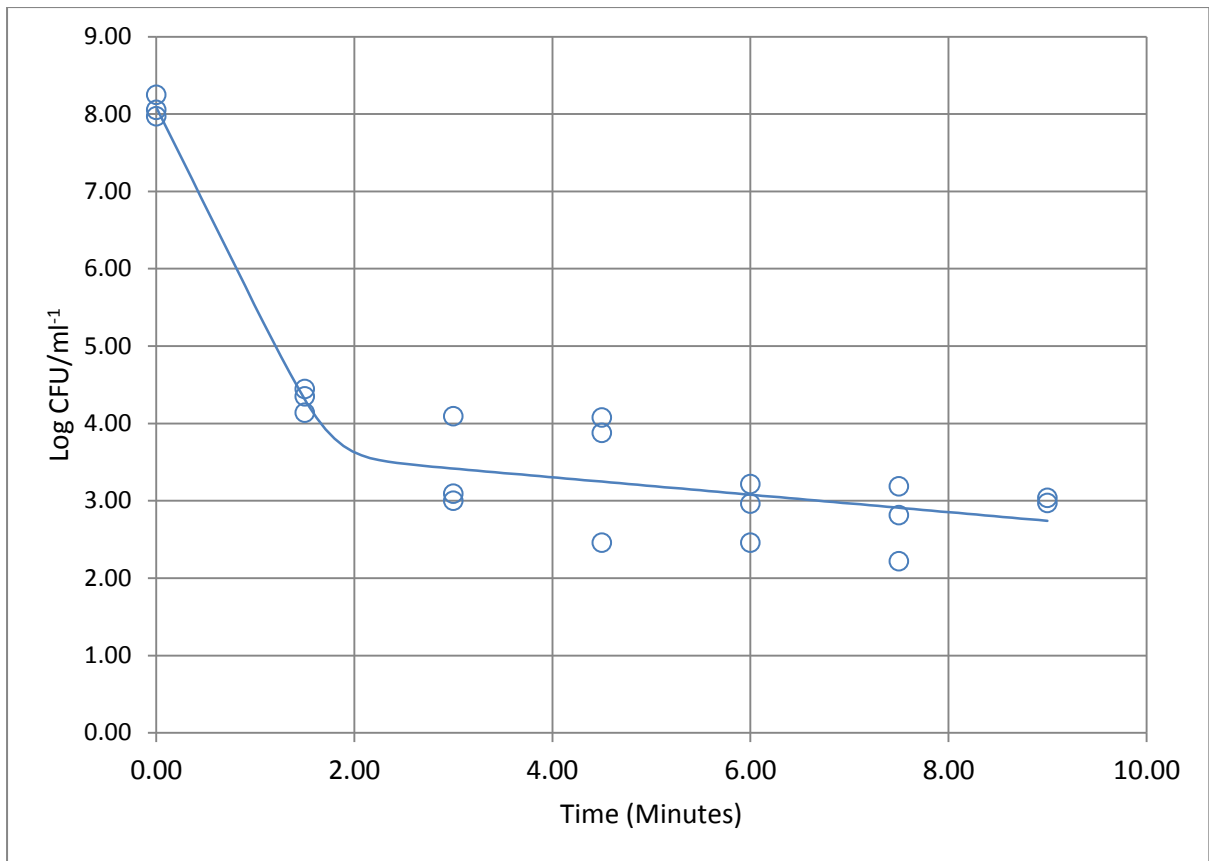


Figure 298. Plot illustrating predicted response using a biphasic model for strain 12662 (ST-257, CC-257) following exposure to pH 4.5 and heating at 60°C.

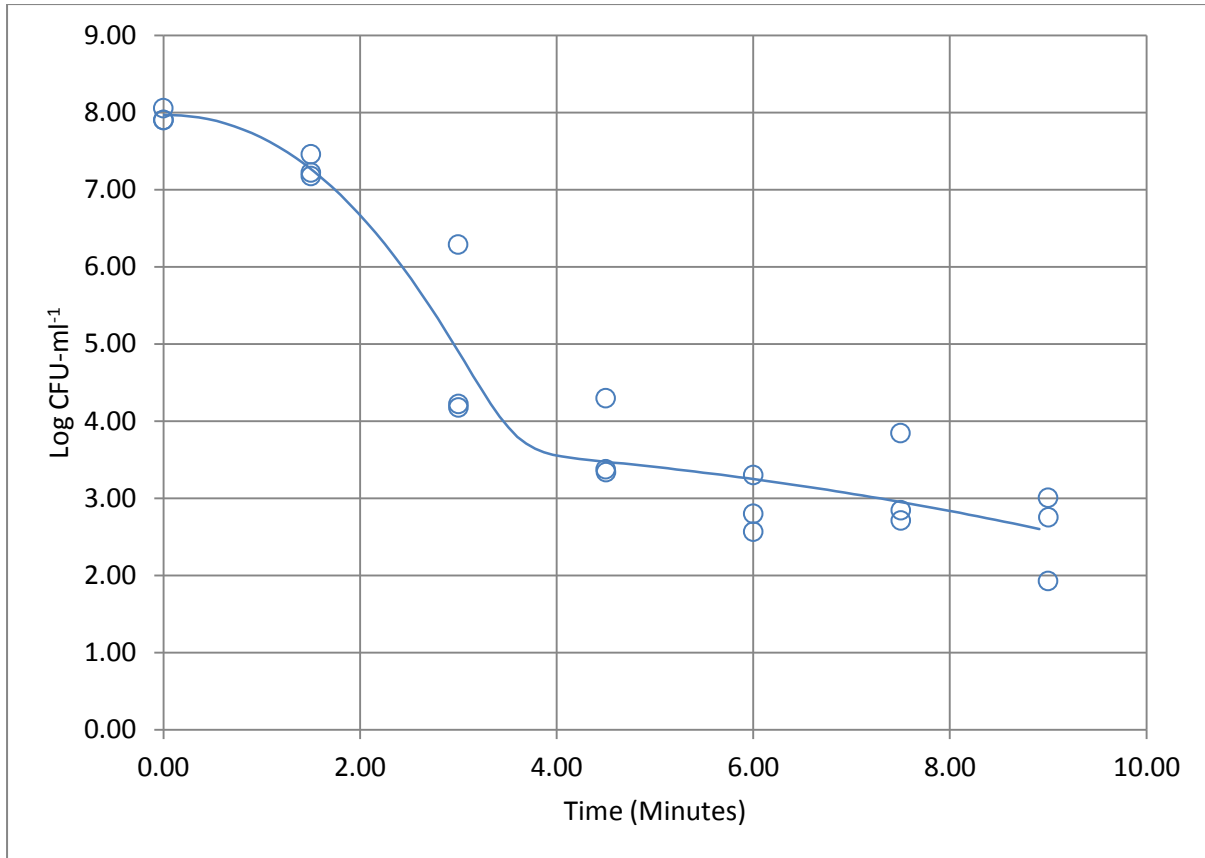


Figure 299. Plot illustrating predicted response curve using a mixed Weibull distribution model for survival of strain 12662 (ST-257, CC-257) following exposure to pH 5.5 and heating at 60°C.

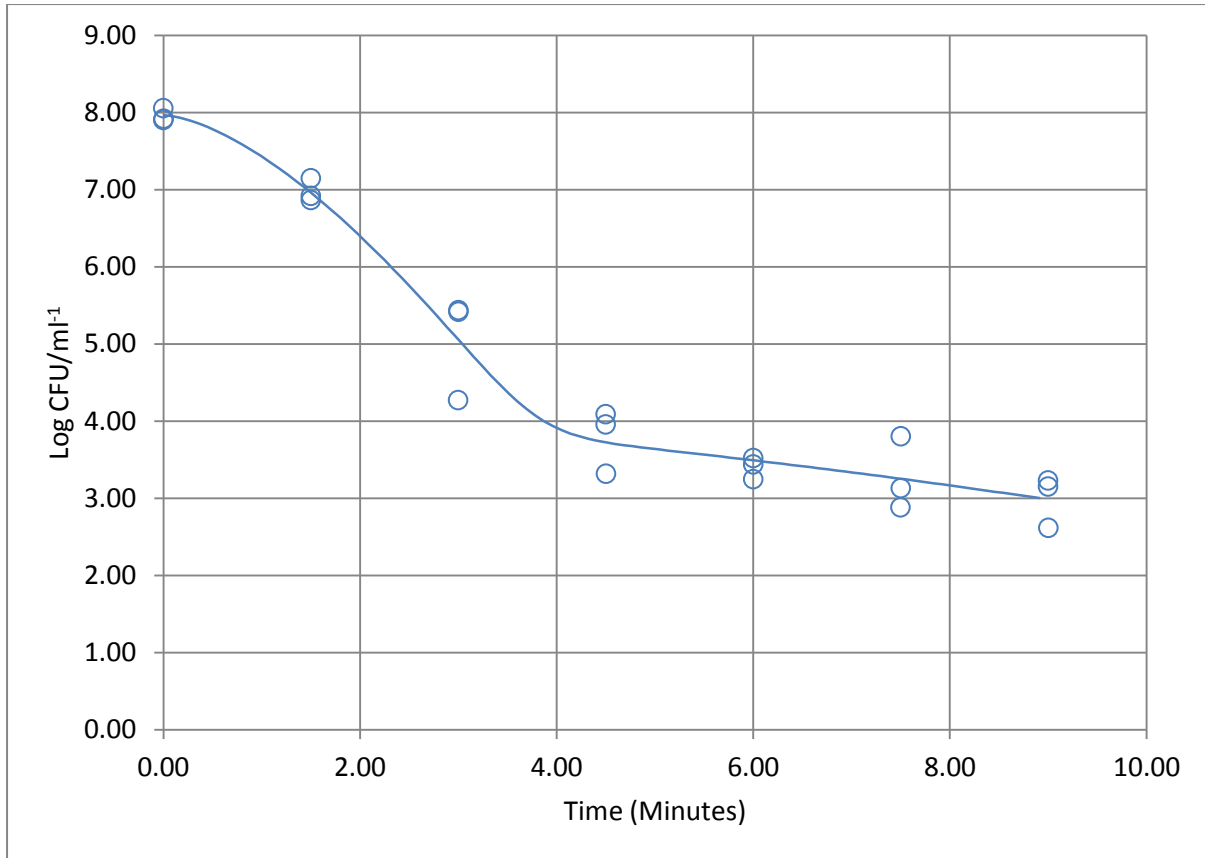


Figure 300. Plot illustrating predicted response curve using a mixed Weibull distribution model for survival of strain 12662 (ST-257, CC-257) following exposure to pH 6.5 and heating at 60°C.

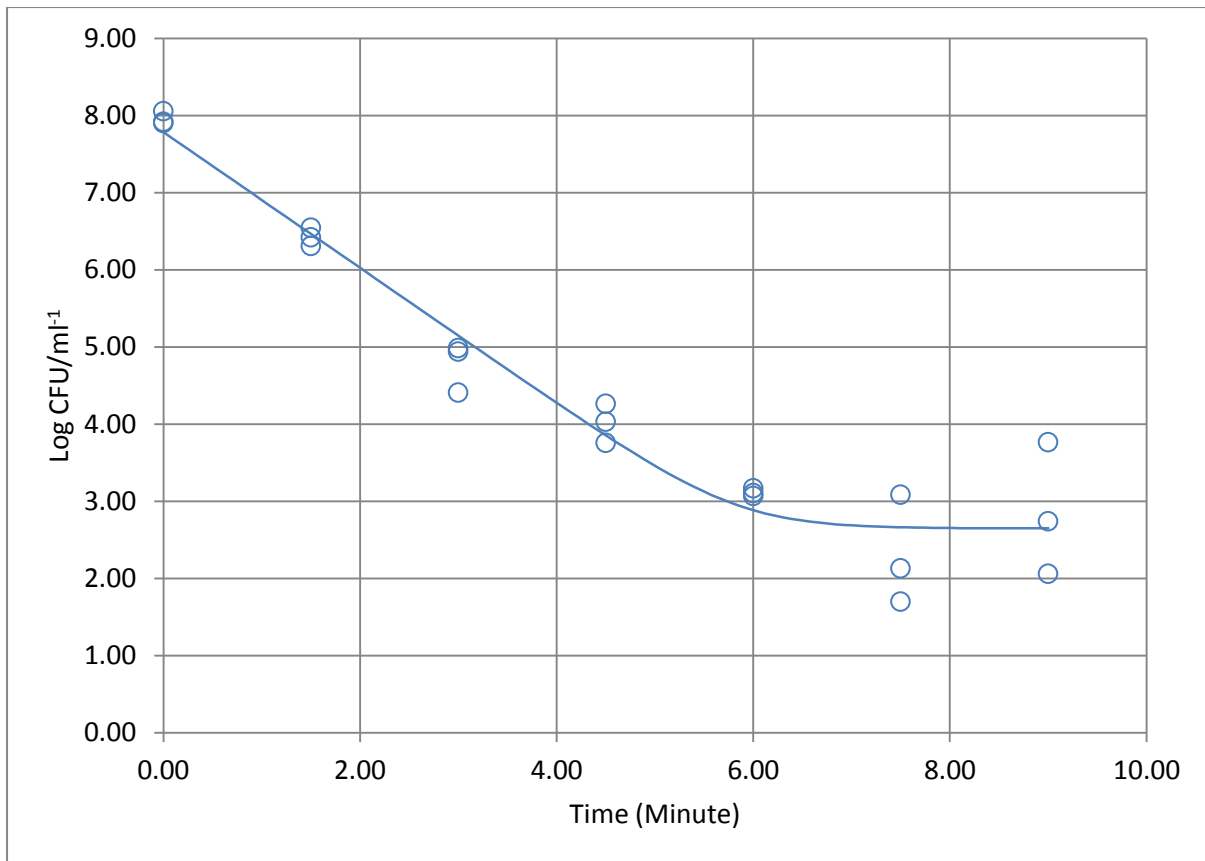


Figure 301. Plot illustrating predicted response using a log-linear model incorporating an asymptotic function for the survival of strain 12662 (ST-257, CC-257) following exposure to pH 7.5 and heating at 60°C.

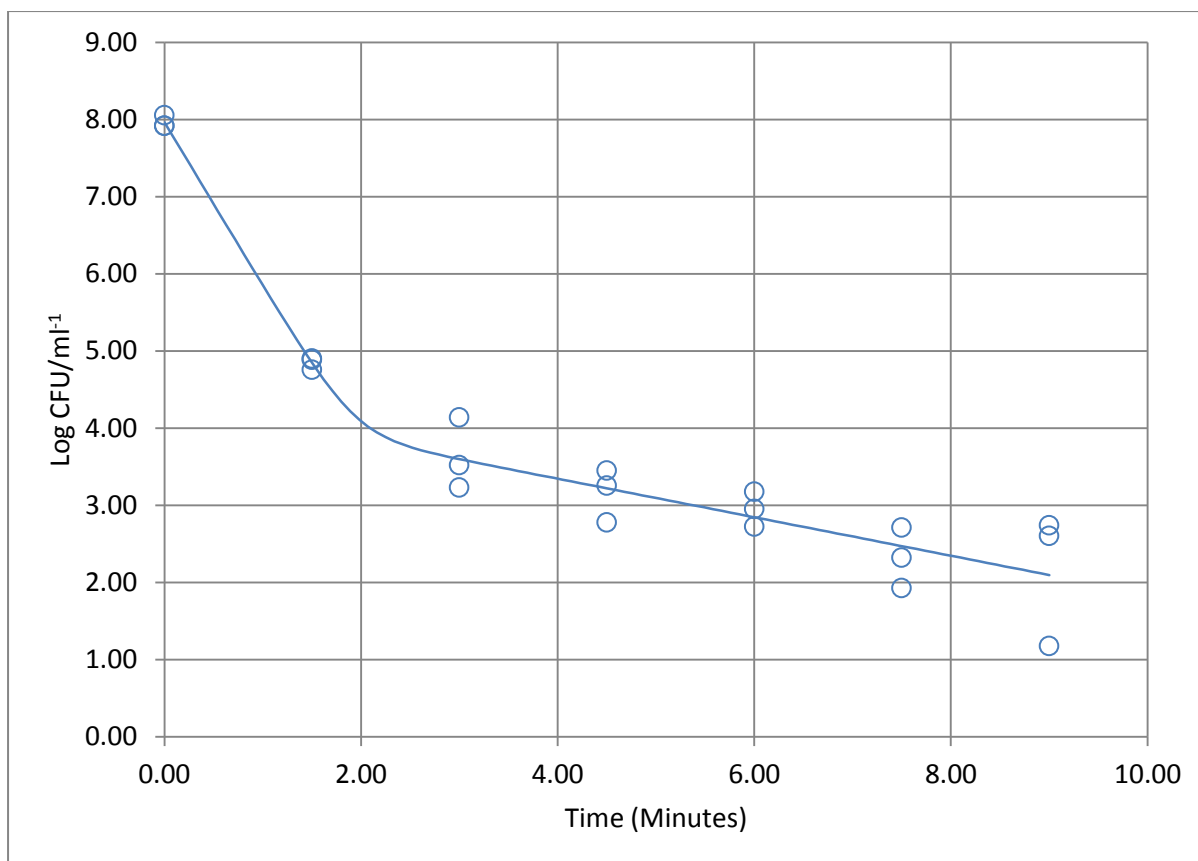


Figure 302. Plot illustrating predicted response using a biphasic model incorporating an asymptotic function for the survival of strain 12662 (ST-257, CC-257) following exposure to pH 8.5 and heating at 60°C.

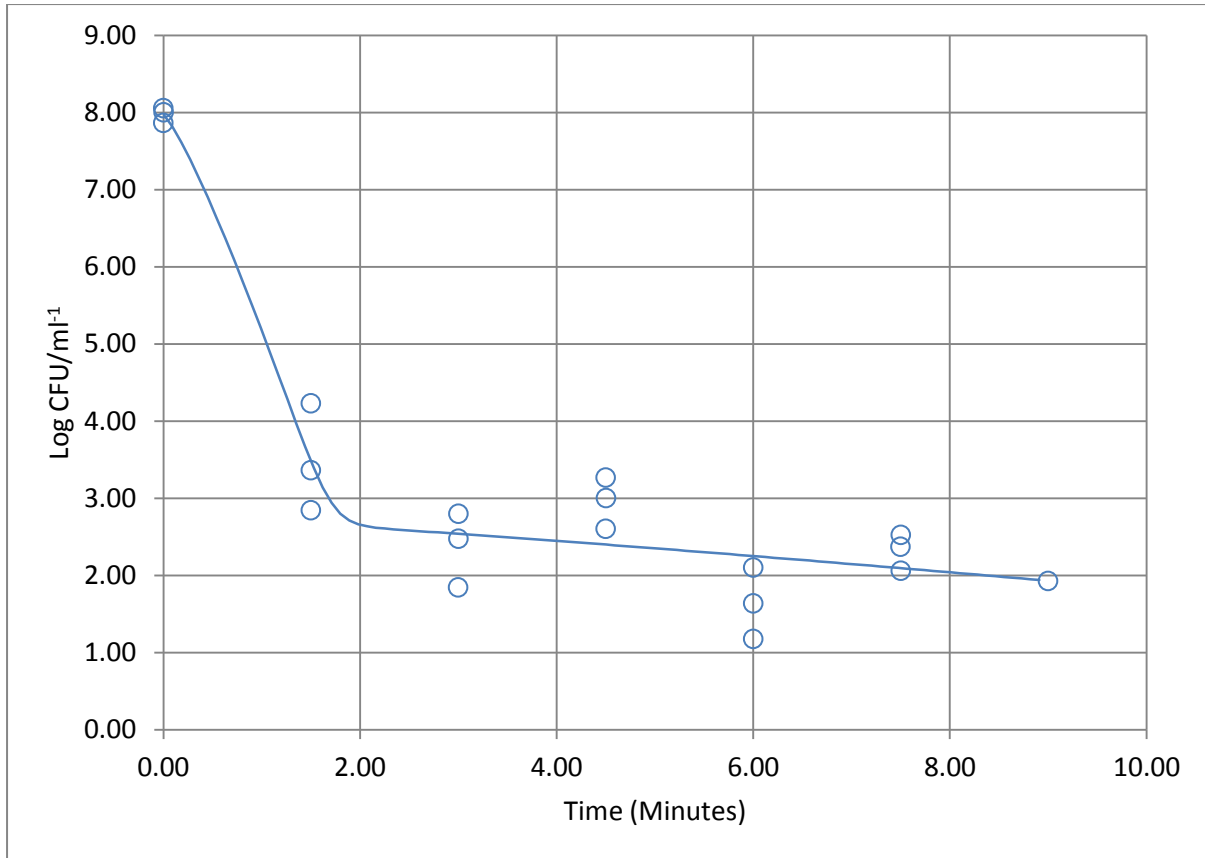


Figure 303. Plot illustrating predicted response curve using a mixed Weibull distribution model for survival of strain 13126 (ST-21, CC-21) following exposure to pH 4.5 and heating at 60°C.

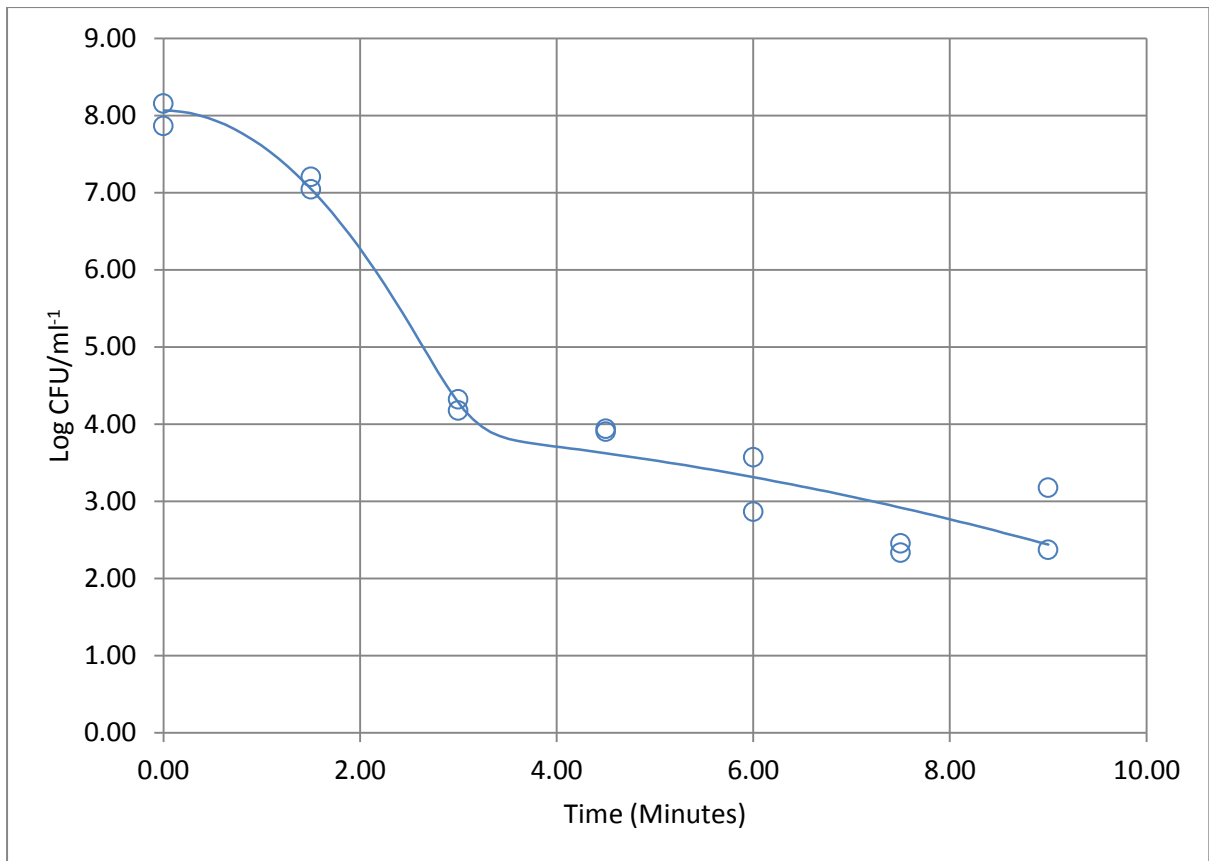


Figure 304. Plot illustrating predicted response curve using a mixed Weibull distribution model for survival of strain 13126 (ST-21, CC-21) following exposure to pH 5.5 and heating at 60°C.

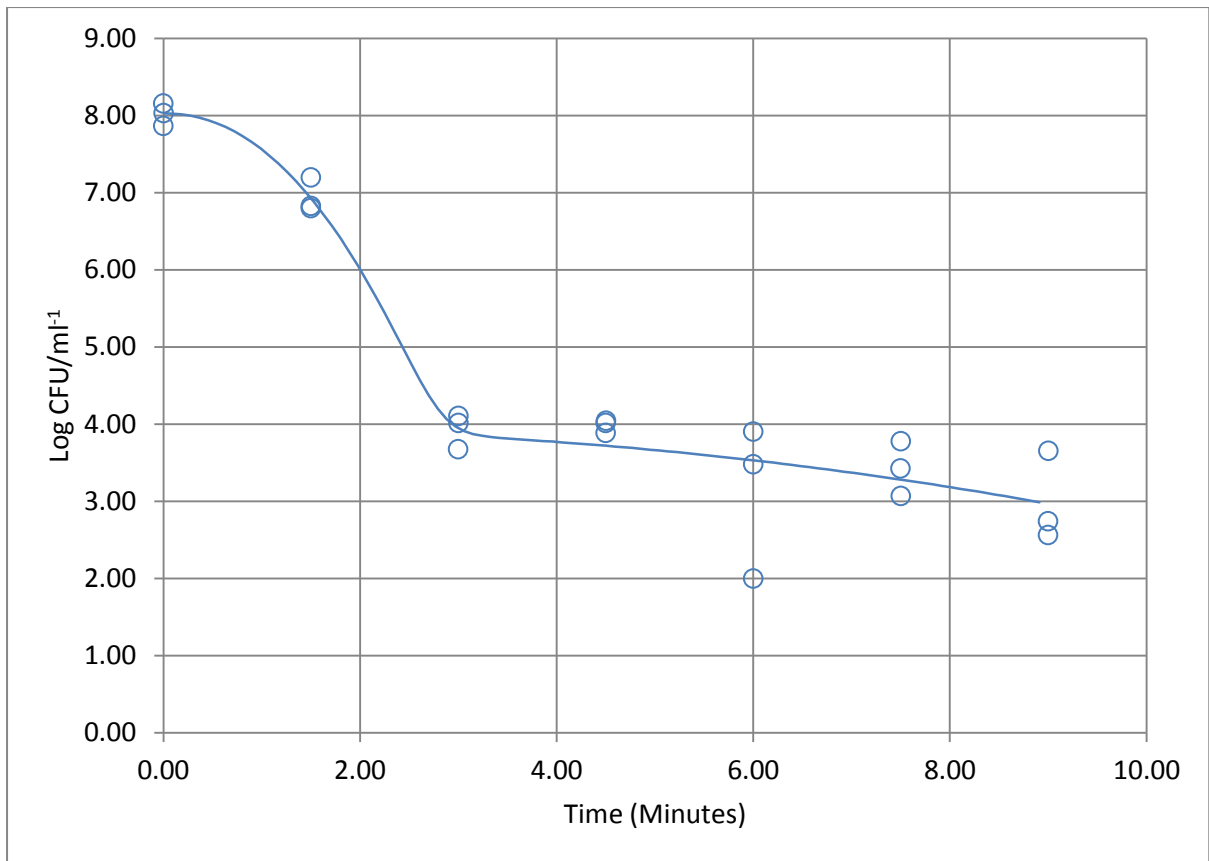


Figure 305. Plot illustrating predicted response curve using a mixed Weibull distribution model for survival of strain 13126 (ST-21, CC-21) following exposure to pH 6.5 and heating at 60°C.

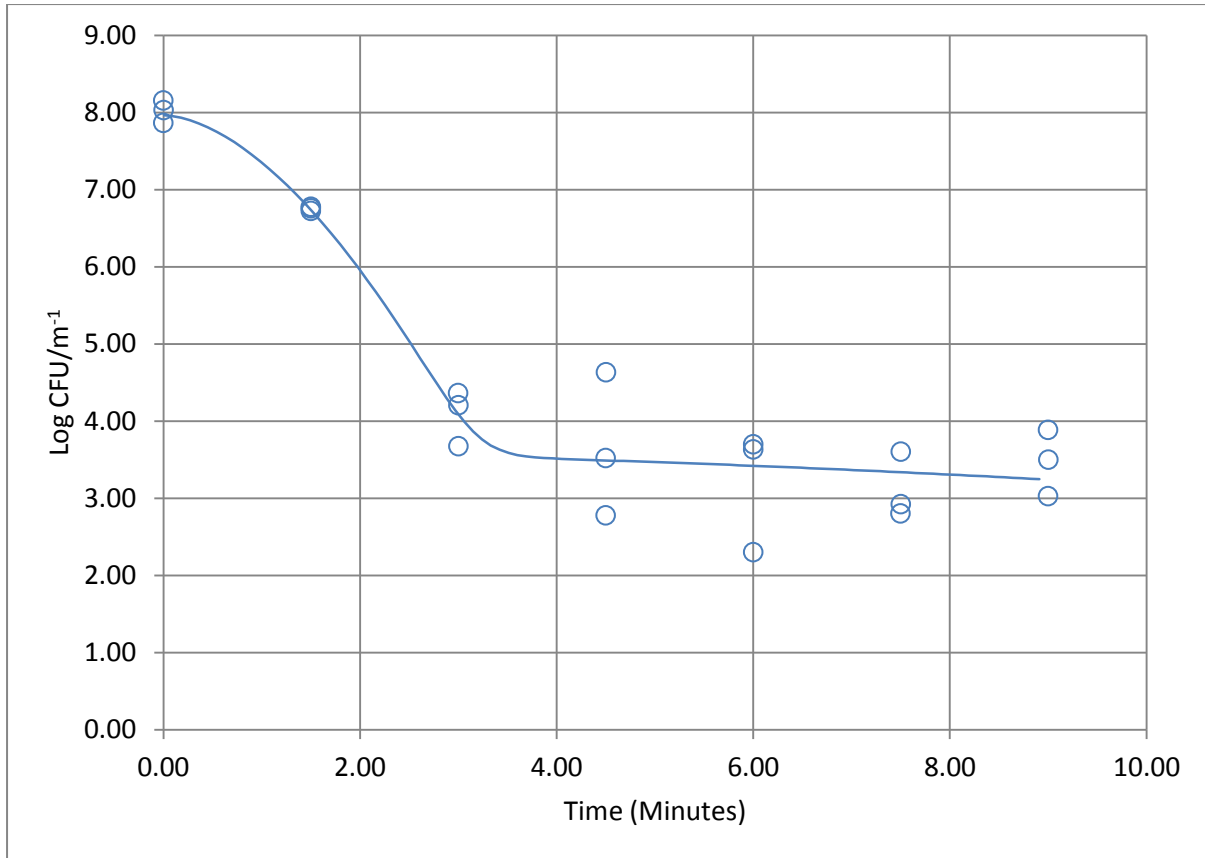


Figure 306. Plot illustrating predicted response curve using a mixed Weibull distribution model for survival of strain 13126 (ST-21, CC-21) following exposure to pH 7.5 and heating at 60°C.

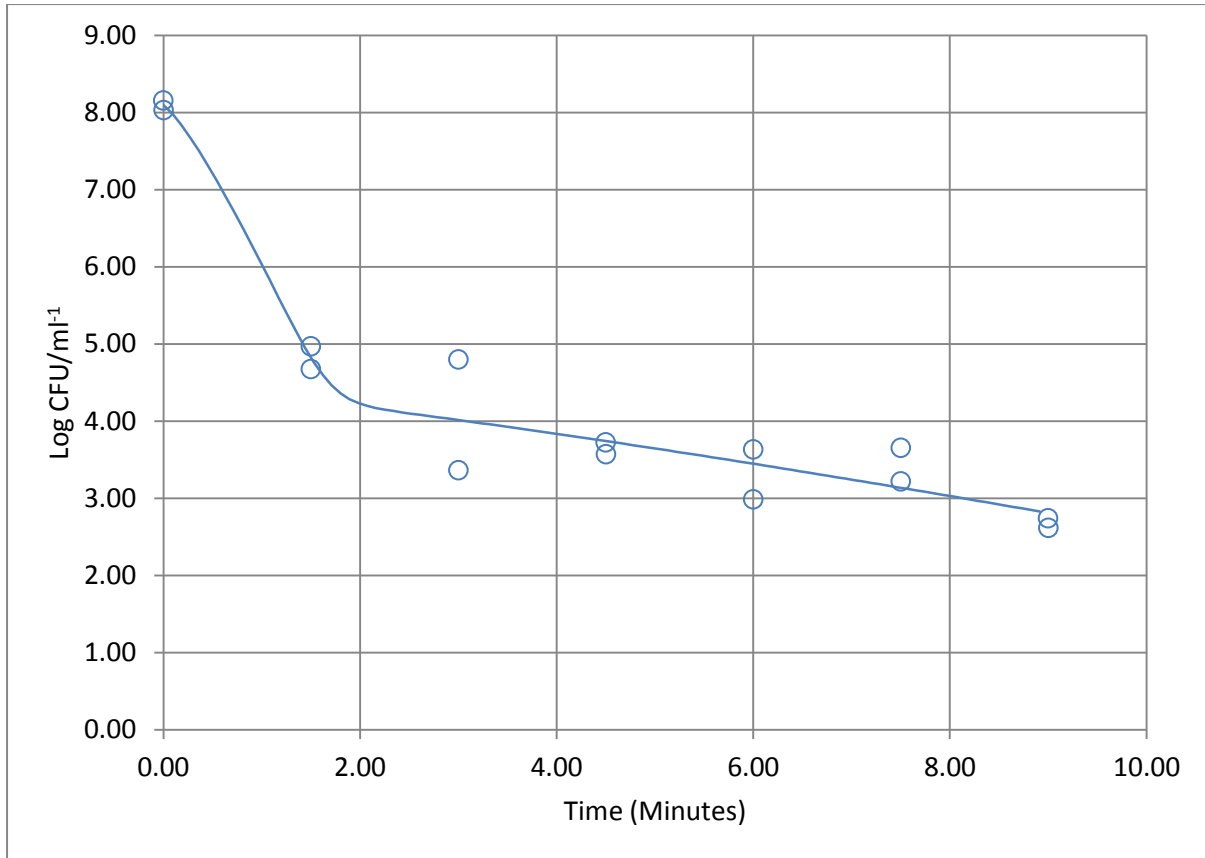


Figure 307. Plot illustrating predicted response curve using a mixed Weibull distribution model for survival of strain 13126 (ST-21, CC-21) following exposure to pH 8.5 and heating at 60°C.

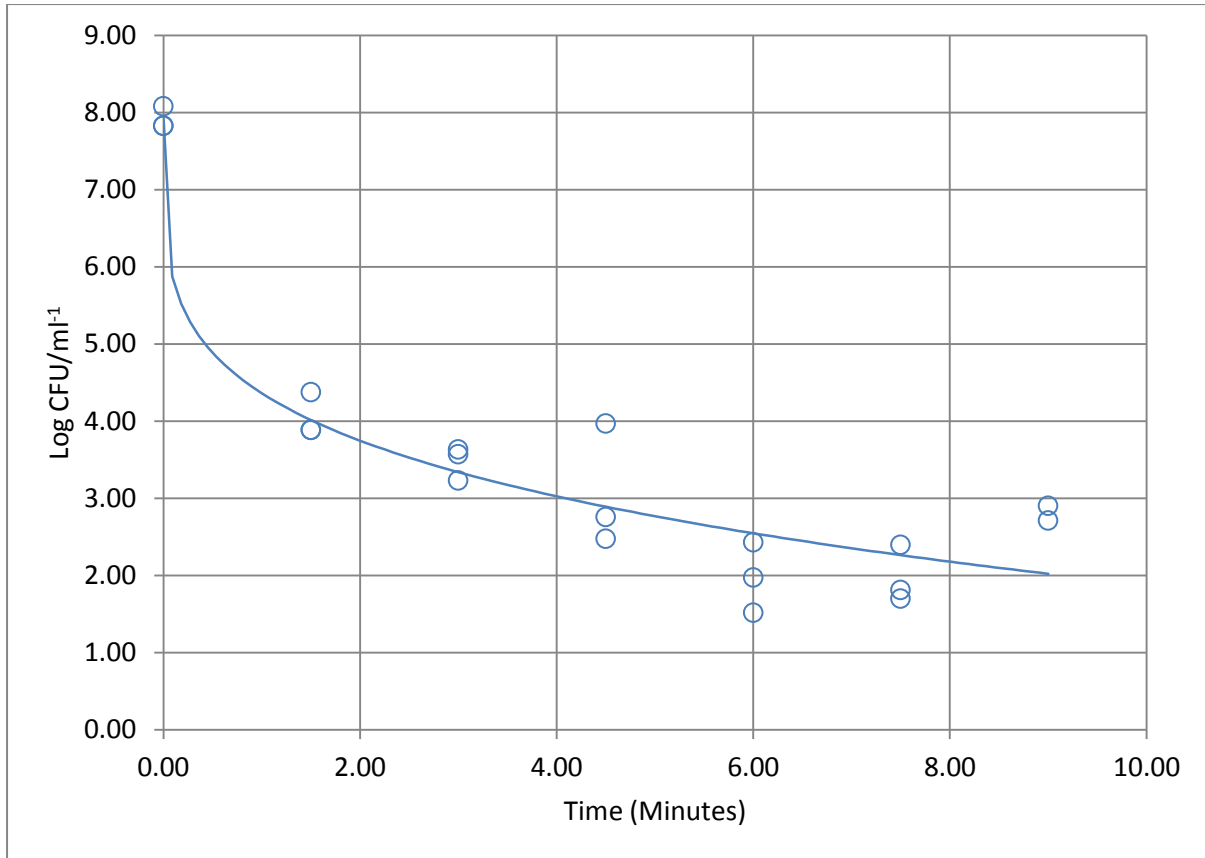


Figure 308. Plot illustrating predicted response curve using a Weibull model for survival of strain 13136 (ST-45, CC-45) following exposure to pH 4.5 and heating at 60°C.

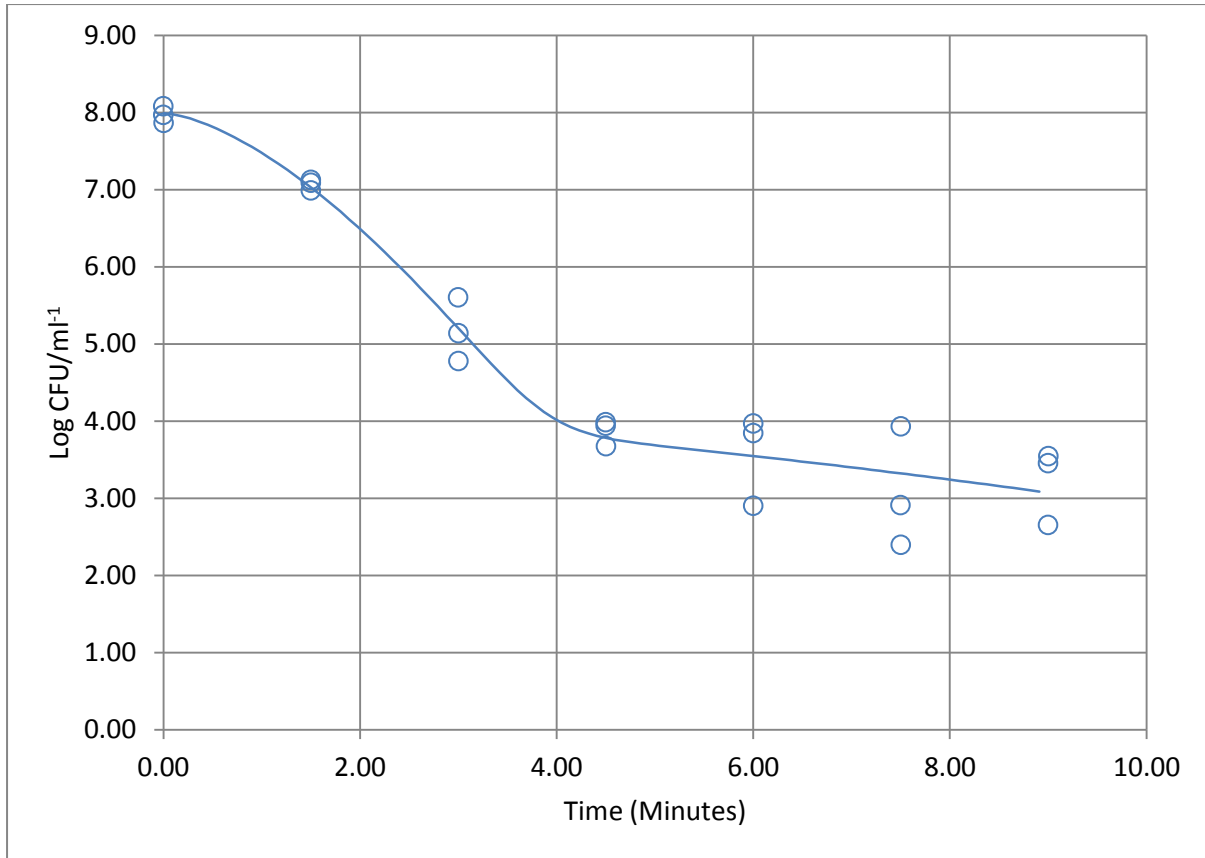


Figure 309. Plot illustrating predicted response curve using a mixed Weibull distribution model for survival of strain 13136 (ST-45, CC-45) following exposure to pH 5.5 and heating at 60°C.

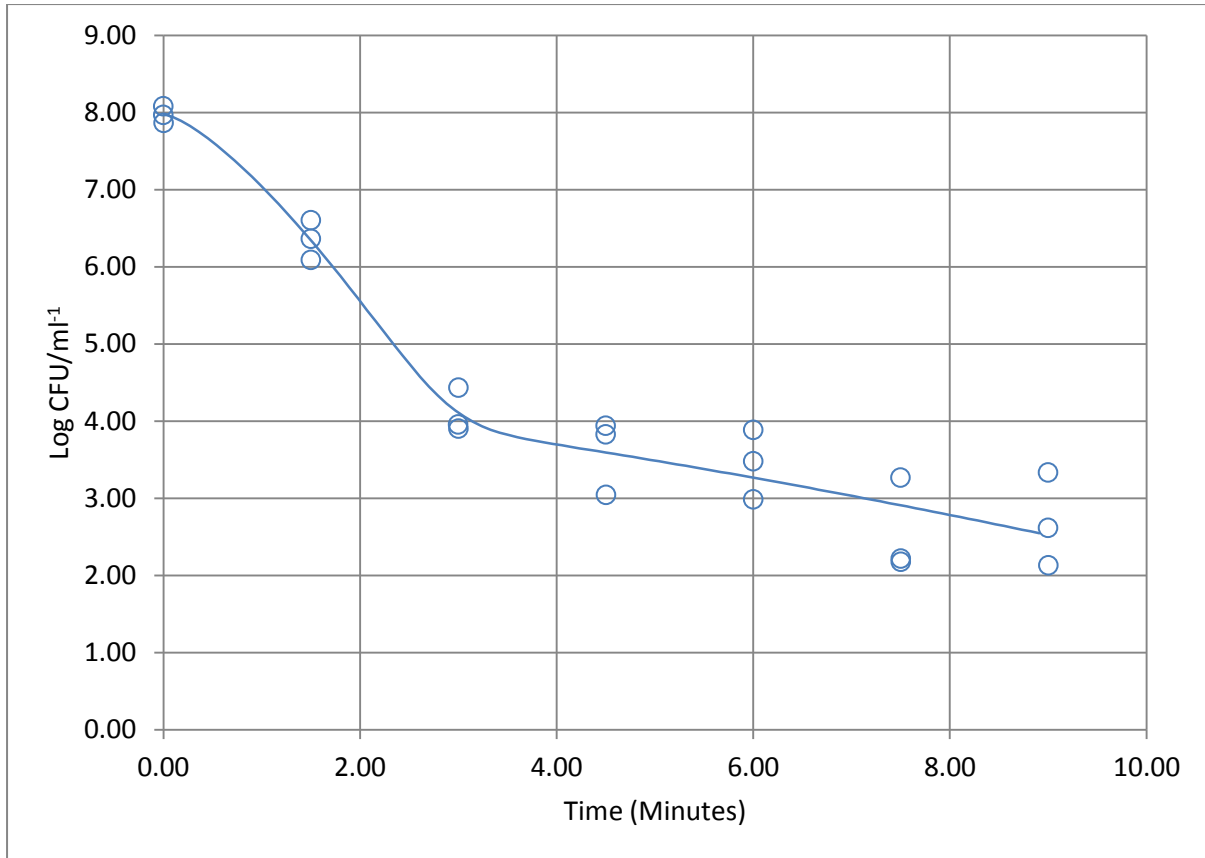


Figure 310. Plot illustrating predicted response curve using a mixed Weibull distribution model for survival of strain 13136 (ST-45, CC-45) following exposure to pH 6.5 and heating at 60°C.

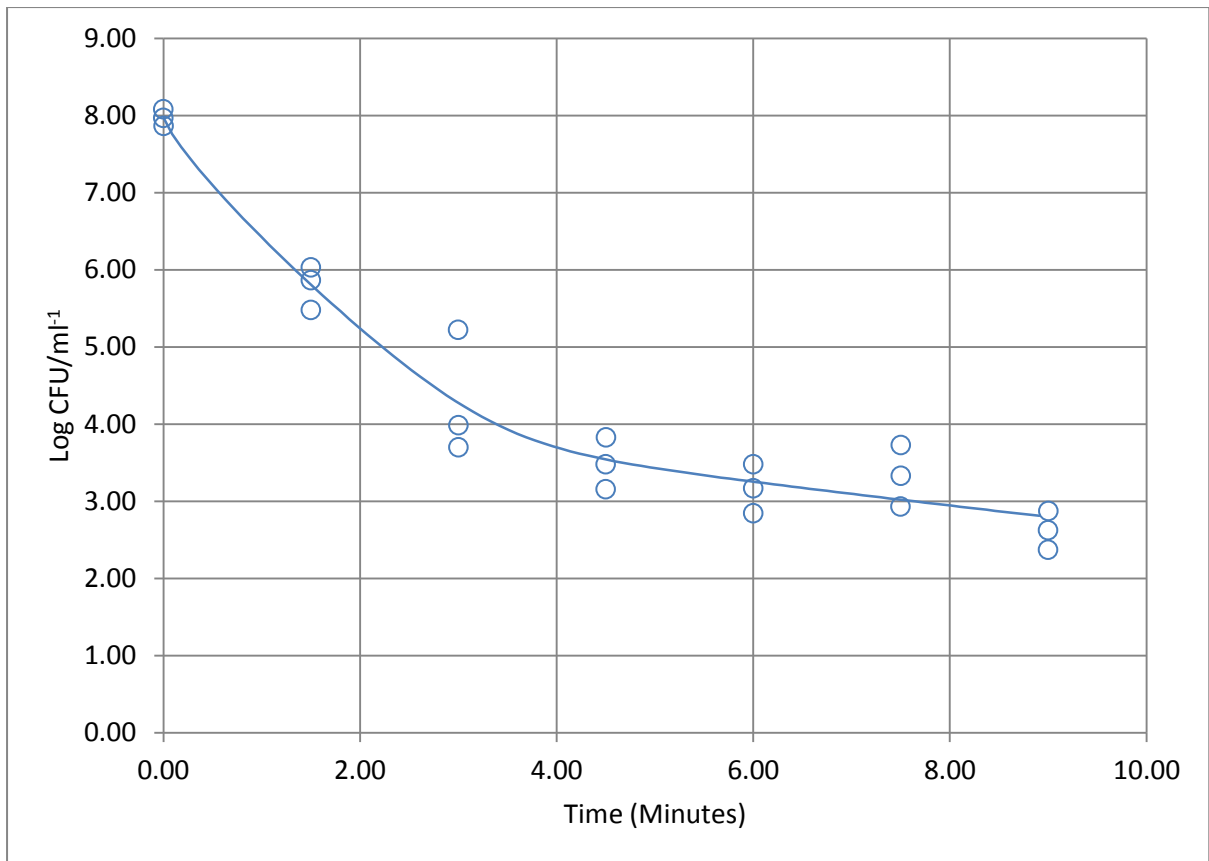


Figure 311. Plot illustrating predicted response curve using a mixed Weibull distribution model for survival of strain 13136 (ST-45, CC-45) following exposure to pH 7.5 and heating at 60°C.

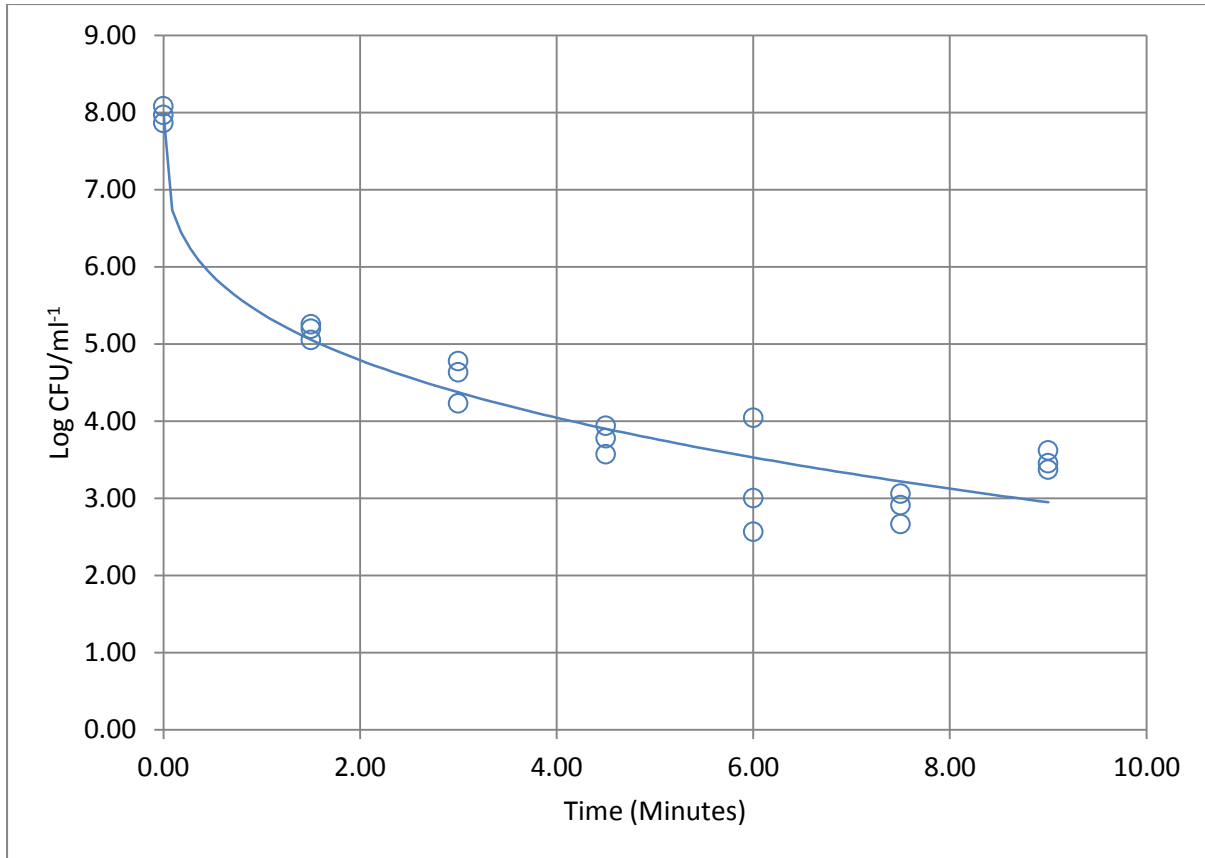


Figure 312. Plot illustrating predicted response curve using Weibull model for the survival of strain 13136 (ST-45, CC-45) following exposure to pH 8.5 and heating at 60°C.

2.3.15 pH and Time-Temperature Simulations: 64°C

Table 292. Assessment of model fit for individual strains following exposure to pH and heating at 64C.

Strain	pH	RMSE	$R^2_{adjusted}$	D-value
12628 (ST-1773, CC-828)	4.5	0.500	0.947	0.001
12628 (ST-1773, CC-828)	5.5	0.613	0.915	0.309
12628 (ST-1773, CC-828)	6.5	0.430	0.950	0.423
12628 (ST-1773, CC-828)	7.5	0.543	0.917	0.341
12628 (ST-1773, CC-828)	8.5	0.479	0.930	0.178
12662 (ST-257, CC-257)	4.5	0.543	0.938	0.137
12662 (ST-257, CC-257)	5.5	0.536	0.931	0.950
12662 (ST-257, CC-257)	6.5	0.469	0.949	0.757
12662 (ST-257, CC-257)	7.5	0.547	0.938	0.432
12662 (ST-257, CC-257)	8.5	0.416	0.952	0.179
13126 (ST-21, CC-21)	4.5	0.585	0.937	0.106
13126 (ST-21, CC-21)	5.5	0.423	0.956	0.712
13126 (ST-21, CC-21)	6.5	0.499	0.945	0.479
13126 (ST-21, CC-21)	7.5	0.417	0.955	0.197
13126 (ST-21, CC-21)	8.5	0.341	0.955	0.258
13136 (ST-45, CC-45)	4.5	0.675	0.900	0.029
13136 (ST-45, CC-45)	5.5	0.582	0.933	0.502
13136 (ST-45, CC-45)	6.5	0.365	0.964	0.611
13136 (ST-45, CC-45)	7.5	0.379	0.963	0.452
13136 (ST-45, CC-45)	8.5	0.563	0.925	0.248

Table 293. Weibull model for survival of strain 12628 (ST-1773, CC-828) following exposure to pH 4.5 and heating at 64°C.

Parameters	Estimates	Standard Error
δ	0.001	0.001
p	0.220	0.034
NO	8.059	0.289

Table 294. Biphasic model for survival of strain 12628 (ST-1773, CC-828) following exposure to pH 5.5 and heating at 64°C.

Parameters	Estimates	Standard Error
F	1.000	0.000
Kmax1	7.468	1.180
Kmax2	0.535	0.369
<i>NO</i>	7.918	0.365

Table 295. Biphasic model incorporating a shoulder-effect for survival of strain 12628 (ST-1773, CC-828) following exposure to pH 6.5 and heating at 64°C.

Parameters	Estimates	Standard Error
F	1.000	0.000
Kmax1	8.623	1.957
Kmax2	0.928	0.256
<i>NO</i>	7.987	0.248
SI	0.165	0.152

Table 296. Biphasic model for survival of strain 12628 (ST-1773, CC-828) following exposure to pH 7.5 and heating at 64°C.

Parameters	Estimates	Standard Error
F	1.000	0.000
Kmax1	8.662	1.253
Kmax2	0.656	0.310
<i>NO</i>	8.027	0.284

Table 297. Biphasic model for survival of strain 12628 (ST-1773, CC-828) following exposure to pH 8.5 and heating at 64°C.

Parameters	Estimates	Standard Error
F	0.999	0.001
Kmax1	13.015	2.061
Kmax2	1.056	0.203
<i>NO</i>	7.988	0.277

Table 298. Biphasic model for survival of strain 12662 (ST-257, CC-257) following exposure to pH 4.5 and heating at 64°C.

Parameters	Estimates	Standard Error
F	1.000	0.000
Kmax1	16.785	2.115
Kmax2	0.694	0.254
<i>N</i> 0	7.968	0.314

Table 299. Mixed Weibull distribution model for survival of strain 12662 (ST-257, CC-257) following exposure to pH 5.5 and heating at 64°C.

Parameters	Estimates	Standard Error
α	4.004	0.550
δ 1	0.950	0.216
ρ	1.913	0.566
<i>N</i> 0	8.019	0.288
δ 2	6.231	3.539

Table 300. Mixed Weibull distribution model for survival of strain 12662 (ST-257, CC-257) following exposure to pH 6.5 and heating at 64°C.

Parameters	Estimates	Standard Error
α	3.868	0.533
δ 1	0.757	0.172
ρ	1.506	0.375
<i>N</i> 0	7.986	0.264
δ 2	4.401	1.644

Table 301. Mixed Weibull distribution model for survival of strain 12662 (ST-257, CC-257) following exposure to pH 7.5 and heating at 64°C.

Parameters	Estimates	Standard Error
α	4.362	0.750
δ 1	0.432	0.150
ρ	1.070	0.316
<i>N</i> 0	8.033	0.321
δ 2	4.127	2.877

Table 302. Biphasic model for survival of strain 12662 (ST-257, CC-257) following exposure to pH 8.5 and heating at 64°C.

Parameters	Estimates	Standard Error
F	1.000	0.000
Kmax1	12.915	1.690
Kmax2	1.077	0.177
<i>NO</i>	8.065	0.240

Table 303. Biphasic model for survival of strain 13126 (ST-21, CC-21) following exposure to pH 4.5 and heating at 64°C.

Parameters	Estimates	Standard Error
F	1.000	0.000
Kmax1	21.763	3.450
Kmax2	0.398	0.343
<i>NO</i>	7.863	0.388

Table 304. Biphasic model for survival of strain 13126 (ST-21, CC-21) following exposure to pH 5.5 and heating at 64°C.

Parameters	Estimates	Standard Error
F	1.000	0.000
Kmax1	5.170	0.701
Kmax2	0.210	0.408
<i>NO</i>	7.785	0.241
SI	0.281	0.196

Table 305. Log-linear model incorporating shoulder-effect for survival of strain 13126 (ST-21, CC-21) following exposure to pH 6.5 and heating at 64°C.

Parameters	Estimates	Standard Error
Kmax	4.841	0.473
Nres	2.687	0.171
<i>NO</i>	7.867	0.224

Table 306. Mixed Weibull distribution model for survival of strain 13126 (ST-21, CC-21) following exposure to pH 7.5 and heating at 64°C.

Parameters	Estimates	Standard Error
α	3.155	0.589
δ_1	0.197	0.088
ρ	0.805	0.237
N_0	7.814	0.249
δ_2	1.551	0.901

Table 307. Mixed Weibull distribution model for survival of strain 13126 (ST-21, CC-21) following exposure to pH 8.5 and heating at 64°C.

Parameters	Estimates	Standard Error
α	3.607	0.394
δ_1	0.258	0.116
ρ	1.679	1.100
N_0	7.818	0.203
δ_2	4.173	1.019

Table 308. Weibull model incorporating an asymptotic function for survival of strain 13136 (ST-45, CC-45) following exposure to pH 4.5 and heating at 64°C.

Parameters	Estimates	Standard Error
Nres	2.420	0.273
δ	0.029	0.051
ρ	0.435	0.212
N_0	7.965	0.434

Table 309. Weibull model incorporating an asymptotic function for survival of strain 13136 (ST-45, CC-45) following exposure to pH 5.5 and heating at 64°C.

Parameters	Estimates	Standard Error
Nres	2.961	0.185
δ	0.502	0.168
ρ	1.334	0.593
N_0	7.912	0.333

Table 310. Weibull model incorporating an asymptotic function for survival of strain 13136 (ST-45, CC-45) following exposure to pH 6.5 and heating at 64°C.

Parameters	Estimates	Standard Error
Nres	3.331	0.122
δ	0.611	0.117
ρ	1.265	0.202
<i>NO</i>	7.904	0.333

Table 311. Mixed Weibull distribution model for survival of strain 13136 (ST-45, CC-45) following exposure to pH 7.5 and heating at 64°C.

Parameters	Estimates	Standard Error
α	3.893	0.378
δ_1	0.452	0.113
ρ	1.247	0.349
<i>NO</i>	7.918	0.225
δ_2	4.039	1.297

Table 312. Mixed Weibull distribution model for survival of strain 13136 (ST-45, CC-45) following exposure to pH 8.5 and heating at 64°C.

Parameters	Estimates	Standard Error
α	3.636	0.615
δ_1	0.248	0.107
ρ	1.003	0.333
<i>NO</i>	7.938	0.336
δ_2	2.221	1.088

2.3.16 pH Time-temperature Simulations: 64°C

Predicted Response Curves:

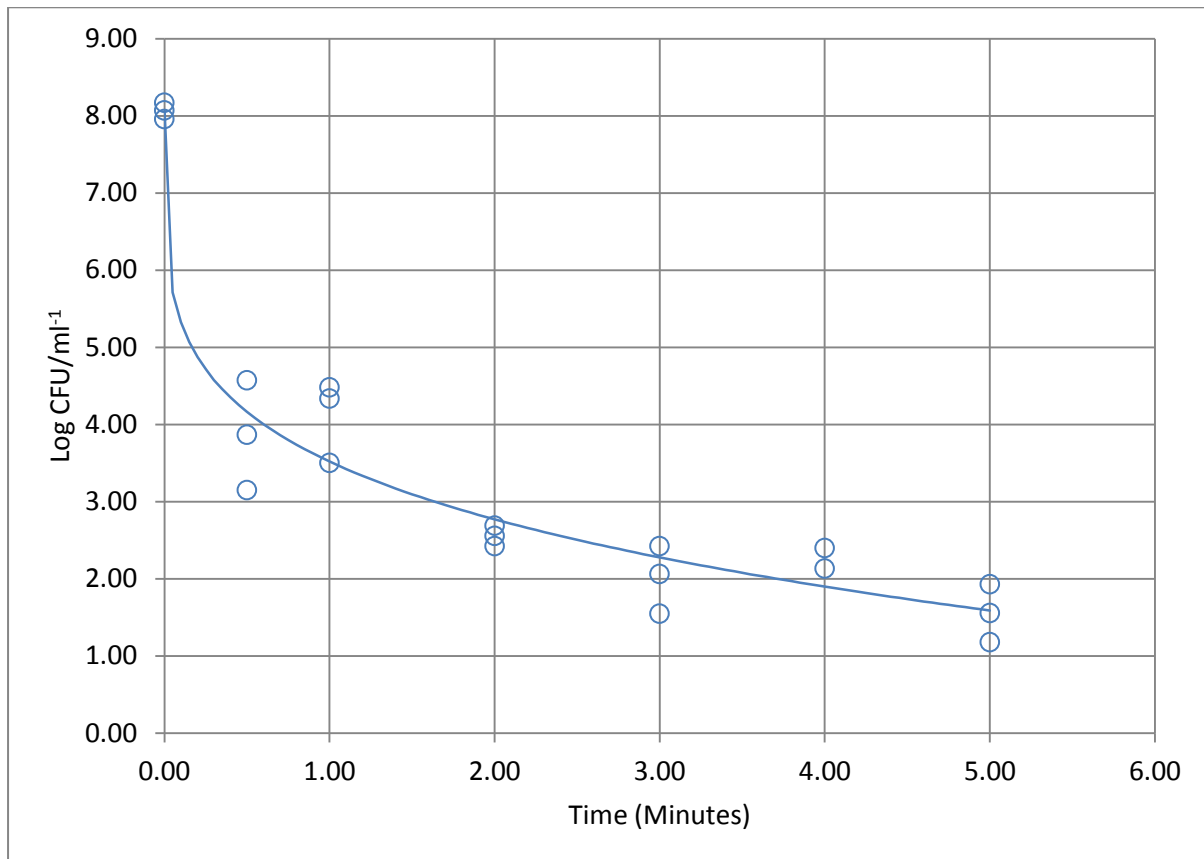


Figure 313. Plot illustrating predicted response curve using a Weibull model for survival of strain 12628 (ST-1773, CC-828) following exposure to pH 4.5 and heating at 64°C.

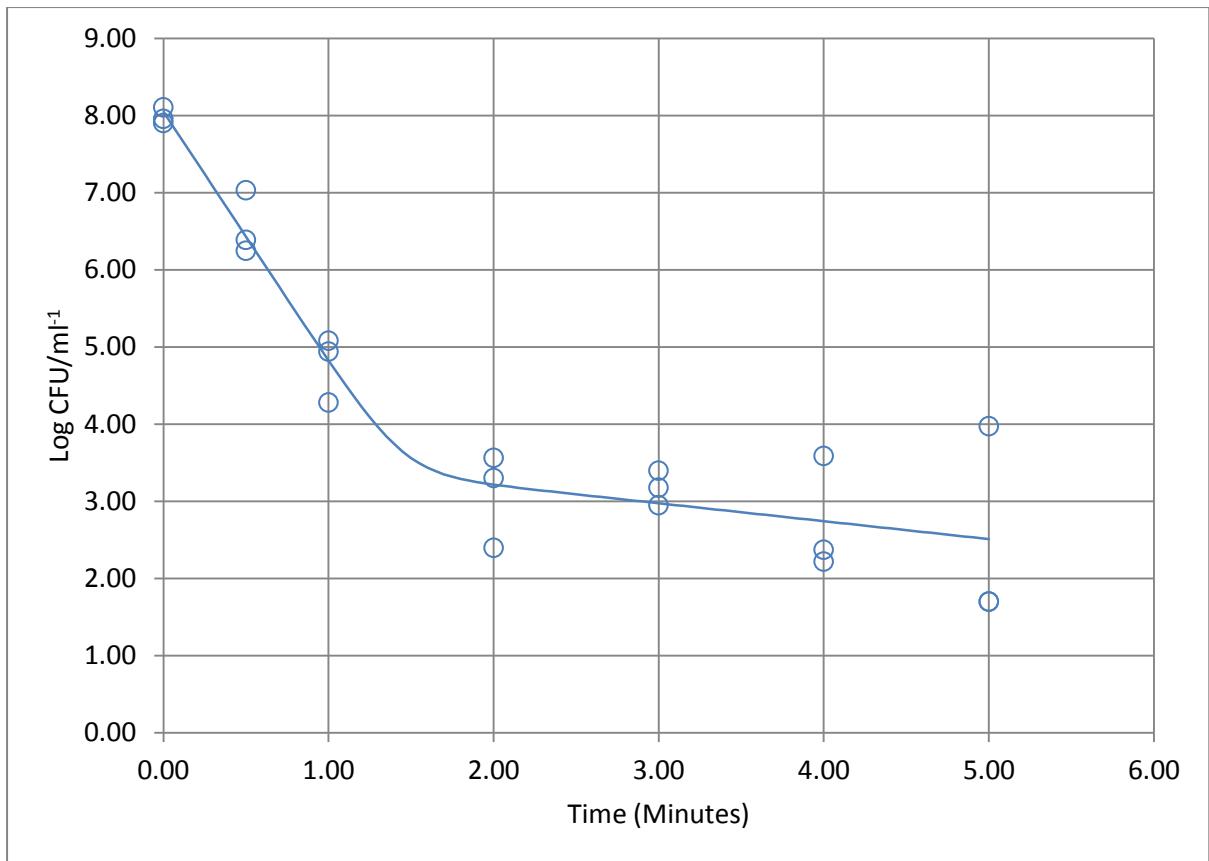


Figure 314. Plot illustrating predicted response curve using biphasic model for survival of strain 12628 (ST-1773, CC-828) following exposure to pH 5.5 and heating at 64°C.

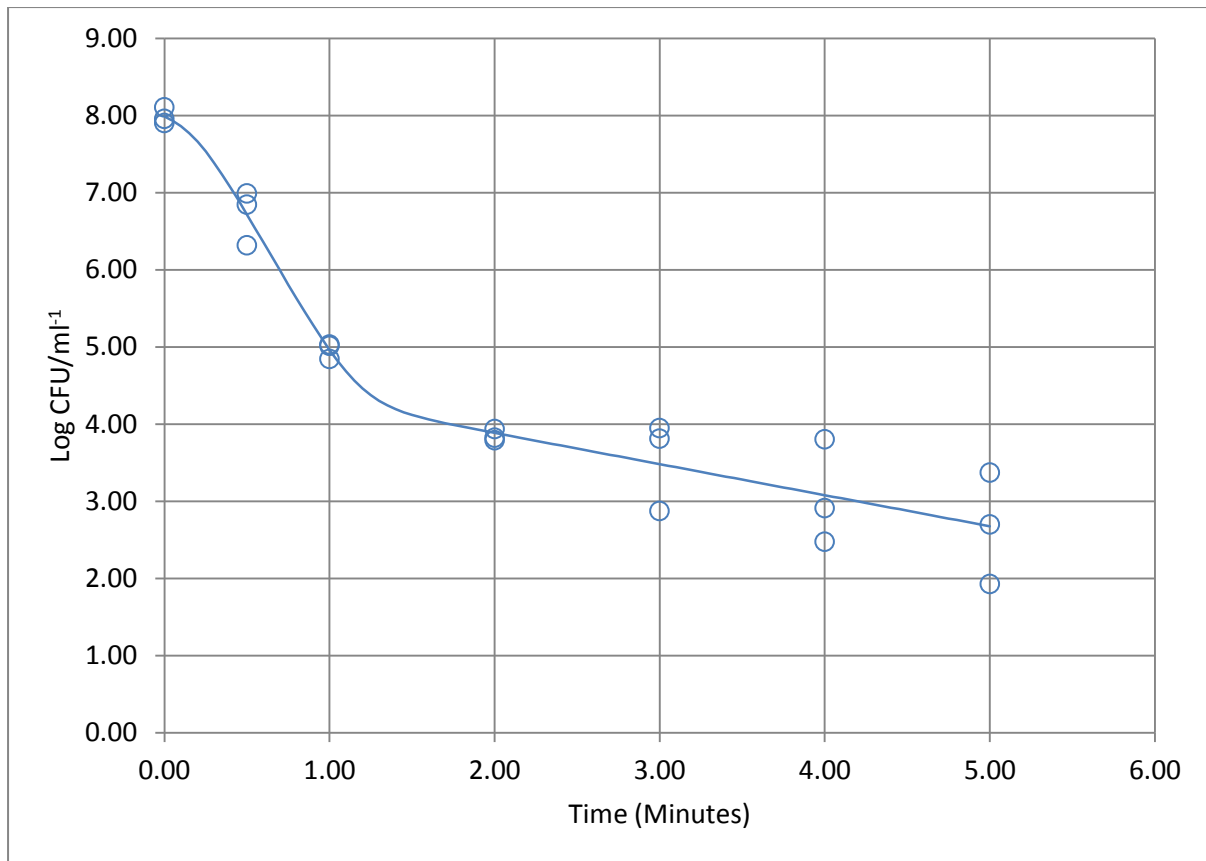


Figure 315. Plot illustrating predicted response curve using a Biphasic model with shoulder-effect for survival of strain 12628 (ST-1773, CC-828) following exposure to pH 6.5 and heating at 64⁰C.

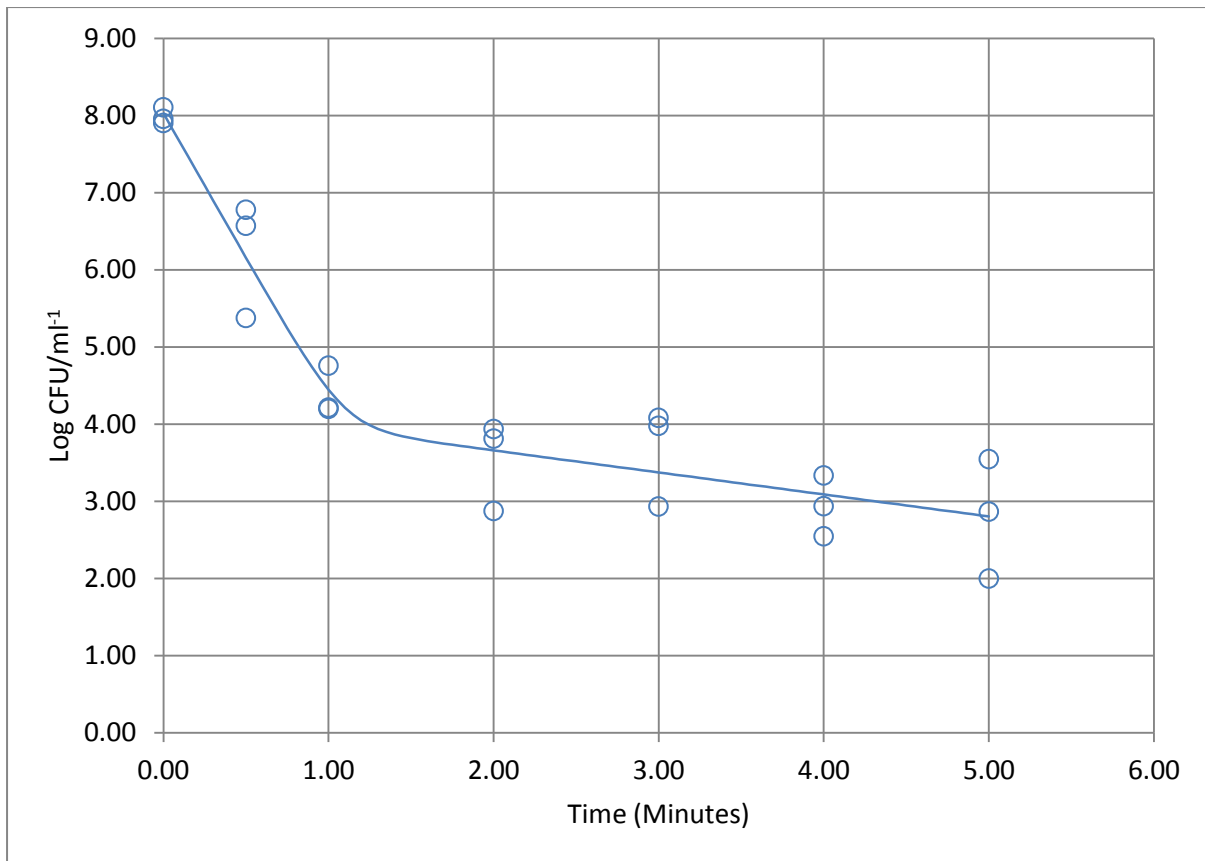


Figure 316. Plot illustrating predicted response curve using a Biphasic model for survival of strain 12628 (ST-1773, CC-828) following exposure to pH 7.5 and heating at 64°C.

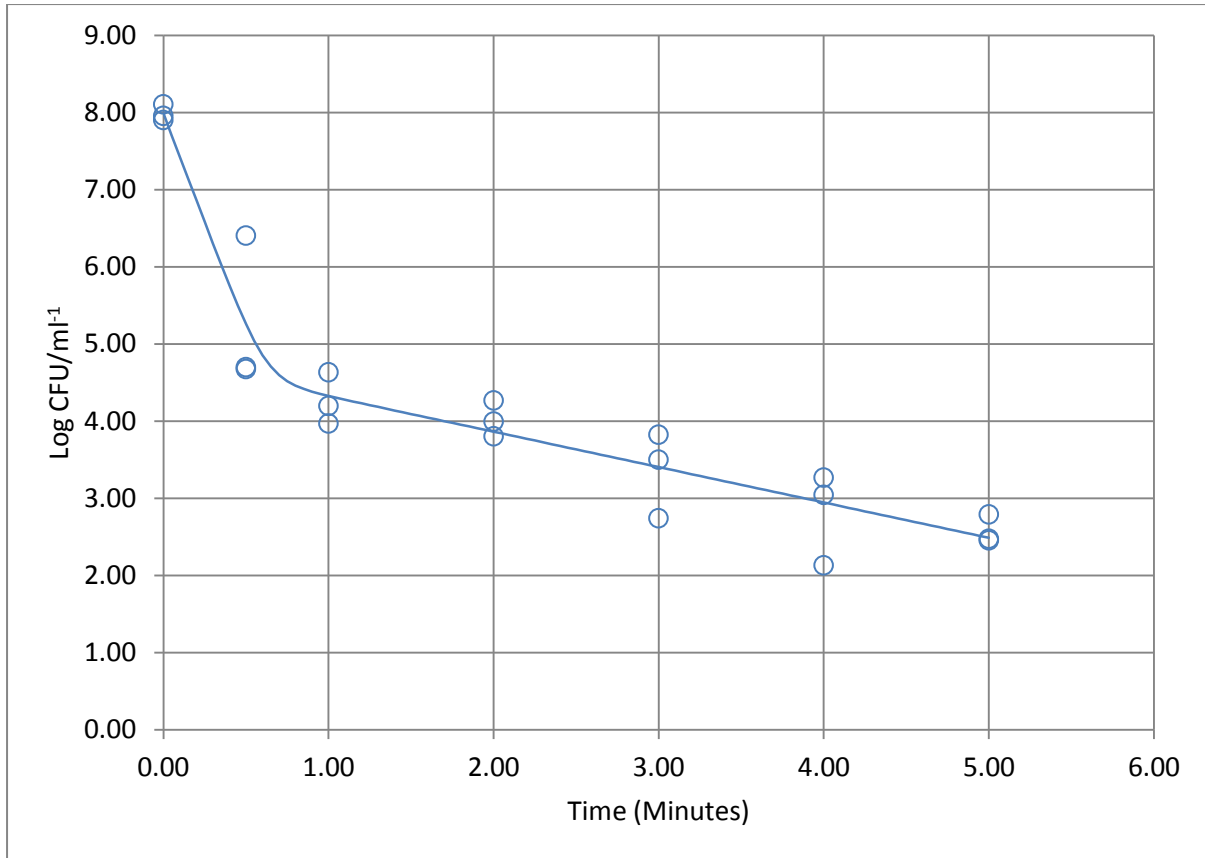


Figure 317. Plot illustrating predicted response curve using a Biphasic model for survival of strain 12628 (ST-1773, CC-828) following exposure to pH 8.5 and heating at 64°C.

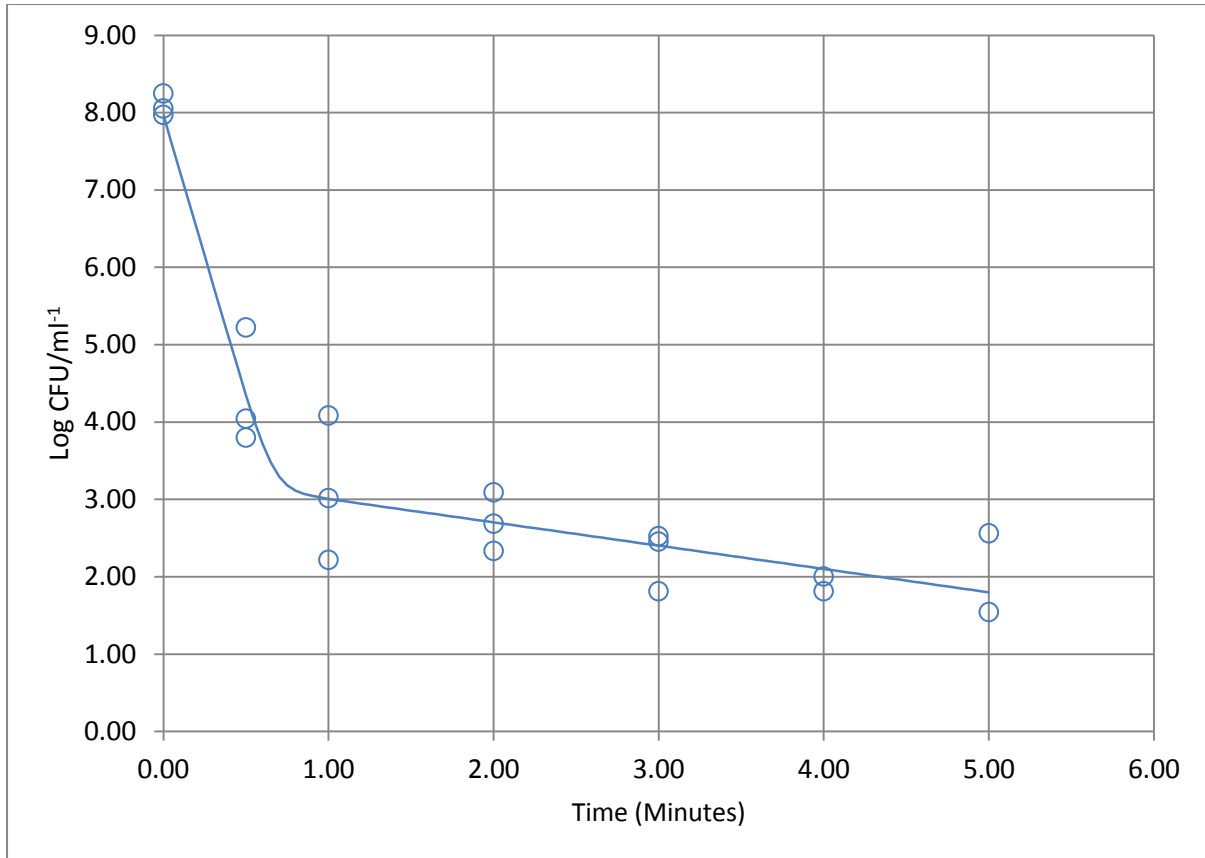


Figure 318. Plot illustrating predicted response curve using a Biphasic model for survival of strain 12662 (ST-257, CC-257) following exposure to pH 4.5 and heating at 64^oC.

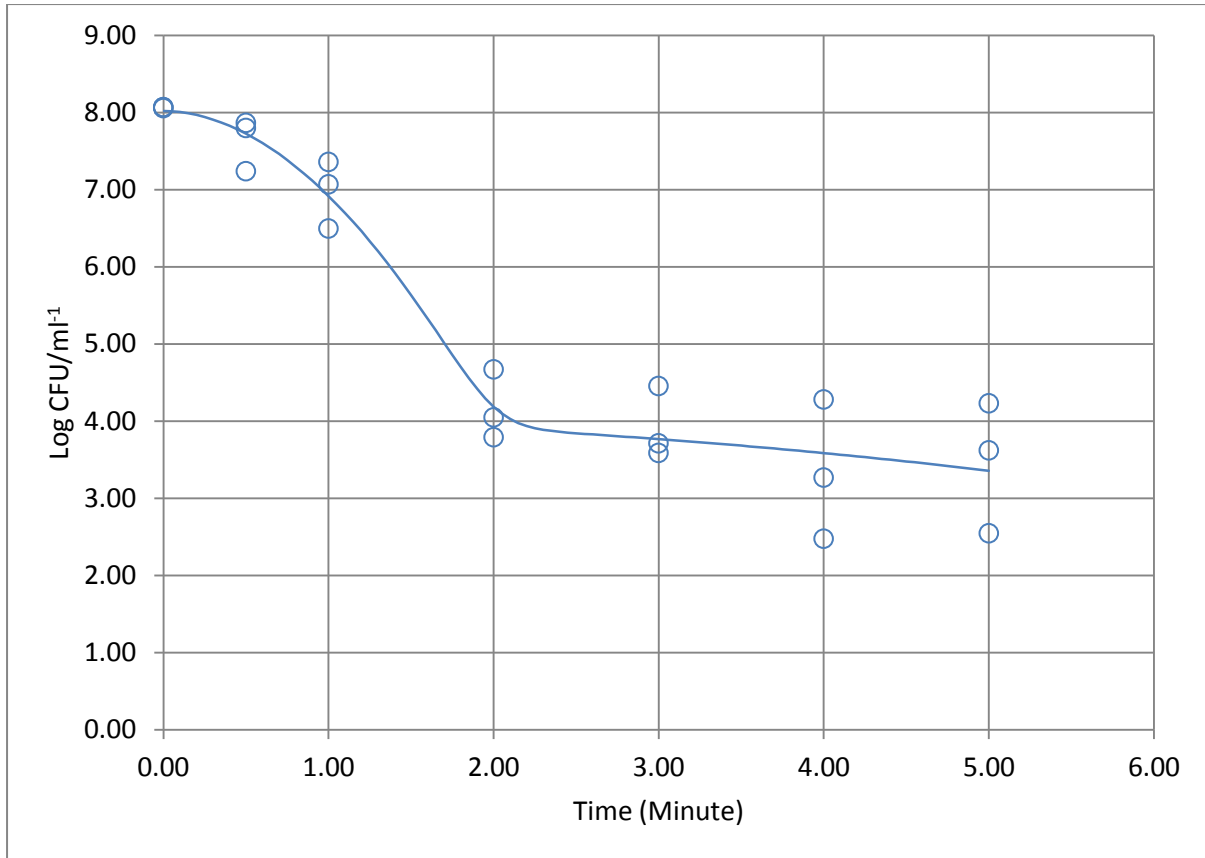


Figure 319. Plot illustrating predicted response curve using a mixed Weibull distribution model for survival of strain 12662 (ST-257, CC-257) following exposure to pH 5.5 and heating at 64°C.

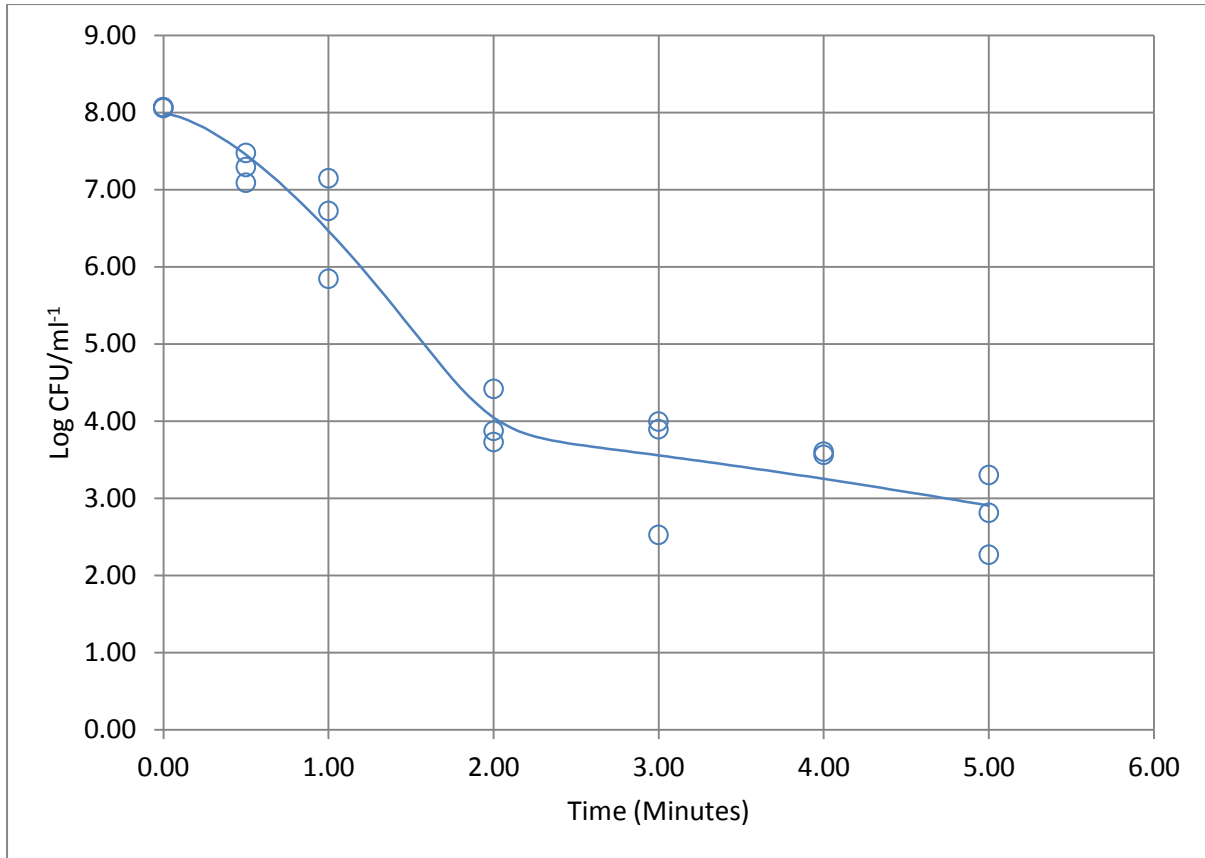


Figure 320. Plot illustrating predicted response curve using a mixed Weibull distribution model for survival of strain 12662 (ST-257, CC-257) following exposure to pH 6.5 and heating at 64°C.

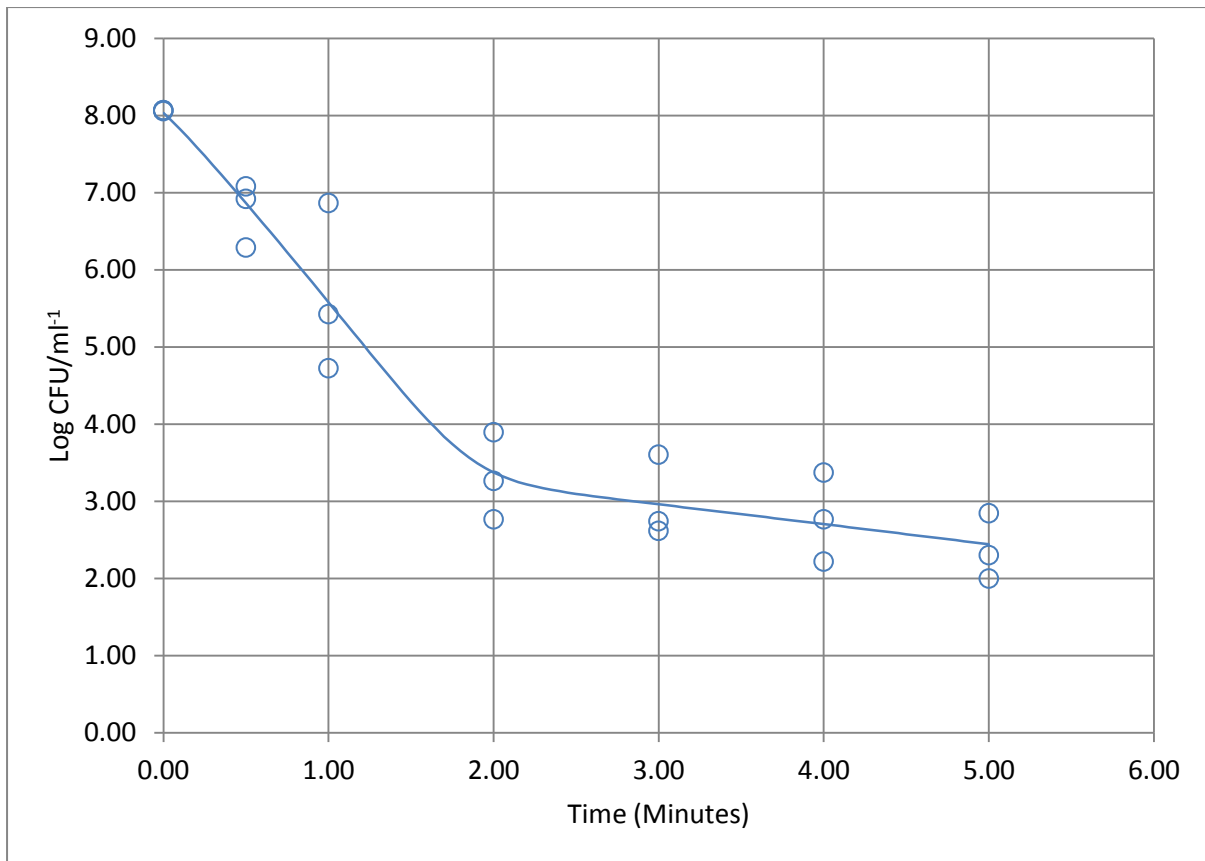


Figure 321. Plot illustrating predicted response curve using a mixed Weibull distribution model for survival of strain 12662 (ST-257, CC-257) following exposure to pH 7.5 and heating at 64°C.

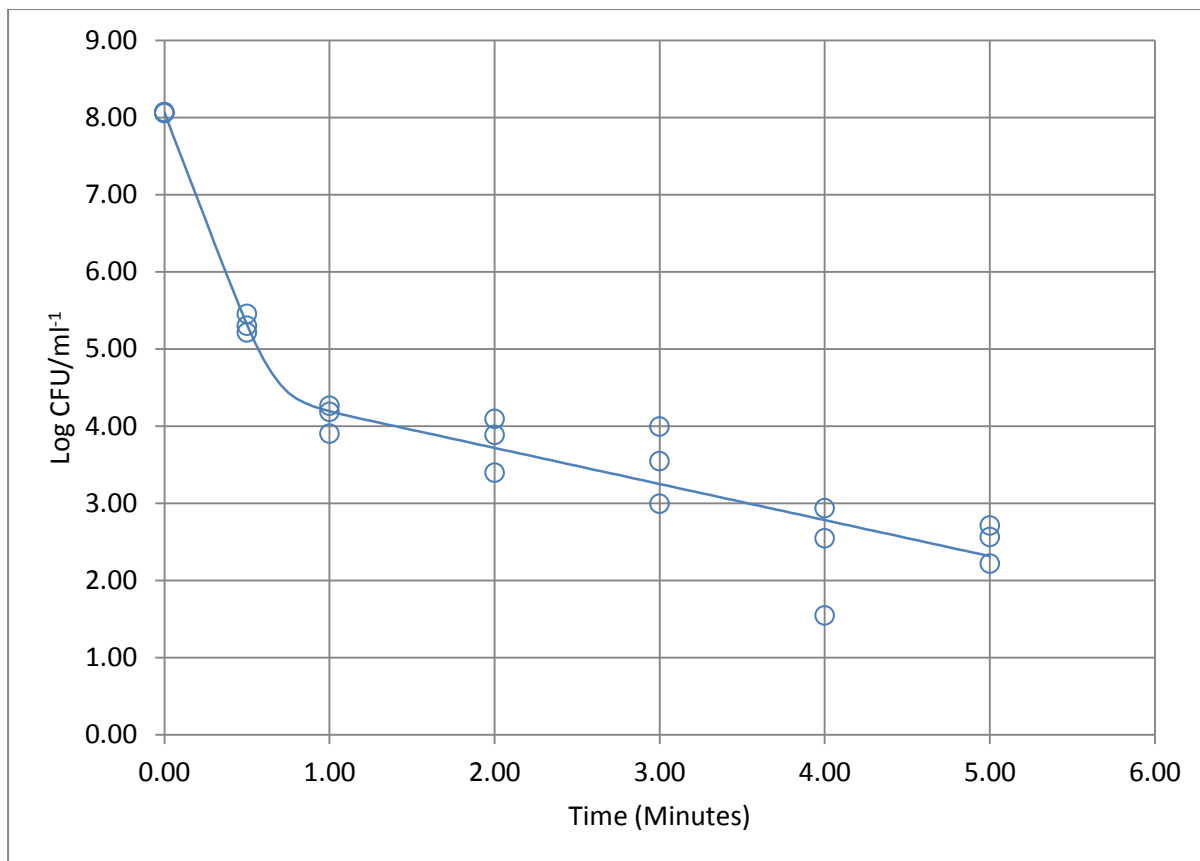


Figure 322. Plot illustrating predicted response curve using a mixed Weibull distribution model for survival of strain 12662 (ST-257, CC-257) following exposure to pH 8.5 and heating at 64⁰C.

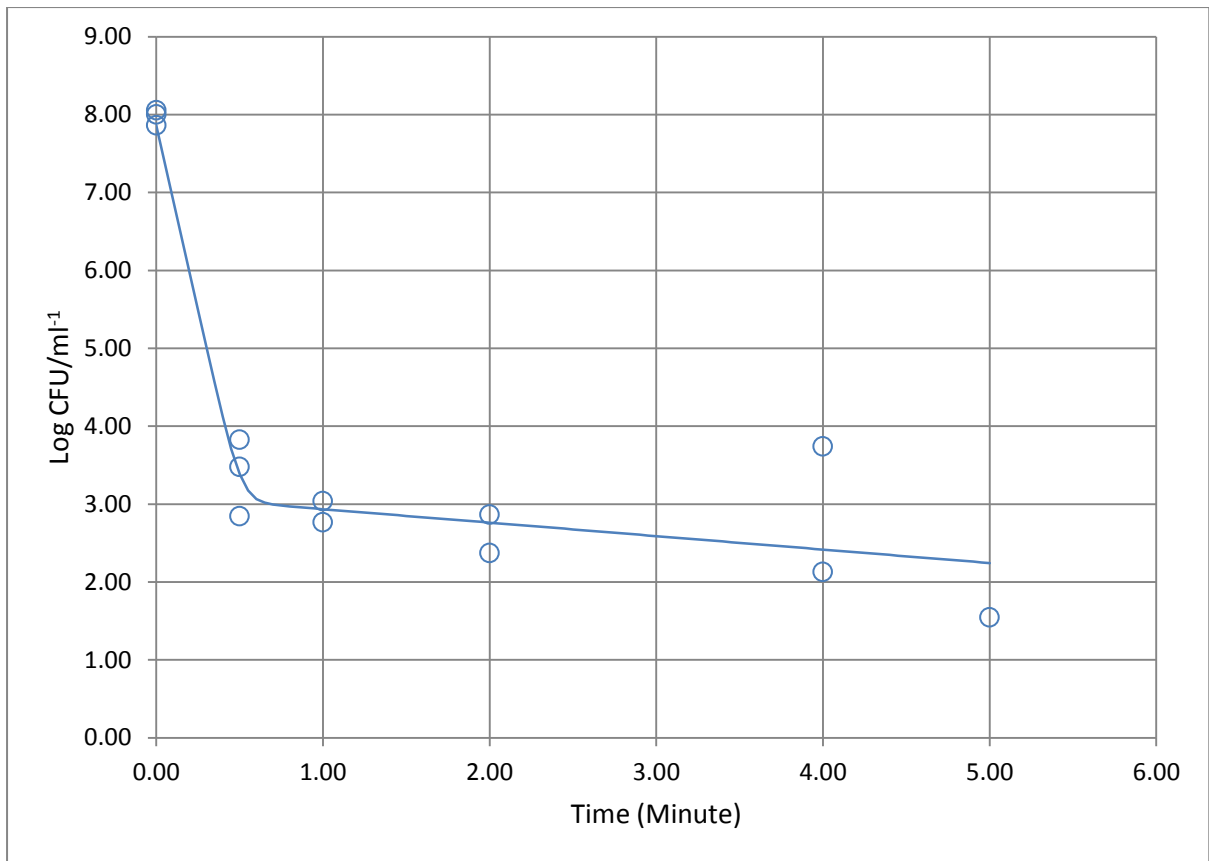


Figure 323. Plot illustrating predicted response curve using a Biphasic model for survival of strain 13126 (ST-21, CC-21) following exposure to pH 4.5 and heating at 64^oC.

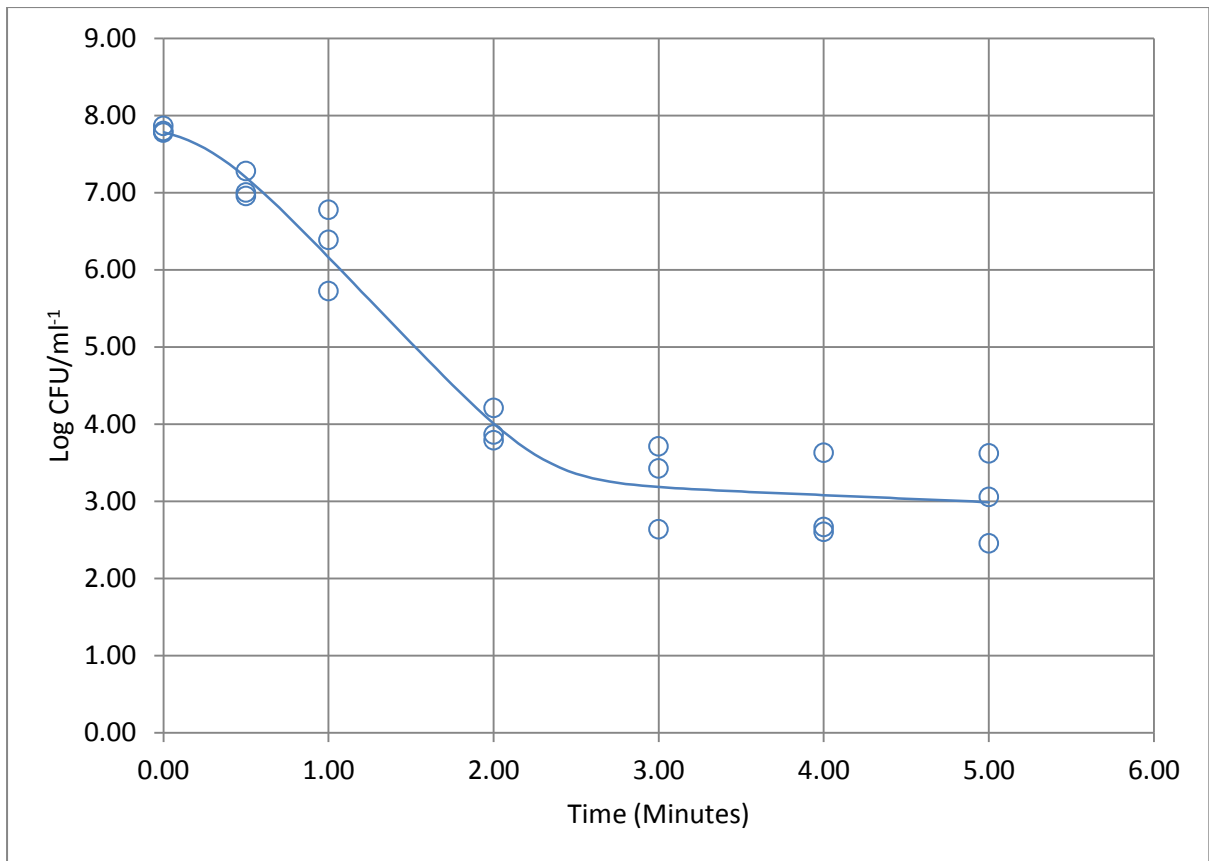


Figure 324. Plot illustrating predicted response curve using a Biphasic model with shoulder effect for survival of strain 13126 (ST-21, CC-21) following exposure to pH 5.5 and heating at 64°C.

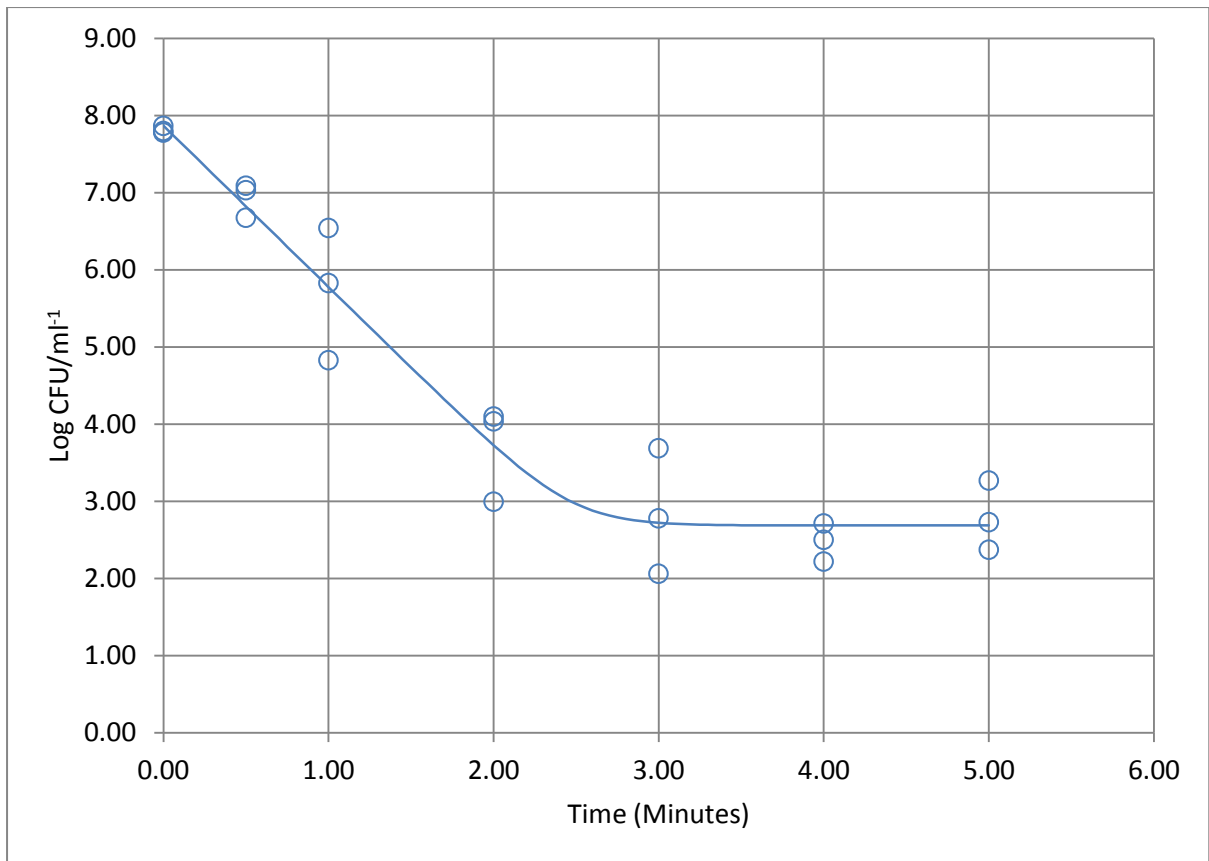


Figure 325. Plot illustrating predicted response curve using a Log-linear model incorporating an asymptotic function for survival of strain 13126 (ST-21, CC-21) following exposure to pH 6.5 and heating at 64°C.

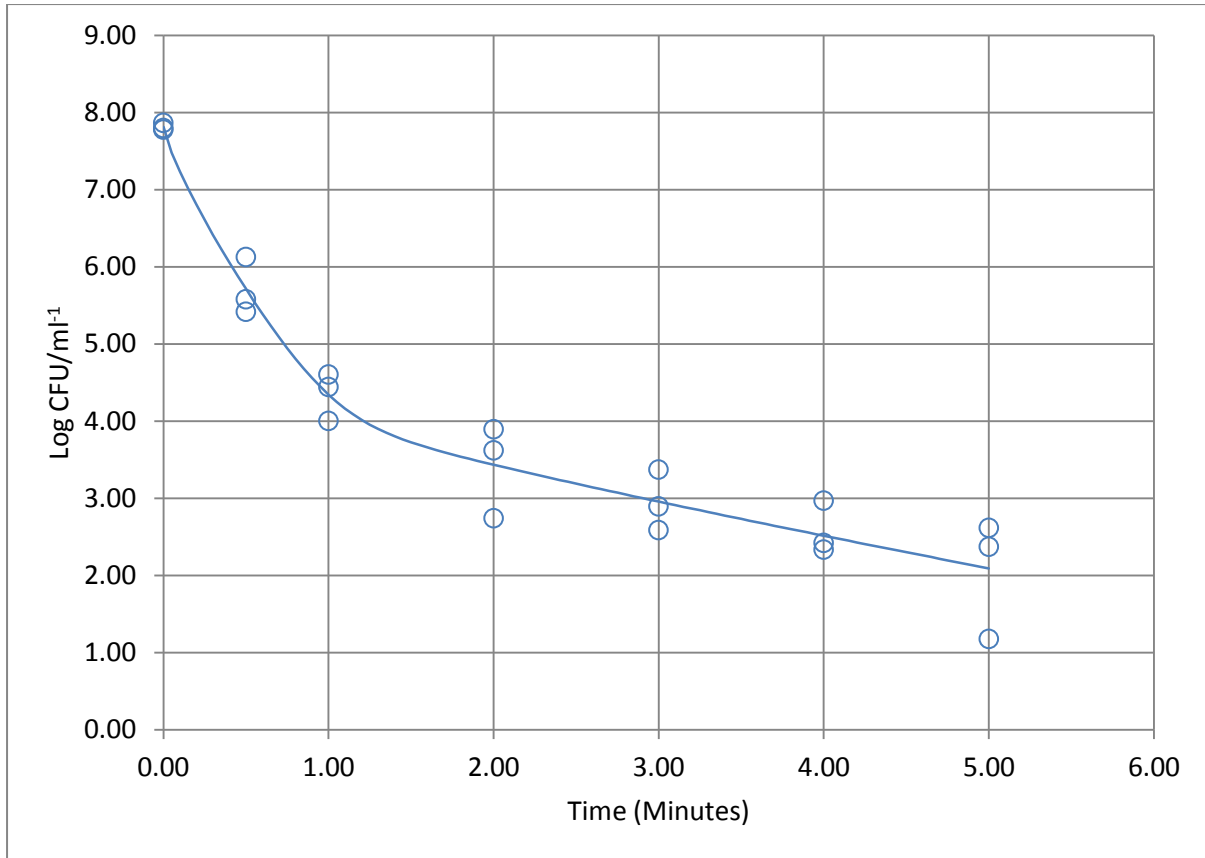


Figure 326. Plot illustrating predicted response curve using a mixed Weibull distribution model for survival of strain 13126 (ST-21, CC-21) following exposure to pH 7.5 and heating at 64^oC.

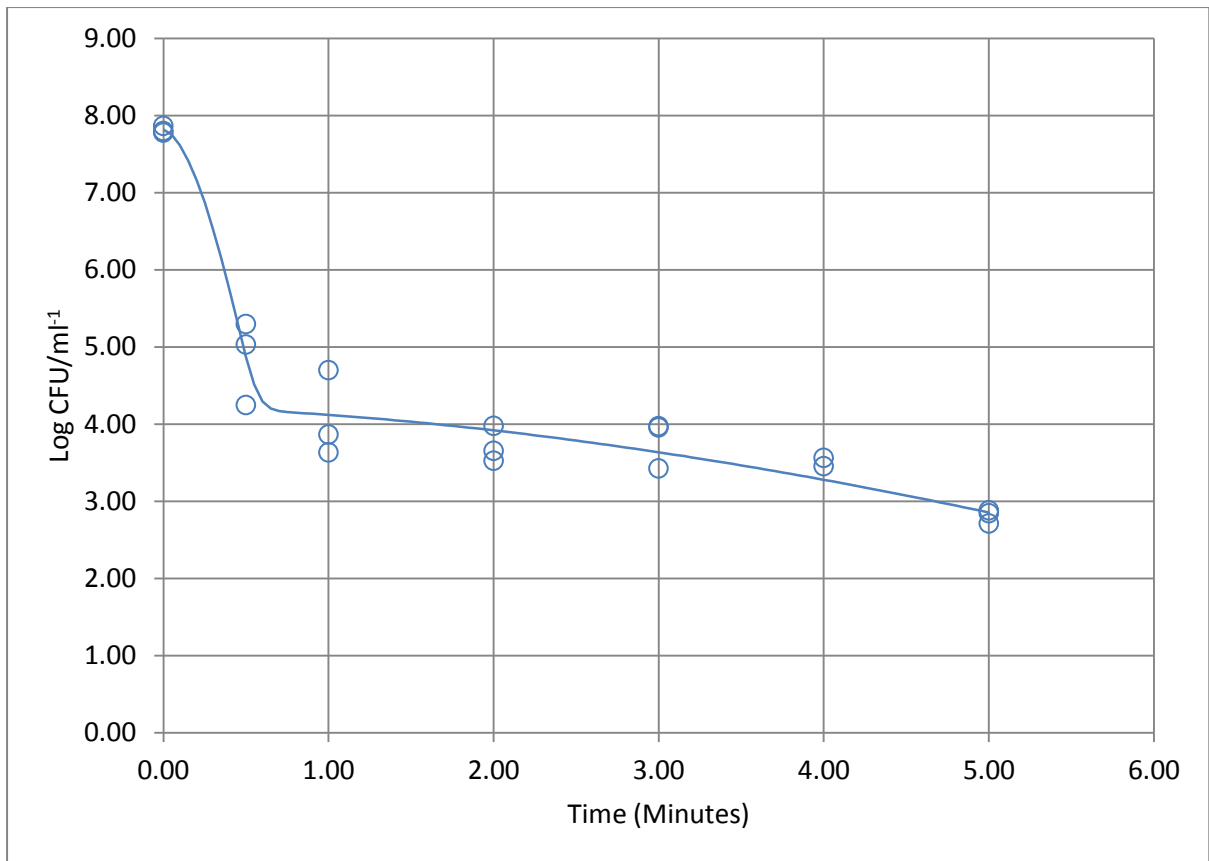


Figure 327. Plot illustrating predicted response curve using a mixed Weibull distribution model for survival of strain 13126 (ST-21, CC-21) following exposure to pH 8.5 and heating at 64°C.

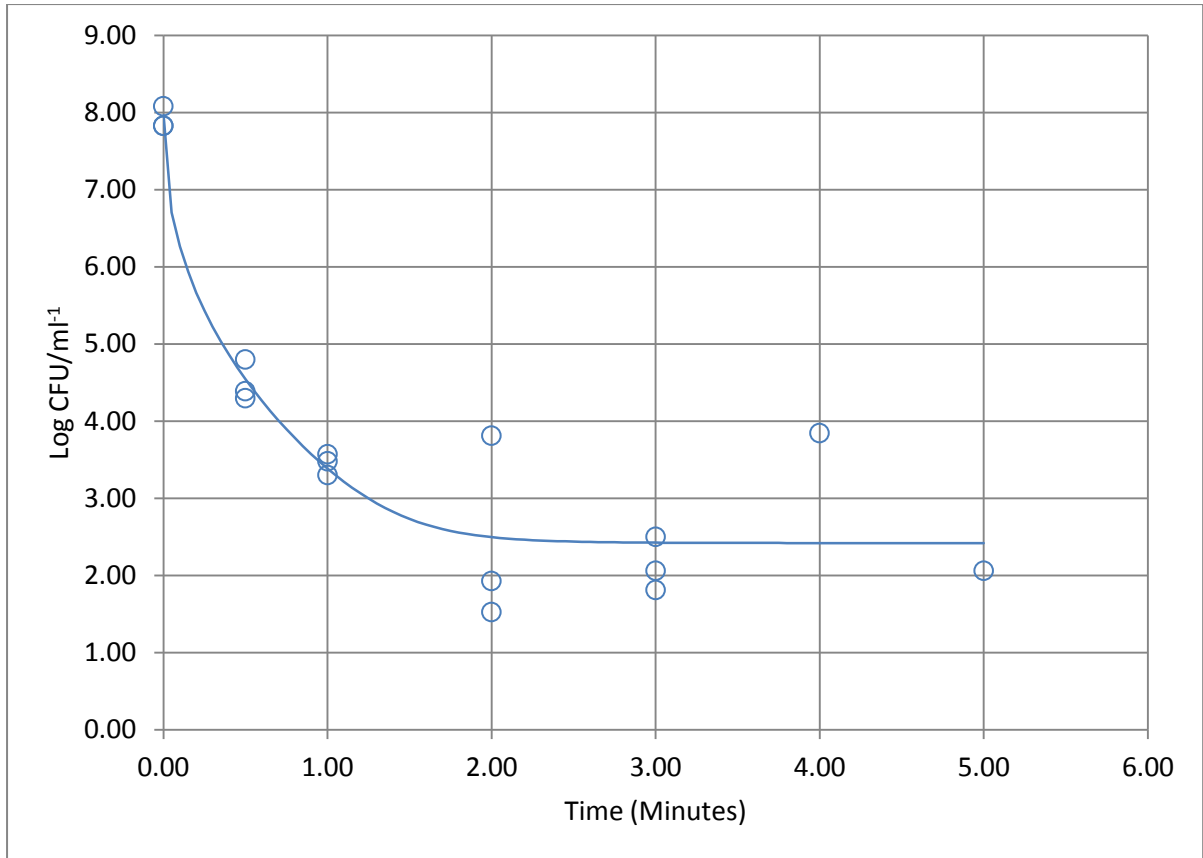


Figure 328. Plot illustrating predicted response curve using a Weibull model incorporating an asymptotic function for survival of strain 13136 (ST-45, CC-45) following exposure to pH 4.5 and heating at 64°C.

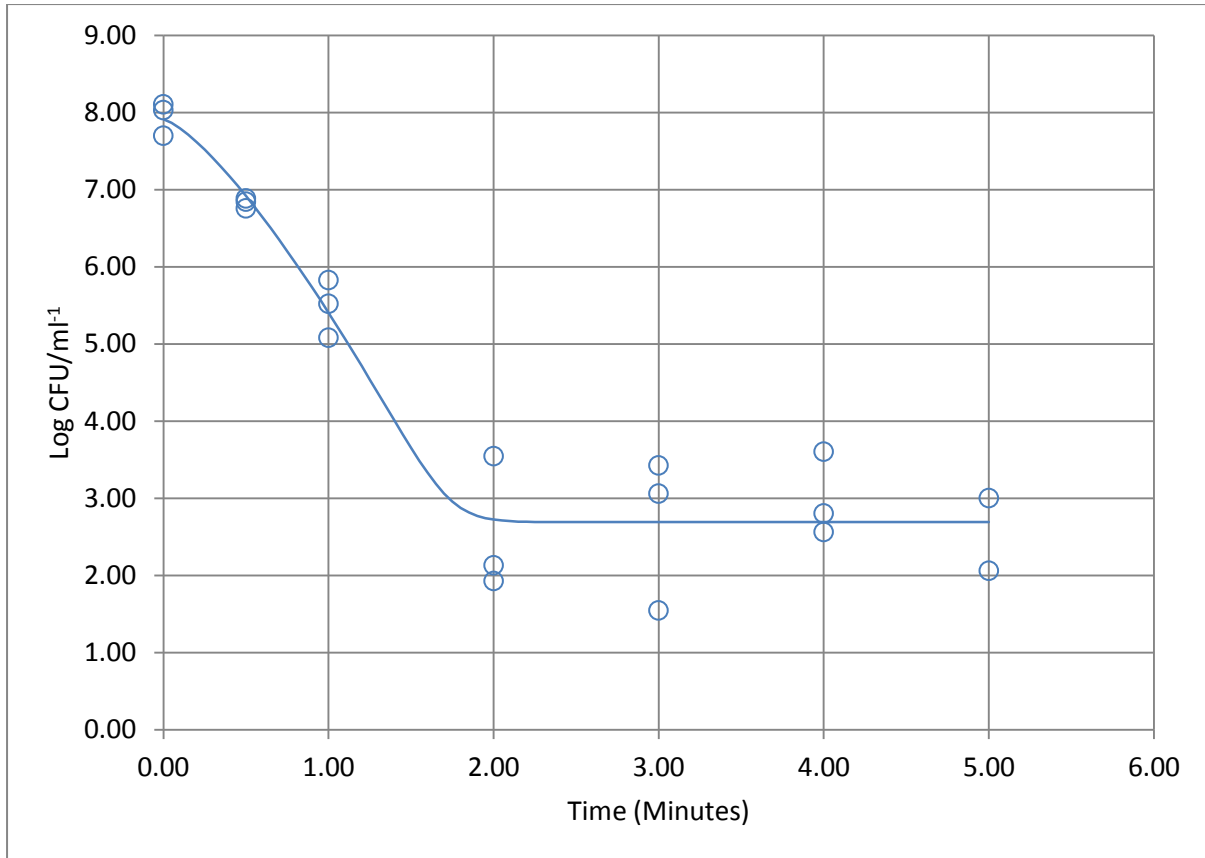


Figure 329. Plot illustrating predicted response curve using a Weibull model incorporating an asymptotic function for survival of strain 13136 (ST-45, CC-45) following exposure to pH 5.5 and heating at 64°C.

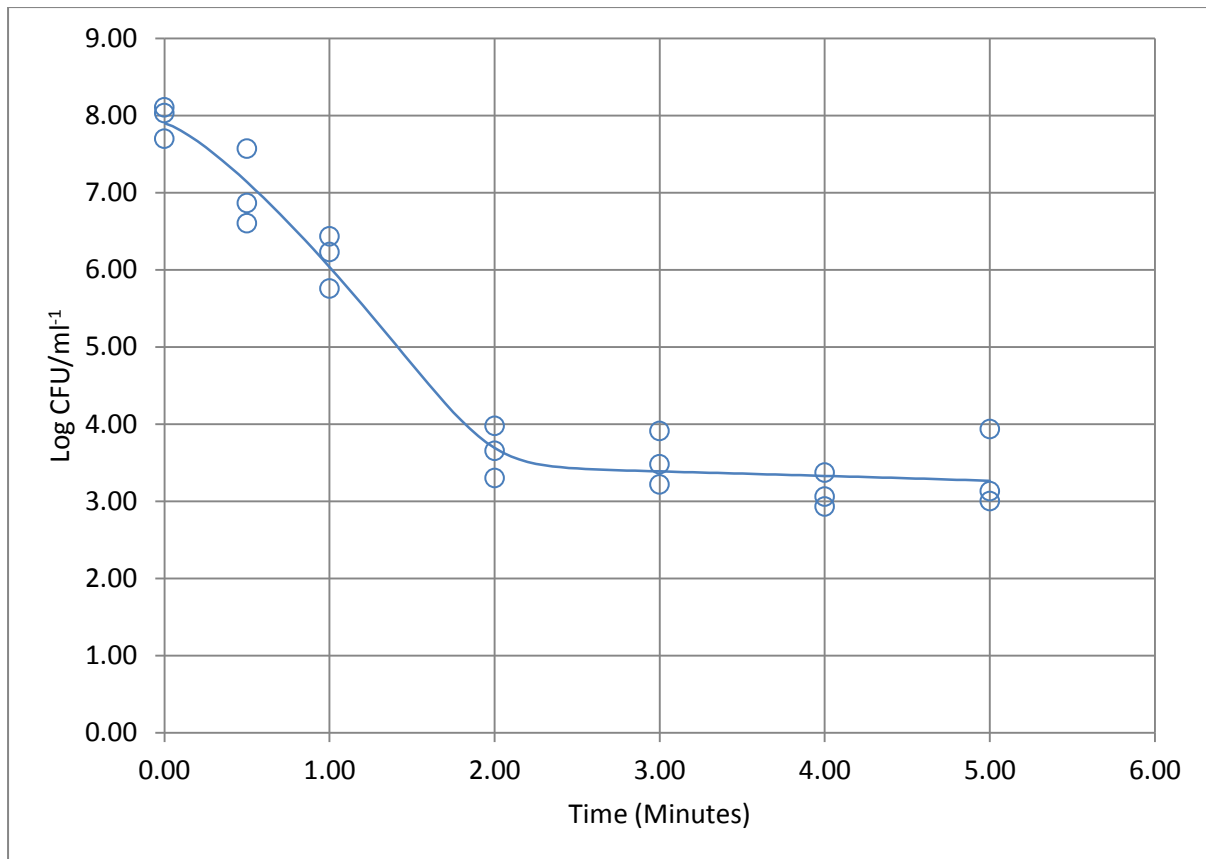


Figure 330. Plot illustrating predicted response curve using a Weibull model incorporating an asymptotic function for survival of strain 13136 (ST-45, CC-45) following exposure to pH 6.5 and heating at 64°C.

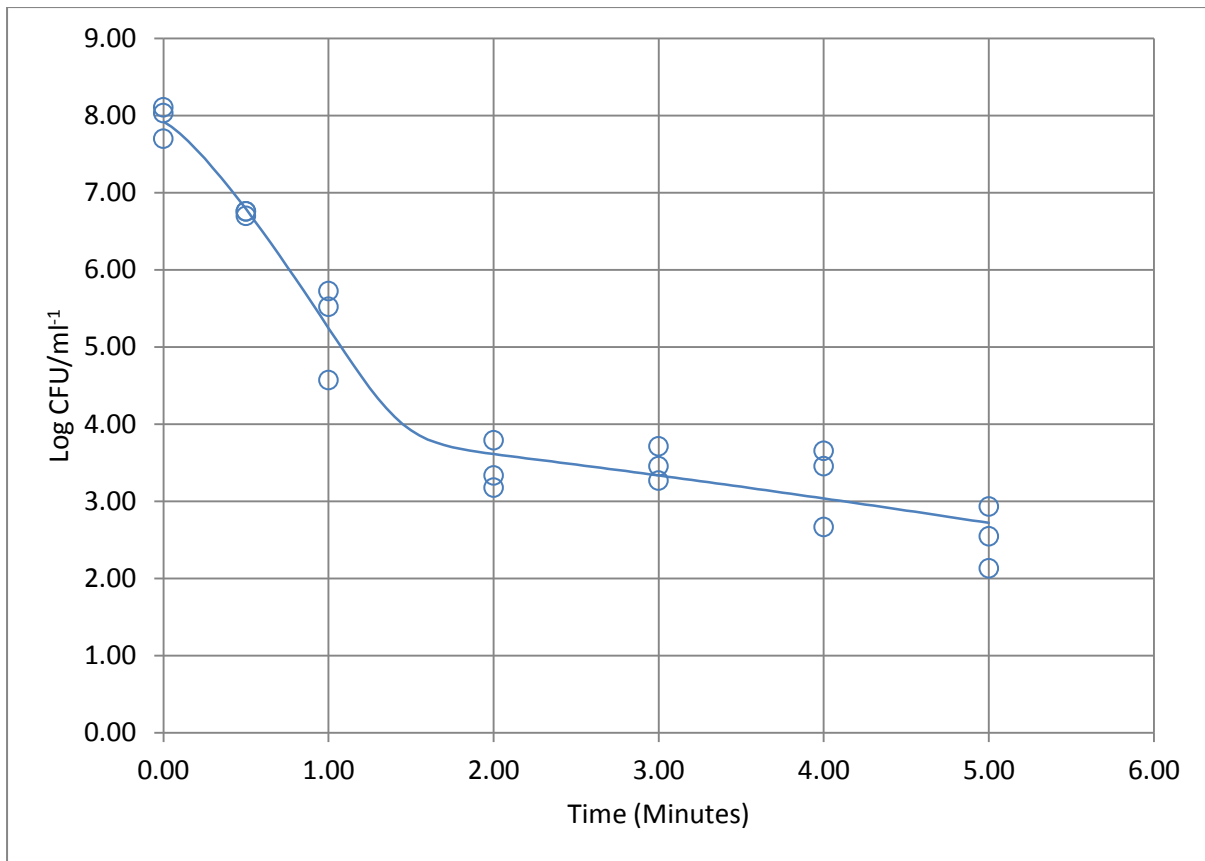


Figure 331. Plot illustrating predicted response curve using a mixed Weibull distribution model for survival of strain 13136 (ST-45, CC-45) following exposure to pH 7.5 and heating at 64°C.

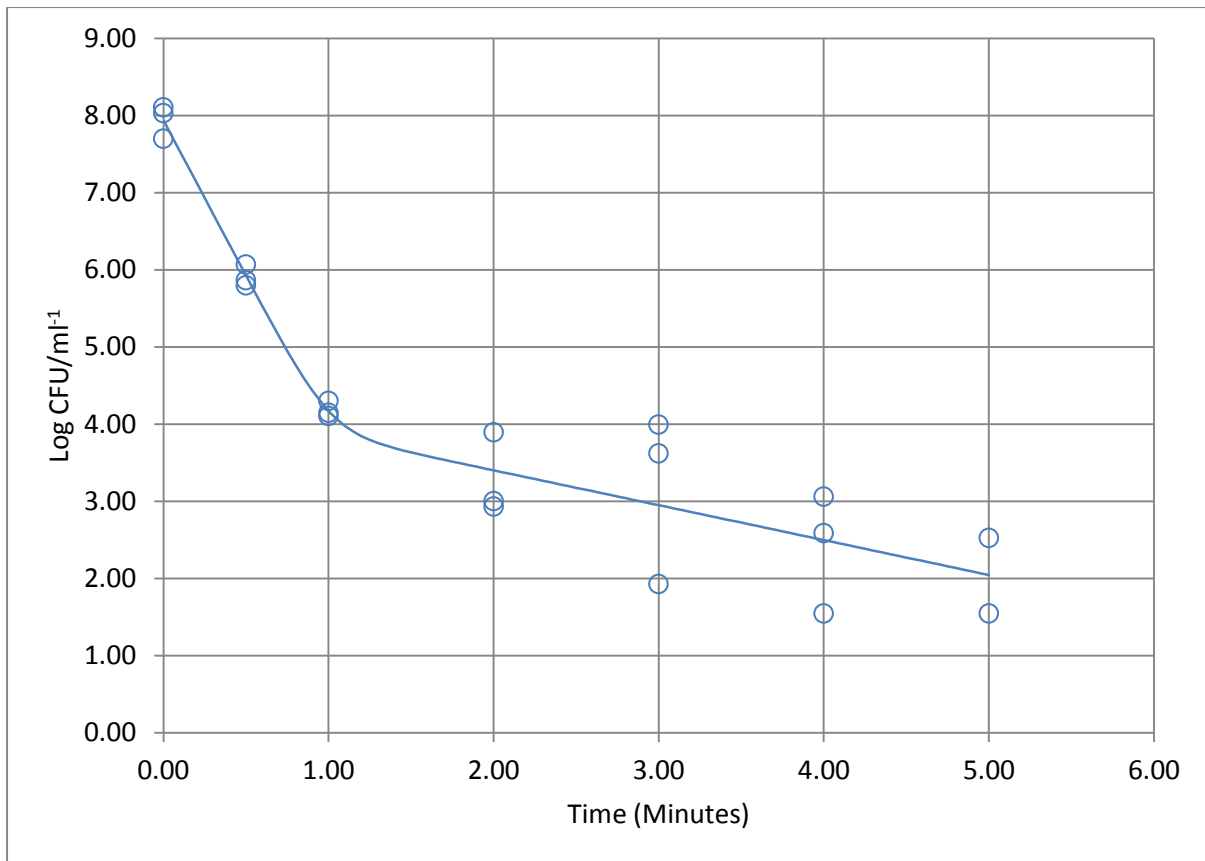


Figure 332. Plot illustrating predicted response curve using a mixed Weibull distribution model for survival of strain 13136 (ST-45, CC-45) following exposure to pH 8.5 and heating at 64⁰C.